THE EFFECTS OF RUNOFF AND UPWELLING EVENTS ON THE WATER QUALITY OF THE SOUTHERN SHELF OF CAYUGA LAKE

A Thesis

Presented to the Faculty of the Graduate School

of Cornell University

in Partial Fulfillment of the Requirements for the Degree of

Master of Science

by

Seth Avram Schweitzer

May 2010

ABSTRACT

The water quality on the southern shelf of Cayuga Lake is of interest locally - it is used for recreation, water supply, and the disposal of treated wastewater, but also more broadly since the factors that control the water quality in this system are common to many lakes and coastal systems. The configuration of a shallow shelf that receives both natural flows and anthropogenic nutrient loads, while at the same time being connected to a larger body of water whose dynamics strongly affect the system is commonly found in many embayment and estuarine systems. The question of what mechanisms control the water quality of the system and how is complicated by the fact that the processes of interest are highly intermittent, both in frequency and in magnitude, and vary both randomly and on seasonal and interannual timescales.

Using an 11 year (1998 - 2008) record of water quality data collected biweekly during the April - October months of each year at 9 sites in the lake, we examine the response of the water quality on the southern shelf of Cayuga Lake to various physical forcing conditions (e.g., surface runoff and internal seiche dynamics) and various loading and flow rates from natural and anthropogenic sources. Several cases of extreme forcing and system response are examined and metrics of correlation of water quality parameters with forcing conditions are calculated.

We hypothesize that in the absence of strong forcing in the form of high flow rates in the tributaries to the shelf, water quality on the shelf and the spatial gradients in water quality on the shelf are controlled by the interaction of basin scale internal waves and the shelf slope.

When the wind blows from the south for a duration greater than the lake's uninodal horizontal seiche period ($T/4$), the thermocline tilts up in the vicinity of the shelf. This leads to reduced exchange between the shelf and the main basin's epilimnion, resulting in higher nutrient levels near loading sources on the shelf. When the wind blows from the north the thermocline is tilted down near the shelf, exchange across the shelf break is increased, resulting in lower levels of nutrients on the shelf.

Gradients in averaged metrics of water quality exist between different parts of the shelf. We suggest that these gradients can in part be explained by effects of the earth's rotation, which cause runup of internal waves on the shelf slope to generally be higher on the western part of the shelf than the eastern, leading to increased mixing with hyplimnetic water and reduced levels of metrics such as chlorophyll-*a* concentrations.

BIOGRAPHICAL SKETCH

The author was born in New York State and immigrated with his family to Israel as a boy. His military service in the Israeli Navy and a following year spent traveling in Asia were perhaps what made him choose to pursue the study of engineering and of water. After completing his B.Sc. In Civil and Environmental Engineering at the Technion, Israel Institute of Technology, the author moved to Ithaca, N.Y. to continue his studies at Cornell University.

For Yael and Daphna, who bring light to every day.

ACKNOWLEDGEMENTS

Sincere thanks go to my advisor, Todd Cowen, and committee members Nelson Hairston and Cliff Kraft for their support and guidance (and for help diving for lost instruments!).

I would also like to thank the Department of Utilities and Energy Management for supporting the work and for the stimulating conversations about the water quality of the southern basin of Cayuga Lake.

The Upstate Freshwater Institute (UFI) collected the majority of the water quality data discussed in the thesis, performed all the laboratory analysis of the water samples and provided much logistical support and advice. I would like to thank Steve Effler, Dave Matthews and everyone else at UFI for all their help.

Like any other project based on field work, this work could not have been completed without the help of many individuals. Tim Brock, Paul Charles and Cameron Willkens kept the equipment going. Fellow students and friends provided support, advice and helping hands in the field. They are (in no particular order) Jack, P.J., Evan, Allie, Rafael, Yong sung, Pete, I-Chi, Jorge, Misty, Tim, Matt, Julia, Ali, Vicki, Franco, Kurt, Sean, Ian, Ryan, Colleen, Matias, C.P., Yoni and Yael.

CONTENTS

Biographical Sketch . . . iii
Dedication . . . iv
Acknowledgements . . . v
Contents . . . vi
List of Figures . . . viii
List of Tables . . . xiii

1 Introduction **1**
1.1 General . . . 1
1.2 Review of related literature . . . 3

2 Methods **7**
2.1 Instruments and data sources . . . 7
2.1.1 RUSS . . . 7
2.1.1.1 RUSS meteorological station . . . 8
2.1.1.2 Underwater profiler . . . 8
2.1.1.3 YSI sondes (660 V1 and V2) and sensors . . . 9
2.1.2 SBE-39 thermistors . . . 9
2.1.3 Game Farm Road (GFR) meteorological station . . . 9
2.1.4 USGS stream gages . . . 10
2.2 Field sampling program . . . 10
2.2.1 Water quality parameters measured . . . 14
2.2.2 Comments on individual sites . . . 16
2.3 Brief overview of statistical methods used . . . 17
2.4 Removal of outlying chlorophyll-*a* samples . . . 18

3 Characterization of Cayuga Lake and its South Shelf **20**
3.1 Physical Characterization of Cayuga Lake . . . 20
3.2 Nutrient loading sources . . . 21

4 Characterization of Physical Forcing Mechanisms **29**
4.1 Surface runoff . . . 29
4.2 Typical annual stratification cycle . . . 31
4.3 The Wedderburn number . . . 33
4.3.1 Calculating the Wedderburn number from observational data . . . 35
4.3.2 Histograms of Wedderburn number in Cayuga Lake . . . 38
4.4 Overview of internal physical processes . . . 40
4.4.1 Internal seiche and (longitudinal) tilting of the thermocline 43
4.4.2 Dynamics (seiching) . . . 46
4.5 Effects of the earth's rotation . . . 47

5 Baseline Conditions and the Response of the Shelf to Forcing Events 52
5.1 Baseline water quality record 53
5.1.1 Turbidity 55
5.1.2 Phosphorus 59
5.1.3 Chlorophyll-*a* 69
5.2 Event related water quality record 76
5.2.1 06/29/2006, shelf-averaged TP = 80.0 $\mu g/L$ 78
5.2.2 08/21/2007, shelf-averaged TP = 51.7$\mu g/L$ 81
5.2.3 09/09/2004, shelf-averaged TP = 49.9 $\mu g/L$ 87
5.3 Temporal correlation of various forcing conditions 91
5.4 Correlation of forcing conditions and water quality observations . 93
5.4.1 South to north gradients 94
5.4.2 East to west gradients 100

6 Discussion 104
6.1 Conceptual models of the impact of internal dynamics on the shelf water mass 104
6.1.1 The shelf as a well-mixed reactor with varying volume . . 104
6.1.2 Lateral tilting of the thermocline near the shelf break . . . 106
6.2 Summary 108

Bibliography 110

LIST OF FIGURES

2.1 Locations of sampling sites, in the context of the entire Cayuga Lake basin 12
2.2 Map of sampling sites on the south shelf 13

4.1 Statistics of flow in Fall Creek 30
4.2 Annual and seasonal (April-October) flow in Fall Creek 30
4.3 Seasonal evolution of temperature-depth profile at the RUSS . . 32
4.4 Seasonal evolution of thermal stratification 33
4.5 Monthly histograms of *Wb* for the period 1998 - 2008. Negative values of *Wb* indicate winds from the south which can lead to an upwards tilt of the thermocline near the southern shelf. 39
4.6 Histogram of wind direction and scatter plot of wind direction and velocity during April - October as measured at the Game Farm Road meteorological station. Dashed line marks approximate orientation of Cayuga Lake's main axis - 340° – 160°. Directions plotted are relative to true north. 43
4.7 Illustration of thermocline tilt under various forcing conditions (not drawn to scale): (a) Winds out of the north, tilting thermocline down at southern shelf, (b) Quiescent state, thermocline not tilted, (c) Winds out of the south, tilting thermocline up at southern shelf, (d) Sustained winds out of the south, causing upwelling of hypolimnetic water onto the southern shelf. 46
4.8 Illustration of internal seiche runup on southern shelf, ignoring the earth's rotation 50
4.9 Illustration of internal seiche runup on southern shelf, with interface tilted due to rotation 50

5.1 Median turbidity levels at each sampling site. a) monthly median turbidity at each site (median of all values in each month across all years) b) annual median turbidity at each site (median of all values in each year) 56
5.2 Monthly median turbidity grouped by site and by month. Order of sites is geographical by distance from the southeast corner of the lake. 57
5.3 Probability distribution function of relative observed Tn at each site. For each sampling site the leftmost bar represents the fraction of all sampling dates on which the site had the highest observed Tn of all sites and so on to the rightmost bar which indicates the fraction of sampling dates on which it had the lowest value. Order of sites is geographical by distance from the southeast corner of the lake. 58

5.4 Box plots of shelf-averaged and mean deepwater (sites 6, 8, Intake) Tn for each month, over the entire record. The horizontal scale is compressed to the right of the dashed black line in order to fit outlying values into the plot. 58
5.5 Median TP levels. a) annual median concentration at each site (all months of each year averaged) b) monthly median concentrations at each site (values of each month in all years averaged) 61
5.6 Probability distribution function (PDF) of relative observed TP at each site. The leftmost bar represents the fraction of sampling dates on which the site had the highest observed TP and so on to the rightmost bar which indicates the fraction of sampling dates on which it had the lowest value. Order of sites is geographical by distance from the southeast corner of the lake. 61
5.7 Median SRP levels. a) annual median concentration at each site (all months of each year averaged) b) monthly median concentrations at each site (values of each month in all years averaged) 62
5.8 Probability distribution function (PDF) of relative observed SRP at each site. For each sampling site the leftmost bar represents the fraction of all sampling dates on which the site had the highest observed SRP of all sites and so on to the rightmost bar which indicates the fraction of sampling dates on which it had the lowest value. Order of sites is geographical by distance from the southeast corner of the lake. 62
5.9 Monthly median TP turbidity grouped by site and by month. Order of sites is geographical by distance from the southeast corner of the lake. 63
5.10 Box plots of shelf-averaged and mean deepwater (sites 6, 8, Intake) TP for each month, over the entire record. The horizontal scale is compressed to the right of the dashed black line in order to fit outlying values into the plot. 64
5.11 Monthly median SRP grouped by site and by month. Order of sites is geographical by distance from the southeast corner of the lake. 65
5.12 Box plots of shelf-averaged and mean deepwater (sites 6, 8, Intake) SRP for each month, over the entire record.The horizontal scale is compressed to the right of the dashed black line in order to fit outlying values into the plot. 66
5.13 Scatter plots of observed shelf-averaged TP and averaged deep water (sites 6, 8, Intake). TP values are in $\mu g/L$. Dashed lines indicate location of perfect correlation (i.e., lines of $x = y$). Plots along the diagonal are histograms of the corresponding metric. Plots that are located symmetrically relative to the diagonal compare the same data, but are presented with different aspect ratios. 67

5.14 Scatter plots of observed TP at the shelf sites, during the stratified season (August - October). Each plot in this figure shows a scatter of two forcing parameters over the eleven year record, with each dot representing a single sampling date. TP values are in $\mu g/L$. Dashed lines indicate location of perfect correlation (i.e., lines of $x = y$). Plots along the diagonal are histograms of the corresponding metric. Plots that are located symmetrically relative to the diagonal compare the same data, but are presented with different aspect ratios. 68
5.15 Probability distribution function (PDF) of relative observed chlorophyll-*a* at each site. For each sampling site the leftmost bar represents the fraction of all sampling dates on which the site had the highest observed chlorophyll-*a* of all sites and so on to the rightmost bar which indicates the fraction of sampling dates on which it had the lowest value. Order of sites is geographical by distance from the southeast corner of the lake. 70
5.16 Median chlorophyll-*a* levels. a) annual median concentration at each site (all months of each year averaged) b) monthly median concentrations at each site (values of each month in all years averaged) 71
5.17 Monthly median chlorophyll-*a* grouped by site and by month. Order of sites is geographical by distance from the southeast corner of the lake. 72
5.18 Box plots of shelf-averaged and mean deepwater (sites 6, 8, Intake) chlorophyll-*a* for each month, over the entire record. The horizontal scale is compressed to the right of the dashed black line in order to fit outlying values into the plot. 73
5.19 Scatter plots of observed shelf-averaged chlorophyll-*a* and averaged deep water (sites 6, 8, Intake). Each plot in this figure shows a scatter of two forcing parameters over the eleven year record, with each dot representing a single sampling date. Chlorophyll-*a* values are in $\mu g/L$. Dashed lines indicate location of perfect correlation (i.e., lines of $x = y$). Plots along the diagonal are histograms of the corresponding metric. Plots that are located symmetrically relative to the diagonal compare the same data, but are presented with different aspect ratios. 74

5.20 Scatter plots of observed chlorophyll-*a* at the shelf sites, during the stratified season (August - October). Each plot in this figure shows a scatter of two forcing parameters over the eleven year record, with each dot representing a single sampling date. Chlorophyll-*a* values are in $\mu g/L$. Dashed lines indicate location of perfect correlation (i.e., lines of $x = y$). Plots along the diagonal are histograms of the corresponding metric. Plots that are located symmetrically relative to the diagonal compare the same data, but are presented with different aspect ratios. 75
5.21 Ranked values of shelf-averaged water quality parameters from the entire 1998 - 2008 period (SRP data are from 2000-2008), and box plots of their distributions. Note the logarithmic scale on the turbidity plot. 77
5.22 Forcing conditions and resulting water quality, 2006 80
5.23 Forcing conditions and resulting water quality, 2007 86
5.24 Comparison of temperature record at RUSS and piling cluster, 08/21/2007. Analysis of the time lag between two measurements of equal temperature at the RUSS and piling thermistors (indicated by the $\oplus$ symbols) yields an upwelling front progression rate of approximately 4 cm/s. 87
5.25 Forcing conditions and resulting water quality, 2004 90
5.26 Temporal correlation of forcing conditions. Each plot in this figure shows a scatter of two forcing parameters over the eleven year record, with each dot representing a single sampling date. Histograms of the various forcing conditions are plotted along the diagonal. Tributary flow is in cfs, LSC and IAWWTF loading are in kg/day TP. Plots that are located symmetrically relative to the diagonal compare the same data, but are presented with different aspect ratios. 92
5.27 Box plots of TP measured at sites 3, 5, 6 during unstratified period (months 4-7), stratified period (months 8-10), stratified period with below median IAWWTF loading and stratified period with above median IAWWTF loading. Bold lines mark median values, grayed area around the median is the 95% confidence interval. The horizontal scale is compressed to the right of the dashed black line in order to fit outlying values into the plot. . . 95
5.28 Box plots of TP measured at sites 3, 5, 6 during stratified period (months 8-10) with IAWWTF above median for any Wb value, and for conditions where the thermocline is tilted up ($Wb < 0$) or down ($Wb > 0$) near the shelf. Bold lines mark median values, grayed area around the median is the 95% confidence interval. The horizontal scale is compressed to the right of the dashed black line in order to fit outlying values into the plot. 96

5.29 Comparison of TP at site1 and site 4 under different Wb number cases, during the stratified season (August - October). Darkened region around the median marks 95% confidence interval of the median. 100
5.30 Comparison of TP at site 1 and site 4 under different forcing conditions, during the stratified season (August - October). TP values are in $\mu g/L$, flow in cfs, LSC and IAWWTF loading in kg/day of TP. 101

6.1 Aerial photo of the southern shelf of Cayuga Lake 108

LIST OF TABLES

2.1 Locations of sampling sites 14

3.1 Estimates of monthly loads of phosphorus to the shelf in kg/day from various loading sources, 1998-2005 23
3.2 Estimates of monthly loads of phosphorus to the shelf in kg/day from various loading sources, 2006-2008 23
3.3 Summary of flow and TP loads entering shelf. The term "flushing time" is used loosely here since the flushing time of the shelf is not controlled by any single parameter. "Flushing times" were calculated by dividing the shelf's volume by the flow rate of the respective discharges and do not make any attempt to include the increased water mass influx from barotropic and baroclinic exchange with the main lake (e.g., Rueda & Cowen, 2005*b*). . . . 25

5.1 p-values of paired Tn comparisons, May - October, n=156. In each case the null hypothesis that the means/medians of respective sets are equal is tested against the listed alternative hypothesis. 57
5.2 p-values of paired TP comparisons, May - October, n=156. In each case the null hypothesis that the means/medians of respective sets are equal is tested against the listed alternative hypothesis. 60
5.3 p-values of paired SRP comparisons, May - October, n=156. In each case the null hypothesis that the means/medians of respective sets are equal is tested against the listed alternative hypothesis. 60
5.4 p-values of paired chlorophyll-*a* comparisons, May - October, n=156. In each case the null hypothesis that the means/medians of respective sets are equal is tested against the listed alternative hypothesis. 70
5.5 p-values of two-sample chlorophyll-*a* comparisons, May - October, n=156. In each case the null hypothesis that the means/medians of respective sets are equal is tested against the listed alternative hypothesis. 71
5.6 Shelf water quality as observed on 06/29/2006 79
5.7 Shelf water quality as observed on 08/21/2007 85
5.8 Shelf water quality as observed on 09/09/2004 89
5.9 Median TP at sites 3, 5, 6 under various forcing conditions 97
5.10 p-values of two-sided TP comparisons. Tests were performed on sampling days in the range August - October when loading from IAWWTF was above median. In each case the null hypothesis that the means/medians of respective sets are equal is tested against the listed alternative hypothesis. 97

5.11 p-values of paired TP comparisons at sites 1 and 4, August - October, n=40 ($Wb > 0$), n=49 ($Wb < 0$). In each case the null hypothesis that the means/medians of respective sets are equal is tested against the listed alternative hypothesis. 102
5.12 p-values of two-sample TP comparisons at sites 1 and 4, August - October, n=40 ($Wb > 0$), n=49 ($Wb < 0$). Δ_{14} refers to the difference in TP between sites 1 and 4. In each case the null hypothesis that the means/medians of respective sets are equal is tested against the listed alternative hypothesis. 102

LIST OF ABBREVIATIONS

Chl	Chlorophyll-*a*
CHWWTP	Cayuga Heights Waste Water Treatment Plant
GFR	Game Farm Road meteorological station
IAWWTF	Ithaca Area Waste Water Treatment Facility
IQR	Inter Quartile Range
LSC	Cornell University Lake Source Cooling facility
NTU	Nephelometric Turbidity Unit
NYSDEC	New York State Department of Environmental Conservation
RTD	Residence Time Distribution
RUSS	Remote Underwater Sampling Station
SRP	Soluble Reactive Phosphorus
Tn, Tn_L	Turbidity
TP	Total Phosphorus
UFI	The Upstate Freshwater Institute

CHAPTER 1

INTRODUCTION

1.1 General

The water quality on the southern shelf of Cayuga Lake is of interest locally - it is used for recreation, water supply, and the disposal of treated wastewater, but also more broadly since the factors that control the water quality in this system are common to many lakes or coastal systems. The configuration of a shallow shelf that receives both natural flows and anthropogenic loads while at the same time being connected to a larger body of water whose dynamics strongly affect the system is commonly found in many embayment and estuarine systems. The question of what mechanisms control the water quality of the system and how is complicated by the fact that the occurrence and magnitude of the processes of interest are highly intermittent, and vary both randomly and on a seasonal and interannual timescale.

Nutrient loading to the southern shelf comes from a number of sources, the most important of which include the inflows from Fall Creek and the Cayuga Inlet and the discharges of point sources located on the shelf (Cornell University, 2009). To understand the effects of this loading on the water quality of the shelf it is necessary to understand the mixing and transport processes that determine the fate of these loads. The length of time that water remains within the boundaries of an aquatic system, in this case the shelf or a region of the shelf, is a useful timescale in the analysis of relevant physical and biological processes (Monsen *et al.*, 2002). This is the residence time which is defined for a particle of water as the period of time that passes between its arrival at some defined

point to the time it exits the system (e.g., Rueda & Cowen, 2005*b*; Monsen *et al.*, 2002). Two particles introduced at the same time and in the same vicinity will follow different paths due to turbulence and chaotic advection, and therefore will have different residence times. For this reason the time scale that particles released at a specific time and place remain in the system is best characterized by a probability density function of residence times - the residence time distribution, or RTD. The residence time on the shelf is a function of the motions of the shelf's waters. These are controlled by several processes, including inflow from the tributaries and point sources as well as surface waves and wind generated currents. However this thesis will argue that the internal seiche dynamics of the lake and the shelf break region are of equal importance in determining mixing and transport on the shelf.

The internal seiching of the lake is not dissimilar to tidal action on an estuary or embayment. The internal seiche motions cause a constant pumping action on the epilimnion which is expected to be felt all the more on the shallow shelf due to nonlinear amplification. Additionally, during extreme events when the thermocline's tilt becomes such that the bottom of the epilimnion is shallower than the lake bottom on the shelf (i.e., upwelling), hypolimnetic water is advected on to the shelf and can have a major impact on the nutrient loading and mixing and transport dynamics on the shelf. The interaction of the internal dynamics and other loading sources and physical processes can also be important, e.g., evidence that upwelling can cause "blocking" of off shelf exchange, effectively lengthening residence time or altering transport and mixing patterns on the shelf. If such episodes coincide with loading events from one or more sources the impact may be significant.

1.2 Review of related literature

Several publications describing the physical limnology of Cayuga Lake exist spanning the past century, although they are separated by significant periods of time. Birge & Juday (1914, 1921) published the first comprehensive survey of the lake, including hydrographic measurements made during an 1875 Cornell University Engineering Department survey (the first such survey of an inland lake in the United States). These measurements are still a primary source of hydrographic data in use today for the lake in its entirety although several more recent and higher resolution surveys have been performed for limited regions of the lake, primarily in connection with various engineering projects.

Internal waves in the Cayuga Lake were first discussed in Henson (1959), in which thermal data collected between 1950 - 1953 off of Taughannock Point were analyzed. The period of the uninodal internal seiche was calculated to be in the 55 - 58 hour range and average amplitudes of 10 m were observed at Taughannock Point, which the author concluded would indicate 15 m amplitudes at the southern end of the lake. The paper describes a single event with more than double this amplitude after "...the winds were reinforcing and occurred in complete synchrony with the seiche movements." i.e., during an upwelling event. Henson *et al.* (1961) published a thorough compilation of physical and chemical characteristics of the lake including a discussion of the thermal dynamics of the lake and basin scale internal waves. The predominant current in the lake was assumed to be northerly due to the fact that more than half of the surface drainage enters the lake in its southern third, and the only outflow is in the north. An argument for the importance of rotation to surface flows was made based on anecdotal observations of turbidity plumes after heavy rainfall

staying near the eastern shore, and measurements made at three locations across a transect of the lake south of Taughannock Point on 06/03/1952 that showed that a depression of isotherms due to warm inflow from streams was tilted such that temperatures were warmer near the surface on the eastern side of the lake.

Sundaram *et al.* (1969) performed an analytical study of the physical effects of thermal discharges from a proposed nuclear power plant that was to be built near Milliken Station. The study includes measurements and discussion of thermal structure and motions of water in the lake. Currents of up to 0.5 m/s in the epilimnion (at a depth of 1.5 m) and up to 0.1 m/s in the hypolimnion (at a depth of 24 m over a lake depth of 34 m) were measured in August of 1968 near Milliken Station. Surface drift was found to be on the order of 2-3% of the wind velocity and the main cause of the epilimnetic currents was found to be internal seiche motions. Seiche periods were calculated to be on the order of 60 hours. Aerial mapping of temperature distribution on the surface of the lake was conducted, and indicated temperature gradients the authors attributed to upwelling due to rotation effects on epilimnetic currents (Ekman transport). Progressive internal waves with short periods on the order of 5 minutes were also observed.

Oglesby (1978) contributed a chapter on Cayuga Lake in the NYSDEC publication, *Lakes of New York State*. This includes a comprehensive review of physical, geological, chemical and biological research conducted on Cayuga Lake until that time. Summer total phosphorus was indicated to range between 15 - 20 $\mu g/L$ throughout the water column and a mass balance for phosphorus indicated a total input of about 139 metric tons per year, or an annual volumetric loading of 14.9 $\mu g/L$ of phosphorus to the lake. Over 60% of this was thought to originate as domestic waste discharges. Average chlorophyll-*a* concentrations in

the epilimnion were reported to have ranged between 6 and 10 $\mu g/L$ although one observation of over 20 $\mu g/L$ was reported in 1972.

Ahrnsbrak (1986) measured currents on the southern shelf of the lake between October 1984 and September 1985, as part of the environmental impact study of relocating the Ithaca Area Wastewater Treatment Facility (IAWWTF) onto the shelf. Summer (May - September) currents were generally weak, with a mean of just over 2 cm/s. 50% of observations were below 2 cm/s, 80% were below 5 cm/s. Winter and early spring currents were generally greater in magnitude than summer currents.

A more recent comparative water quality study of the Finger Lakes including sections on Cayuga Lake was prepared by Callinan (2001) of NYSDEC. Substantial declines in total phosphorus over the preceding decades were reported, along with smaller declines in chlorophyll-*a* and moderate increases in water clarity. A longitudinal gradient in trophic conditions in the lake was described, with decreasing levels of total phosphorus and chlorophyll-*a* and increasing water clarity found at locations farther from the south shelf and closer to the deep basin. Increases in populations of zebra mussels (*Dreissena sp.*) were cited as a possible cause for the downward trend in chlorophyll-*a* and upward trend in water clarity within the south shelf area.

Using X-ray energy spectroscopy (SAX) analysis of water samples collected from the lake, Effler *et al.* (2002) showed that inorganic tripton, rather than phytoplankton is the primary regulator of turbidity on the south shelf, and recommended that efforts to improve water clarity in the region consider controlling particulates suspended in surface runoff rather than reductions in phosphorus loading. Haith *et al.* (2009) modeled sediment and nutrient loads en-

tering Cayuga Lake with the goal of producing baseline information required for eventual management of water quality. The main (67.5%) loading source of phosphorus to the lake was found to be surface runoff, primarily from agricultural land.

Effler *et al.* (Submitted December 2009) analyzed long term water quality records in Cayuga Lake in the context of preparation for water quality modeling for purposes of establishing a TMDL (Total Maximum Daily Load) for the lake. The flushing rate for the southern shelf was estimated to be on the order of one day.

Several studies of the lake and primarily its southern shelf have been performed in relation to Cornell University's Lake Source Cooling (LSC) facility. These include the Draft Environmental Impact Statement (DEIS - Stearns & Wheler, 1997) and annual reports on lake monitoring related to the facility's operation generated each year beginning in 1998 (UFI, 2000*a*,*b*, 2001, 2002, 2003, 2004, 2005, 2006, 2007; Cornell University, 2008, 2009). The DEIS includes discussion of the thermal dynamics of the lake, and various ecological issues related to the operation of the facility. The annual reports summarize the results of water samples and other data collected in the lake each in relation to the facility's operation. This lake monitoring is the main source of the data used in this thesis.

CHAPTER 2

METHODS

2.1 Instruments and data sources

2.1.1 RUSS

The RUSS, or Remote Underwater Sampling Station, is an instrument platform moored on Cayuga Lake at a fixed location near the shelf break over a lake depth of approximately 29 *m*. Various instruments can be mounted on the platform including a Campbell Scientific meteorological station on the surface buoy and water quality sensors mounted on an underwater payload that profiles the water column under the main surface float. The main float also includes solar panels, batteries and charge control circuits, and an RF transmitter/receiver to communicate wirelessly with a base station. The instrument is controlled by an on board computer that manages data acquisition and short term storage, control of the underwater profiler and communications with the base station.

The RUSS was built by Apprise Technologies of Duluth MN and has been deployed in a similar location on Cayuga Lake since 2001, generally during the warmer months of the year (April - October). Since the RUSS was not deployed during the entire period discussed in this thesis meteorological data used in the thesis were taken from the Game Farm Road station located on the main Cornell campus.

2.1.1.1 RUSS meteorological station

A Campbell Scientific meteorological station is mounted on the RUSS' surface platform that includes the following sensors:

- R.M. Young 05106 Wind Monitor-MA anemometer
- Campbell Scientific HMP45C Relative humidity/air temperature sensor
- Surface water temperature sensor
- Li-Cor LI200x pyranometer

2.1.1.2 Underwater profiler

The RUSS underwater profiler is a buoyancy controlled device that is connected to the main buoy only by means of a single cable that provides power and communications. The profiler consists of two plastic canisters, an electric pump and the sonde housing. It can be configured to carry either a Hydrolabs or YSI sonde fitted with various sensors. Buoyancy of the profiler is controlled by pumping water in or out of the watertight canisters, thereby changing the specific gravity of the entire unit, causing it to move up or down in the water column as needed. This buoyancy controlled mechanism theoretically provides better energy efficiency and the advantage of isolation from movements of the surface buoy when compared to other possible mechanisms (e.g., being lowered by a winch).

The profiler will generally be "parked" at a given depth and then take several water column profiles a day. Depending on the amount of available solar energy to power the unit 4-6 profiles a day may be collected. Data collected by

the profiler is stored on the main buoy's computer until being uploaded to the base station by wireless RF transmission.

2.1.1.3 YSI sondes (660 V1 and V2) and sensors

At various times the underwater profiler was fitted with either a YSI 6600 V1 or V2 sonde carrying some combination of the following sensors:

Temperature/Salinity

pH/Oxidation-Reduction Potential (ORP)

Chlorophyll-a

Turbidity

Dissolved Oxygen (DO)

Optical DO

Pressure

2.1.2 SBE-39 thermistors

The thermal records at the piling cluster were taken by means of Seabird SBE-39 thermistors.

2.1.3 Game Farm Road (GFR) meteorological station

The Game Farm Road (GFR) weather station is located on the Cornell University campus approximately 5 miles east of the southern end of the lake and operated

by the Northeast Regional Climate Center. Data collected by the weather station include air temperature, precipitation, relative humidity, wind speed and direction, and solar radiation.

Meteorological (primarily wind) data used in this thesis were taken from measurements made at the GFR station. Although the RUSS station has the advantage of taking measurements above the surface of the lake itself, it was first deployed in 2001 and was not deployed continuously throughout the entire study period. Therefore the GFR data were used for the sake of consistency.

All wind directions presented in the thesis are referenced to the true north. Magnetic declination in the region is approximately $12°6'W$ (2010).

2.1.4 USGS stream gages

USGS stream gages are installed on Fall Creek[1] and the Cayuga Inlet[2]. The gage on the Cayuga Inlet is located near enough to the lake that it is controlled by lake level (e.g., surface waves and seiches) and not the flow through the Inlet. For this reason the Fall Creek gage was the main source for surface flow data in this study.

2.2 Field sampling program

Most of the water quality data presented in this study were collected as part of the NYSDEC permit-required in-lake monitoring of Cornell's Lake source Cool-

[1]USGS 04234000, Lat 42°27'12", Long 76°28'23" NAD27
[2]USGS 04233500, Lat 42°26'45", Long 76°30'45" NAD27

ing (LSC) facility. Water samples were collected biweekly between April and October of each year at nine sites. Water sample collection before 2007 was done by the Upstate Freshwater Institute (UFI). Beginning in 2007 the samples were collected by the author and colleagues at the DeFrees Hydraulics Laboratory, School of Civil & Environmental Engineering.

The sampling site location configuration includes an east - west transect on the shelf at lake depths of approximately 4-5 *m* (sites 1, 3, 4) and a north - south transect located approximately at the lake's centerline including three sites on the shelf at depths of up to 6 *m* (sites 2, 3, 5) and one site farther north over a lake depth of 40 *m* (site 6). One more shelf site is located in the southeast corner of the shelf (site 7). In addition, two sites located farther north over deep water were also sampled - the LSC Intake site (Intake) off of Glenwood Point (directly above the location of the intake pipe to the LSC facility) and site 8 near Taughannock Point, approximately 10 *km* north of the shelf (figure 2.1, 2.2, table 2.1). Equal volumes were collected by submersible pump from a few centimeters below the surface and from 2 *m* below the surface at all sites, and additionally from 4 *m* below the surface at sites 5, 6, 8, and Intake (the sites where the lake is deep enough to permit this). These subsamples were then mixed together to create a single water sample from each site. The samples were analyzed for total phosphorus (TP), soluble reactive phosphorus (SRP), chlorophyll-*a* (Chl) and turbidity (Tn). All laboratory analysis of water samples was performed by UFI using standard procedures.

In addition to the collection of water samples, water temperature on the shelf was recorded continuously at one location. Thermistors were attached to a cluster of pilings located near site 3 (referred to as the "piling thermistors") at a near

bottom depth of approximately 3 *m*. Temperatures were recorded at least hourly during the sampling season (April - October) and at least daily during the rest of the year since July 1998. Details of lab and field protocols are available in the annual reports (UFI, 2000*a*,*b*, 2001, 2002, 2003, 2004, 2005, 2006, 2007; Cornell University, 2008, 2009).

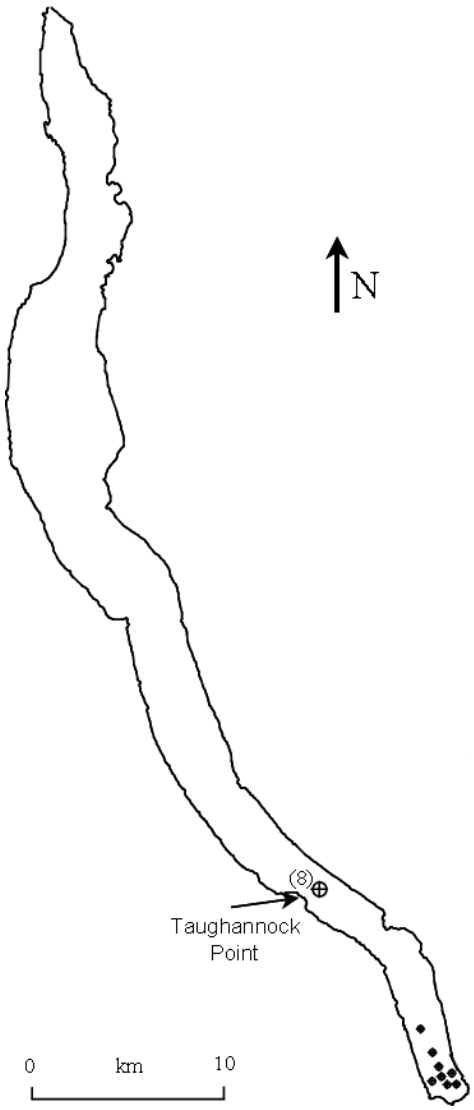

Figure 2.1: Locations of sampling sites, in the context of the entire Cayuga Lake basin

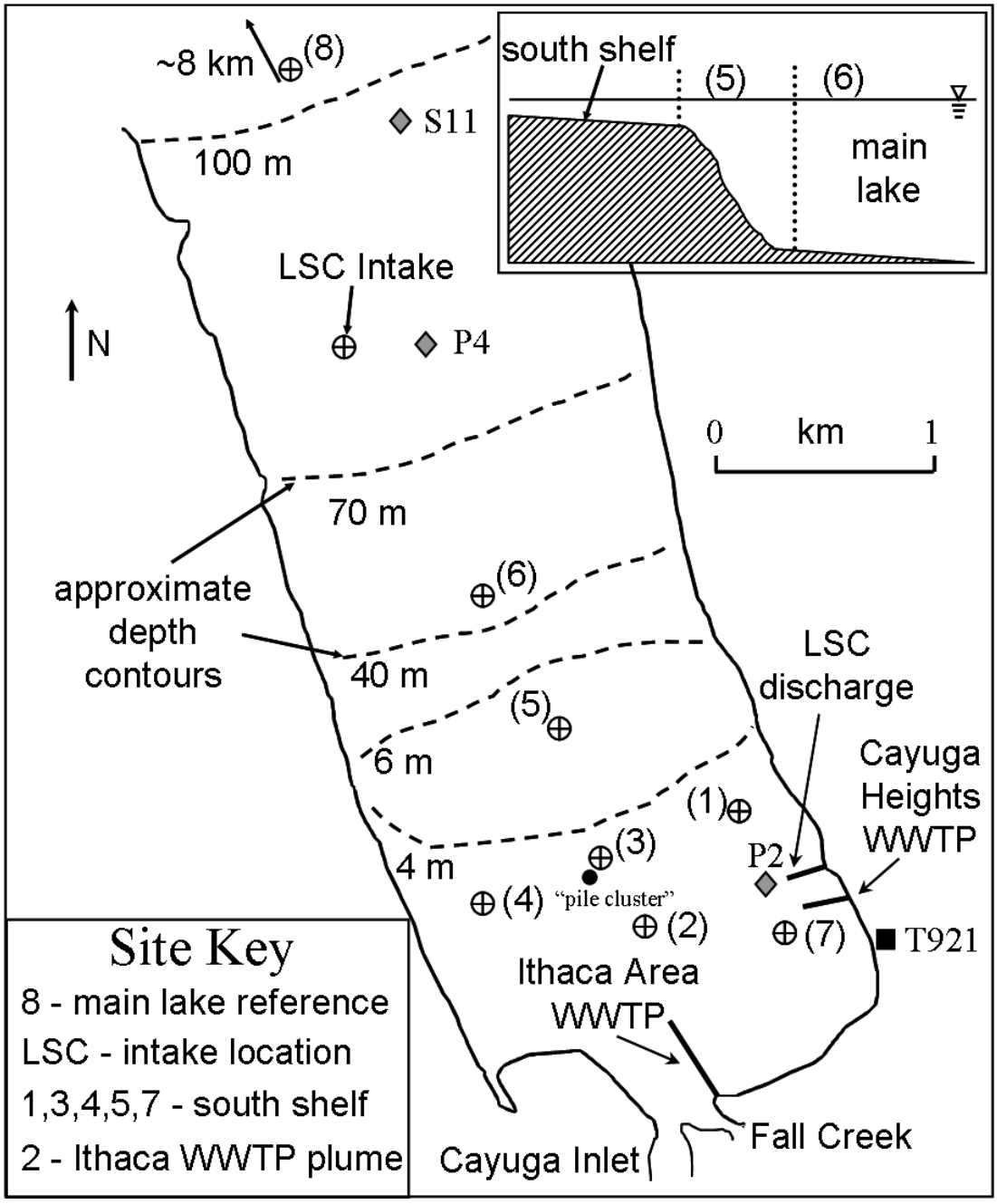

Figure 2.2: Map of sampling sites on the south shelf

Table 2.1: Locations of sampling sites

Site No.	Latitude	Longitude	Lake Depth (*m*)	Location description
1	N 42°28.3′	W 76°30.5′	5	East shelf
2	28.0′	30.8′	3	South shelf
3	28.2′	30.9′	4	Center of shelf
4	28.2′	31.4′	4	West shelf
5	28.5′	31.1′	6	North shelf
6	28.8′	31.3′	40	Shelf break
7	28.0′	30.3′	3.5	Southeast shelf
8	33.0′	35.0′	110	Taughannock Pt.
LSC Intake	29.4′	31.8′	78	Glenwood Pt.

2.2.1 Water quality parameters measured

The following is a brief introduction of the water quality parameters that were measured in the monitoring program. Further details on the significance of these metrics in Cayuga Lake can be found in the LSC monitoring annual reports (UFI, 2000*a*,*b*, 2001, 2002, 2003, 2004, 2005, 2006, 2007; Cornell University, 2008, 2009).

Total Phosphorus (TP) Phosphorus is generally considered to be the limiting nutrient in Cayuga Lake and in most lakes in the region (e.g., Oglesby & Schaffner, 1978; Oglesby, 1978; GFLRPC, 2000; Callinan, 2001). Total phosphorus includes particulate and dissolved matter. This is important since much of the particulate phosphorus (PP) entering the lake is bound

to sediments (Effler *et al.*, 2002), and will eventually settle to the bottom of the lake, effectively leaving the system (becoming unavailable for phytoplankton uptake). The major source of particulate phosphorus loading to the shelf (and the entire lake) is the tributaries (Haith *et al.*, 2009). Effler *et al.* (2002) showed that inorganic tripton (rather than phytoplankton) is primarily responsible for the higher TP measured on the shelf relative to the main body of the lake.

Soluble Reactive Phosphorus (SRP) SRP is a fraction of dissolved phosphorus considered to be most available for biological uptake. Thus low levels of SRP could indicate either low levels of loading, or high levels of biological activity.

Turbidity (Tn or Tn_L) Turbidity is a measure of the amount of blocking of light that exists in water, i.e., it is an inverse measure of water clarity. Turbidity is regulated by scattering particles in the water column including phytoplankton, clay, silt and other organic and inorganic matter. The main source of turbidity on the shelf is inorganic tripton (Effler *et al.*, 2002). High turbidity values have been observed on the shelf following high surface runoff events (UFI, 2000*a*,*b*, 2001, 2002, 2003, 2004, 2005, 2006, 2007; Cornell University, 2008, 2009).

Chlorophyll-*a* (Chl) Chlorophyll is a principal photosynthetic pigment common to all phytoplankton and is widely used as a surrogate measure of trophic state.

2.2.2 Comments on individual sites

Site 2 is located adjacent to the outflow of the IAWWTF. Water samples collected at this site are considered to be strongly influenced by this outfall and not representative of water on the shelf in this region (UFI, 2000*a*,*b*, 2001, 2002, 2003, 2004, 2005, 2006, 2007; Cornell University, 2008, 2009). Beginning in 2005 the IAWWTF upgraded its phosphorus treatment capabilities (added a tertiary treatment phase). This has significantly reduced the nutrient load in the effluent. As a result water samples collected at site 2 since 2005 have been closer in the measured parameters to those collected at nearby sites although often still somewhat elevated. Site 2 has largely been excluded from the discussion in this thesis.

Site 7 is located close to the shore in the southeastern corner of the shelf. It is proximate to the outfalls of CHWWTP and the LSC facility as well as to inflows from small tributaries draining nearby suburban neighborhoods. Total phosphorus (TP) has been observed to be elevated locally in the vicinity of this site relative to the rest of the shelf (UFI, 2000*a*,*b*, 2001, 2002, 2003, 2004, 2005, 2006, 2007; Cornell University, 2008, 2009).

Site 8 is located near the centerline of the lake approximately 10 *km* north of the shelf off of Taughannock Pt. It was selected to represent a reference of conditions in the main lake, well away from the southern shelf.

2.3 Brief overview of statistical methods used

This section provides a brief overview of the various statistical methods of hypothesis testing used in the thesis and defines nomenclature used throughout the thesis. All statistical analysis was performed using R (R Development Core Team, 2009).

paired t-test Student's t-test of the null hypothesis that the differences between pairs in two sets of data are a random sample from a normal distribution with mean zero, against the alternative hypothesis that the mean is not zero . For example, comparing the differences between sets of observations made at two different locations but at the same times to determine whether it is fair to say there is a difference in water quality metrics between the two locations.

two-sample t-test Welch's two sample t-test of the null hypothesis that two samples are drawn from normal distributions with equal means and possibly unequal variances. For example, comparing sets of observations at two different sites in the lake taken at different times to determine whether it is fair to say there is a difference in water quality metrics between the two locations.

signed rank test Wilcoxon signed rank test. A nonparametric (distribution free), paired test of the null hypothesis that the differences between pairs of observations come from a continuous, symmetric distribution with zero median, against the alternative that the distribution does not have zero median.

rank sum test Wilcoxon rank sum test (equivalent to a Mann-Whitney U-test).

Nonparametric (distribution free) test of the null hypothesis that data in two sets are independent samples from identical continuous distributions with equal medians, against the alternative that they do not have equal medians.

The paired and two-sample t-tests assume that the data being analyzed are normally distributed. This assumption is not always valid for the data discussed in this thesis. The data in question are bounded by zero on one side but contain numerous observations of much larger magnitude than the mean (i.e., they are right skewed). The nonparametric tests do not make such assumptions about the distribution of the data. These tests calculate the test statistic on the ranking of the underlying data, and are therefore less sensitive to skewness and outlying extreme values in the data.

However, under the central limit theorem samples of large size can be treated approximately as being normally distributed. Furthermore, while two sets of observations might not be normally distributed, the differences between observations in those two sets often are. In this thesis, whenever these tests were utilized, both a parametric and the corresponding nonparametric tests were performed and the results of each is presented. In most cases the two methods agreed quite well.

2.4 Removal of outlying chlorophyll-*a* samples

UFI (2008) performed an outlier analysis on chlorophyll-*a* data collected prior to 2006. Observations determined to be statistical outliers were compared to in-situ chlorophyll-*a* measurements, and those that did not fall inside of the 99%

prediction interval from in-situ fluorometry were considered to be spurious data points and were discarded. Since most of the observations that were determined to be outliers were collected at times and sites at which dense macrophyte beds generally exist, the authors hypothesized that the extreme values were the result of small pieces of macrophytes contaminating the samples.

A total of seven chlorophyll-*a* observations were determined to be spurious outliers. Six of the seven observations were of chlorophyll-*a* concentrations greater[3] than 20 $\mu g/L$. The entire pre-2006 record contains a total of seven chlorophyll-*a* observations greater than 20 $\mu g/L$, six of which were identified as spurious outliers. The seventh was measured at site 2, which is adjacent to the outfall of the IAWWTF and largely excluded from the discussion in this thesis due to the effects of the outfall. The outlier analysis was only performed on the data collected prior to 2006 and no similar analysis exists for subsequent years. In order to extend the treatment of outliers to the data collected in 2006 and later, all chlorophyll-*a* values greater than 20 $\mu g/L$ were treated as suspect and dropped from the record for the purpose of this thesis. A total of thirteen values were discarded, eight from the years 1998-2005 and five from the years 2006-2008.

[3]The 06/15/00 site 1 value is reported in UFI (2008) as 17.1 $\mu g/L$. This is a mean of 3 replicates collected at that site. The median value of the replicates is 20.6 $\mu g/L$. Median values of replicate samples are used throughout the thesis.

CHAPTER 3

CHARACTERIZATION OF CAYUGA LAKE AND ITS SOUTH SHELF

The purpose of this characterization is to provide context for this thesis as well as to create an easy reference for future work.

3.1 Physical Characterization of Cayuga Lake

The dimensions listed here are as presented by Oglesby (1978), largely based on the original measurements made by Birge & Juday (1914).

Location (center) 42°41′30″ N, 76°41′20″ W

Surface elevation 116.4 m above sea level

Catchment area 2033 km^2

Surface area 172.1 km^2

Length 61.4 km

Maximum width 5.6 km

Average width 2.8 km

Shore length 153.4 km

Maximum depth 132.6 m

Mean depth 54.5 m

Volume $9,379.4 \times 10^6\, m^3$, calculated for lake elevation of 116 m, 50% of lake volume is above 40 m depth and 50% below

Southern shelf boundaries The southern shelf is defined for the purposes of this thesis as the portion of the southern basin south of the 6 m isobath

Southern shelf volume $8 \cdot 10^6\ m^3$ (up to the 6 *m* isobath, Effler *et al.*, Submitted December 2009)

Shelf break defined loosely as the area immediately north of the southern shelf in which the bottom depth steeply increases from 6 *m* or less to several tens of meters of depth

3.2 Nutrient loading sources

Two main tributaries enter Cayuga Lake near the southern end of the lake, namely Fall Creek and the Cayuga Inlet. Six Mile Creek and Cascadilla Creek flow into the Cayuga Inlet just upstream of entering the lake. Together these streams account for approximately 40% of the total inflow to the lake (UFI, 2000*a*; GFLRPC, 2000) and account for a significant portion of the total nutrient loads to the lake - Haith *et al.* (2009) estimated that 67.5% of all phosphorus entering the lake does so through surface runoff, mainly from agricultural lands, with the rest divided between groundwater discharge (23%) wastewater treatment systems (7.2%) and septic systems (2.3%).

Other loading sources to the southern shelf include discharge from IAWWTF and CHWWTP and flow from several small streams. The wastewater treatment plant effluents are characterized by high phosphorus and very low turbidity, e.g., typically <0.1 NTU for IAWWTF (J. Lozano, personal communication). Additionally, Cornell's LSC facility discharges on to the shelf. The LSC discharge consists of hypolimnetic water that has been circulated through heat exchangers. The LSC facility does not introduce any new water or loading to the lake, but transports water internally from the deeper part of the lake onto the shelf.

Estimates of monthly phosphorus loads from the main sources are presented in table 3.1 for 1998 - 2005 and table 3.2 for 2006 - 2008. The estimates for the tributaries are taken from the draft Environmental Impact Statement for the LSC facility (Stearns & Wheler, 1997). The authors of that document attempted to estimate the total soluble phosphorus (TSP) for an average hydraulic year in Fall Creek and the Cayuga Inlet. The values presented are therefore a general estimate and do not take in to account interannual variations in precipitation and surface runoff or land use. The loading estimates for IAWWTF, CHWWTP and LSC are mean monthly TP loadings calculated from the respective facilities' permit reporting (further details are available in UFI, 2000*a*,*b*, 2001, 2002, 2003, 2004, 2005, 2006, 2007; Cornell University, 2008, 2009).

Other possible sources of nutrient loading include groundwater flow, leakage from failed septic systems on lakefront properties, discharge from minor tributaries draining suburban areas and excretion and defecation of transient flocks of geese and other birds near the water or ice off of Stewart Park (e.g., Kitchell *et al.*, 1999).

It has been shown by Effler *et al.* (2002) that the main component of turbidity in southern Cayuga Lake is mineral (tripton) and not biological. The main source of turbidity on the shelf is suspended sediment from the tributaries. Other possible sources include resuspension of sediment by wave action or other water movements. Therefore turbidity can perhaps be used as a marker for inflow from the tributaries, whereas high phosphorus content coupled with low turbidity is indicative of waters discharged from the point sources or, for more moderate phosphorus increases coupled with low turbidity, upwelled from the hypolimnion. However, caution must be used as neither tur-

bidity nor phosphorus can truly be considered to be passive tracers, since other sources for both exist.

Table 3.1: Estimates of monthly loads of phosphorus to the shelf in kg/day from various loading sources, 1998-2005

	IAWWTF	**CHWWTP**	**Tributaries**	**LSC**
May	15.0	4.4	29.0	1.0
June	8.9	5.2	15.8	1.3
July	12.6	4.2	8.8	1.4
August	15.1	3.8	6.0	1.4
September	19.4	4.7	7.5	1.2
October	13.3	5.2	13.1	0.7

Table 3.2: Estimates of monthly loads of phosphorus to the shelf in kg/day from various loading sources, 2006-2008

	IAWWTF	**CHWWTP**	**Tributaries**	**LSC**
May	5.0	2.8	29.0	1.1
June	4.3	2.9	15.8	1.8
July	4.6	2.7	8.8	2.0
August	4.6	3.0	6.0	1.8
September	4.2	2.6	7.5	1.3
October	2.8	2.7	13.1	1.1

There are two main causes for the differences in loading levels before and after 2005/2006. TP loading from the two wastewater treatment plants was reduced due to upgrades in the plants' treatment systems, most importantly the installation of tertiary treatment at IAWWTF. The increase in loading from LSC

is due to increased TP in the lake's hypolimnion that occurred over 2004 - 2005 (UFI, 2006, 2007; Cornell University, 2008, 2009) for reasons that are not well understood. From table 3.1 and table 3.2 it is apparent the tributaries are overall the main source of phosphorus loading to the shelf (which is consistent with the modeling results of Haith *et al.*, 2009). It can be expected that loading from the tributaries will be even more significant relative to the other sources during the months not shown in these tables (data were not available) since surface runoff is even higher during those months (section 4.1). However, during July - October in years prior to 2006 loading from the wastewater treatment plants, especially IAWWTF, was significantly higher than loading from the tributaries. Following the upgrades to these facilities the summed phosphorus loading from the two wastewater treatment plants has been on the order of the loading from the tributaries during low surface runoff months, and much lower than the loading from the tributaries when surface flow rates are high (table 3.2).

The volume of the shelf, from the southern shoreline to the 6 m depth contour (just north of site 5) has been estimated by UFI to be approximately $8 \cdot 10^6 m^3$ (Effler *et al.*, Submitted December 2009). Using this volume and some typical flow and loading rates from the various inputs to the shelf, the following calculations were performed to give rough estimates of the relative importance of the different sources (summarized in table 3.3):

Table 3.3: Summary of flow and TP loads entering shelf. The term "flushing time" is used loosely here since the flushing time of the shelf is not controlled by any single parameter. "Flushing times" were calculated by dividing the shelf's volume by the flow rate of the respective discharges and do not make any attempt to include the increased water mass influx from barotropic and baroclinic exchange with the main lake (e.g., Rueda & Cowen, 2005*b*).

		Discharge $[m^3/s]$	**"Flushing time"** $[days]$	**Mass loading** $[kg/day]$	**Volumetric loading** $[\mu g/L]$
Tributaries	*summer base flow*	1.55	60		
	moderate flow event	42	2.2		
	major flow event	105	0.9		
IAWWTF	*median 1998-2005*	0.42	220	11.4	1.4
	median 2006-2008			3.6	0.5
	median 1998-2008			9.2	1.2
CHWWTP	*typical summer flow*	0.05	1,852	3	0.375
LSC	*maximum permitted flow*	2	46		

Total volume of Cayuga Lake:

$9.4 \cdot 10^9\, m^3$ (Birge & Juday, 1914)

Southern shelf volume:

$8 \cdot 10^6\, m^3$ (up to the 6 m depth contour, Effler *et al.*, Submitted December 2009)

Southern shelf proportion of entire lake's volume:

$$\frac{8 \cdot 10^6\, m^3}{9.4 \cdot 10^9\, m^3} = 8.5 \cdot 10^{-4} = 0.085\%$$

TP mass corresponding to a $1 \mu g/L$ increase on shelf:

$$1 \tfrac{\mu g}{L} \times 8 \cdot 10^6\, m^3 = 8\, kg$$

TP mass corresponding to a $1 \mu g/L$ increase in entire lake:

$$1 \tfrac{\mu g}{L} \times 9.4 \cdot 10^9 m^3 = 9,400\, kg = 9.4\, metric\ tons$$

Summer tributary flow:

$1.6\, m^3/s$ total tributary flow (calculated using $0.85\, m^3/s$ typical baseline August Fall Creek flow rate from USGS stream gage data and assuming that Cayuga Inlet flow rate is 85% of Fall Creek flow; Effler *et al.*, Submitted December 2009).

Time required to fill shelf volume at this flow rate:

$$\frac{8 \cdot 10^6\, m^3}{1.55\, m^3/s} \approx 60\, days$$

Moderate storm tributary flow:

$42\, m^3/s$ total tributary flow (calculated using $22.7\, m^3/s$ Fall creek flow rate and assuming that Cayuga Inlet flow rate is 85% of Fall Creek flow).

Time required to fill shelf volume at this flow rate:

$$\frac{8 \cdot 10^6 m^3}{42\, m^3/s} \approx 2.2\, days$$

Major storm tributary flow:

105 m^3/s total tributary flow (calculated using 56.6 m^3/s Fall creek flow rate and assuming the Cayuga Inlet flow rate is 85% of Fall Creek flow).

Time required to fill shelf volume at this flow rate:

$$\frac{8 \cdot 10^6 m^3}{105\, m^3/s} \approx 0.9\, days$$

LSC flow rate:

2 m^3/s at maximum permitted flow rate (actual flow rate is usually well below this value).

Time required to fill shelf volume at this flow rate:

$$\frac{8 \cdot 10^6 m^3}{2\, m^3/s} \approx 46\, days$$

IAWWTF flow rate:

0.42 m^3/s high range of flow (but not maximum; from discharge permit reporting)

Time required to fill shelf volume at this flow rate:

$$\frac{8 \cdot 10^6 m^3}{0.42\, m^3/s} \approx 220\, days$$

IAWWTF TP loading (median daily loading):

1998-2005: 11.4 kg/day

2006-2008: 3.6 kg/day

1998-2008: 9.2 kg/day

(source: discharge permit reporting)

Median daily TP load from IAWWTF / shelf volume:

1998-2005: $\frac{11.4kg}{8 \cdot 10^6 m^3} = 1.4\,\mu g/L$

2006-2008: $\frac{3.6kg}{8 \cdot 10^6 m^3} = 0.5\,\mu g/L$

1998-2008: $\frac{9.2kg}{8 \cdot 10^6 m^3} = 1.2\,\mu g/L$

CHWWTP flow rate:

$0.05\,m^3/s$ typical summer flow (from discharge permit reporting).

Time required to fill shelf volume at this flow rate:

$\frac{8 \cdot 10^6 m^3}{0.05\,m^3/s} \approx 5\,years$

CHWWTP TP loading:

$3\,kg/day$ (conservative summer month estimate from discharge permit reporting).

CHWWTP TP loading / shelf volume:

$\frac{3\,kg}{8 \cdot 10^6 m^3} = 0.375\,\mu g/L$

CHAPTER 4

CHARACTERIZATION OF PHYSICAL FORCING MECHANISMS

4.1 Surface runoff

Surface runoff is expected to be the dominant source of nutrient loading to the southern shelf (e.g., Haith *et al.*, 2009; UFI, 2000*a*; Cornell University, 2009). The relative fraction of loading from surface runoff to the lake has increased significantly over the period 1998 - 2008 due to improvements in treatment processes at the waste water treatment facilities that reduced loading from these sources (UFI, 2007; Cornell University, 2008, 2009). Flow rates in Fall Creek have been recorded by the USGS continuously since 1925. This is the primary source of data on surface flows used in this thesis and is used to estimate the relative total surface flow entering the shelf. Flow rates in the Cayuga Inlet have been estimated to be approximately 85% of the flow rate in Fall Creek (Effler *et al.*, Submitted December 2009). Strong seasonal variations in flow rate exist with the peak flow rate occurring in early April as a result of snow melt, and very low flow rates during the summer months. Daily statistics of flow are presented in figure 4.1. Tributary flow during the study period varied significantly - total flow during the sampling season (April - October) in 1999 was the third lowest of the 84 years in the interval 1925 - 2008 while in 2004 the total flow during the sampling season was the second highest of that 84 year interval (figure 4.2).

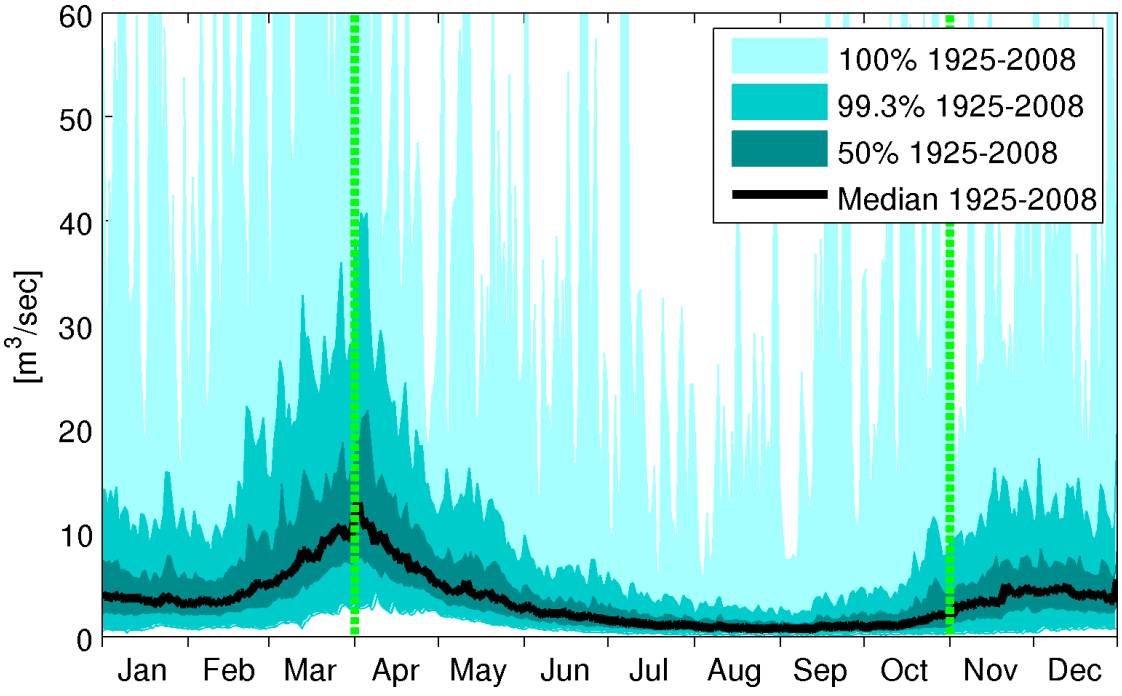

Figure 4.1: Statistics of flow in Fall Creek

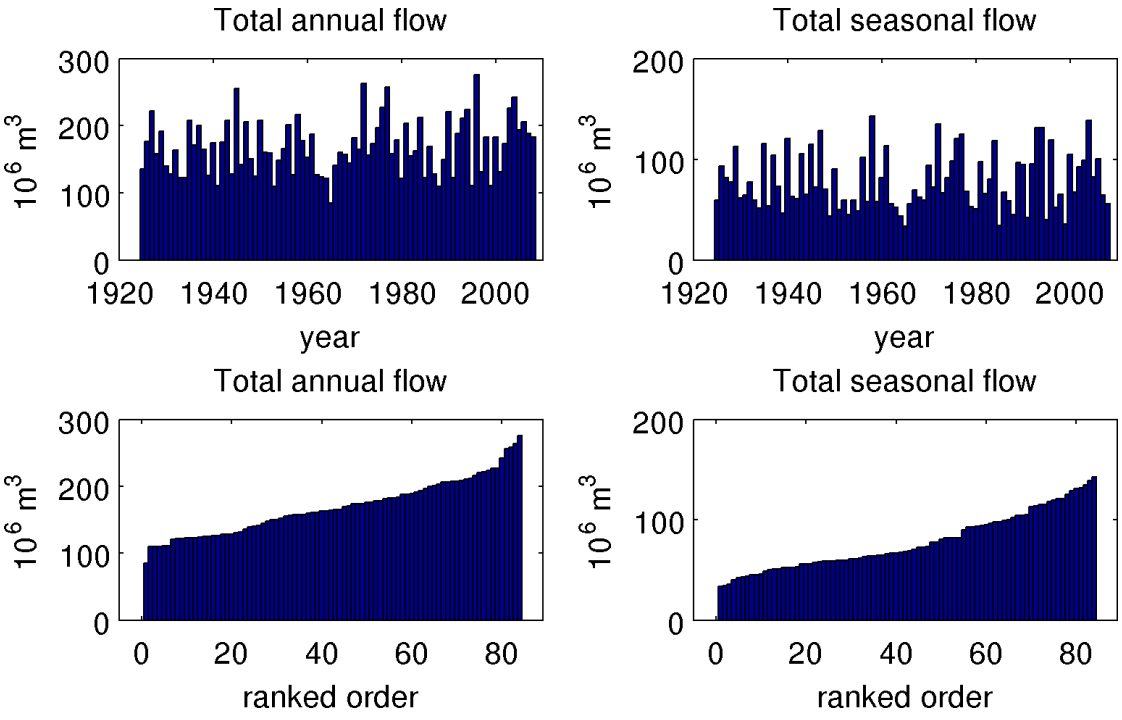

Figure 4.2: Annual and seasonal (April-October) flow in Fall Creek

4.2 Typical annual stratification cycle

Water column temperature - depth profiles collected by the RUSS during the years 2001 - 2005 were analyzed to calculate the average thermal profile of the water column. Average temperatures were calculated in 1 *m* steps between the depths of 3 and 25 *m* within a 3 *m* depth window and a 21 day time window (e.g., to calculate the mean temperature at a depth of 18 meters on October 15 all available data falling between 16.5 *m* and 19.5 *m* collected between October 4 and October 25 of any year such data were available were averaged to a single value). Water column data from the RUSS are available intermittently (both in time and in vertical position). The depth and time windows used here were selected to allow reasonably high temporal and spatial resolution while still ensuring that enough measurements were available for averaging within each window to create a smooth profile. The averaging time period is long enough to filter out the effects of internal waves and disturbances of the mean stratification profile. Average profiles were calculated for each day of the year. Thermocline depths used in this thesis are based on the depth of the largest temperature gradient (between two adjacent 1 *m* depth bins). Hypolimnion temperatures used are the mean temperature measured below the thermocline depth. Average epilimnion temperatures were calculated as the mean temperature above the thermocline (although for most calculations in the thesis the temperature record at the piling thermistors was used for the eplilimnion temperature). The vertical temperature profiles collected by the RUSS are limited to a maximum depth of approximately 25 *m* due to the lake bottom depth at the location the RUSS is moored. In a typical year the thermocline approaches this depth during October. Therefore the thermocline depths calculated after this month are

not as accurate as those calculated for preceding months (however by this point in the season stratification has become weak so determining the depth of the thermocline becomes less important for the analysis performed in the thesis). Monthly profiles are presented in figure 4.4 and figure 4.3 for illustration.

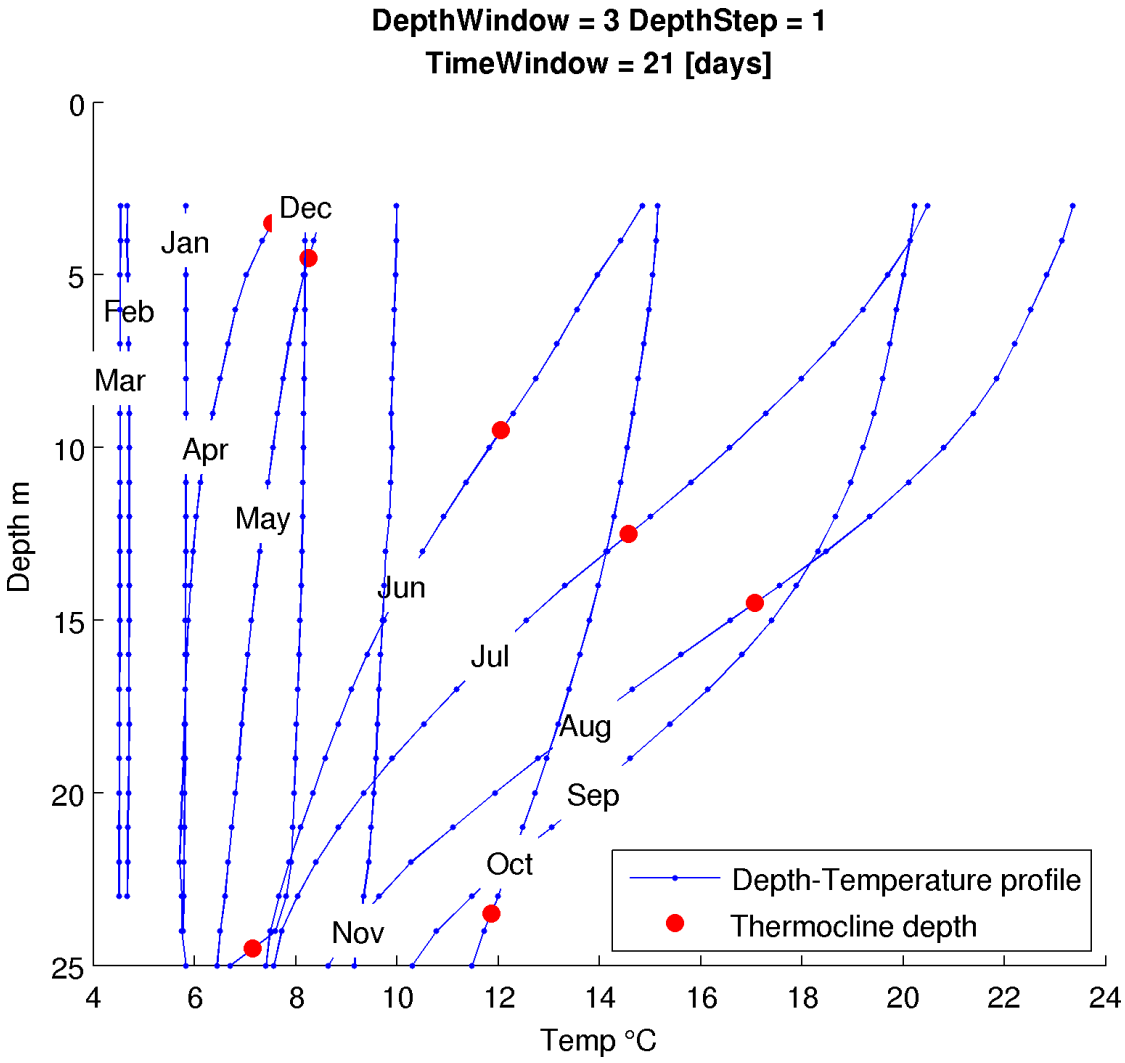

Figure 4.3: Seasonal evolution of temperature-depth profile at the RUSS

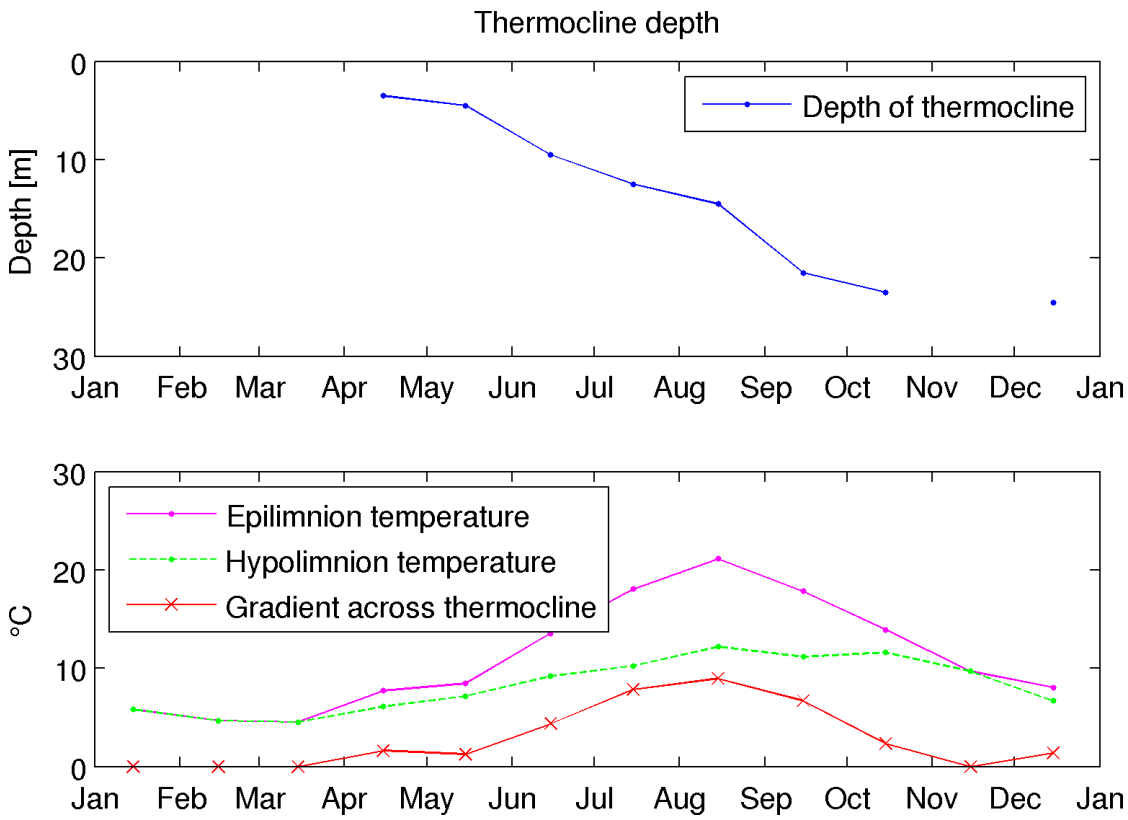

Figure 4.4: Seasonal evolution of thermal stratification

4.3 The Wedderburn number

The Wedderburn number (*Wb*, equation 4.1) represents the balance between the gravitational force which preserves the stable stratification of the body of water, and the wind stress acting on the surface of the water which can disrupt this balance. *Wb* is essentially the surface Richardson number multiplied by the aspect ratio of the upper layer of the lake (e.g., Imberger & Hamblin, 1982; Imberger, 1985; Monismith, 1985).

$$Wb = \frac{g' h_1^2}{u_\star^2 L} \tag{4.1}$$

where:

$g' = g\frac{\rho_2 - \rho_1}{\rho_2}$ gravitational acceleration modified by the relative density of the stratified layers

ρ_1 density of water in the epilimnion, calculated here from temperature measured at the piling cluster using empirical formula from Maidment, 1993

ρ_2 density of water in the hypolimnion, calculated here from average temperature measured by the RUSS using empirical formula from Maidment, 1993

h_1 depth (thickness) of the epilimnion, calculated here as the point of sharpest gradient in the averaged water column temperature profile measured by the RUSS

$u_\star$ friction velocity $u_\star = \left(\frac{\rho_a}{\rho_1}\right)^{1/2} U_{10} \cdot C_{10}^{1/2}$ where ρ_a is the density of air and C_{10} is a drag coefficient found using the method described in Amorocho & Devries, 1980; U_{10} is the wind velocity at an elevation of 10 m above the ground, measured at the Game Farm Road (GFR) weather station

L length of Cayuga Lake along its long axis, at the depth of the thermocline

4.3.1 Calculating the Wedderburn number from observational data

Using the average temperature - depth profiles calculated from historic RUSS records (described in section 4.2), the hypolimnion density and the average epilimnion thickness were calculated (with 1 day temporal resolution). The temperature record measured at the piling cluster was used to represent the epilimnion temperature (resolution of 1 hour or less April - October, 1 day or less during the other months of the year). The component of the wind along the main axis of the lake, approximated at 340° relative to true north, was calculated from GFR data and used to find $u_\star^2$ (While the RUSS measures the wind directly above the surface of the lake these data were not available for the entire study period. Therefore wind data from the nearby GFR station were used throughout for consistency). $u_\star^2$ was calculated according to the method of Amorocho & Devries (1980) using a drag coefficient C_{10} calculated as a function of U_{10}. Wb was calculated from these values using an approximate length along the main axis of the lake at the depth of the thermocline of $L = 48\,km$. This length is an approximation of the length of the lake without the northern (~10 km) and southern (~2 km) shelves.

The uninodal seiche period (T) is the period of the longest internal oscillation of the lake - it is the length of time it takes an internal seiche to go through an entire cycle from maximum upwards tilt on one end of the lake to maximum downwards tilt, and back again. Hence one quarter of this period is the time lapse between horizontal and maximum tilt. T is a function of the lake's geometry and stratification (depth of and difference in density across the internal interface). If a steady wind is applied to an undisturbed, stably stratified lake

(i.e., in which the thermocline is horizontal and stationary), the free surface and the thermocline will both begin to tilt. The period of time a steady wind must blow before the entire length of the lake becomes tilted is equal to one-quarter of the uninodal seiche period, $T/4$ (Spigel & Imberger, 1980; Boegman *et al.*, 2005). This $T/4$ response time of the lake effectively acts as a filter on the wind signal - higher frequency wind events, with durations less than $T/4$, will have less of an effect on the internal dynamics of the lake than events lasting $T/4$ or longer, even if the shorter events are of greater magnitude.

The data were therefore smoothed by averaging the wind over the period $T/4$ (14.4 hours), i.e., Wb at each moment in time was calculated from the averaged component of the wind along the lake's main axis during the preceding period $T/4$. This period $T = 2.4$ days is the internal seiche period calculated and verified from observations by Henson (1959) and calculated by Effler *et al.* (Submitted December 2009). Since the time between measurements is not the same in each of the records used, the records with larger intervals between measurements were linearly interpolated to match the timestamps of the higher frequency records.

When $|Wb| \sim 1$ the force of the wind is sufficient to tilt the thermocline to such an extent that it will approach the free surface (e.g., Imberger & Hamblin, 1982; figure 4.7). For this to happen in practice $|Wb|$ must remain near or less than 1 for longer than one-quarter of the lake's uninodal horizontal seiche period ($T/4$).

When $|Wb| \gg 1$ the wind is not strong enough to disturb the stable density stratification of the lake. In the analysis performed for this thesis a cutoff value of $|Wb| > 15$ was chosen (based on an empirical examination of the Wb and thermal record) as the value above which the effect of the wind is neglected in

the analysis. Essentially any value of $|Wb| > 15$ can be treated as infinite (e.g., there is no new insight to be gained from knowing that $Wb \sim 10^3$ vs. $Wb \sim 10^2$, both of these would just mean that the stratification is such that the wind stress is negligible). When the lake is not stratified $Wb \approx 0$ since $\rho_1 \approx \rho_2$ and hence $g' \rightarrow 0$ and $h_1 \rightarrow 0$. In the analysis presented here values $|Wb| < 0.05$ were treated as indicating the lake not being stratified.

Even when $|Wb| > 1$ but is approaching unity the thermocline will be tilted significantly. The sign convention used in this thesis is that $Wb < 0$ indicates winds out of the south, that will tilt the thermocline up at the south and down at the north end of the lake, $Wb > 0$ indicate winds out of the north and the opposite tilt of the thermocline. If the thermocline tilts sufficiently that its depth is near to or shallower than the depth on the shelf the result will be reduced exchange between the shelf and the off-shelf epilimnion, and increased exchange between the hypolimnion and the shelf's waters.

Once the wind relaxes, or shifts significantly in direction, the disturbed layers of the lake will begin to rock, or seiche, back and forth until the motions of the water are dampened by friction at the bottom, or, as is generally the case in practice, until the next wind event begins and creates a new disturbance of the stratification field.

The temporal resolution of Wb is that of the wind data from GFR, i.e., hourly. Wb at each point in time is calculated using wind and epilimnion temperature measurements taken at or around that point in time. However the accuracy of the result is reduced by the fact that the stratification data (depth of thermocline and temperature of hypolimnion) used are a daily average taken across multiple years and do not take into account either interannual or localized (in time and

space) variations in the actual stratification. Furthermore, the stratification data were measured at a single point (the RUSS) near the southern shelf break of the lake and the wind data were measured at a single location approximately 5 miles east of the southern end of the lake. However, despite these limitations comparison by eye of the calculated Wb numbers and the actual thermal record measured at the piling cluster shows very reasonable results (e.g., figure 5.22, figure 5.23, figure 5.25).

4.3.2 Histograms of Wedderburn number in Cayuga Lake

Using the method described in section 4.3.1 a time history of the Wedderburn number in Cayuga Lake was calculated for the period 1998 - 2008. Histograms of the results for the entire 1998 - 2008 period broken down by month are presented in figure 4.5. From equation 4.1 it is clear that when the lake is not stratified we will have $Wb \approx 0$ since $\rho_1 \approx \rho_2$ and hence $g' \to 0$ and $h_1 \to 0$. This explains the narrow distributions of Wb observed in March - May and to a lesser extent June and November, months during which the lake is not usually stratified or stratification is weak. Conversely, the wider distributions observed in July - October indicate that the effects of upwelling events should be more significant. Note that during these months most of the mass of the distribution is in the tails, i.e., $|Wb| > 20$. This means that most of the time the wind is not strong enough to perturb the stratification of the lake, or does not blow for a long enough time to have a significant effect (recall that Wb represents a balance between the wind and the lake's stratification).

The monthly histograms of Wb also describe the typical seasonal stratifica-

tion cycle. A narrow distribution around zero indicates that the lake is not generally stratified. This is the case in March - June. A wide distribution with a large proportion of the histogram's mass in the tails indicates strong stratification, as is the case in August - October. The fact that during most months the distribution has more mass on the negative side indicates that stronger, sustained winds tend to blow out of the south more than the north in this region, resulting in an upwards tilt of the thermocline near the shelf.

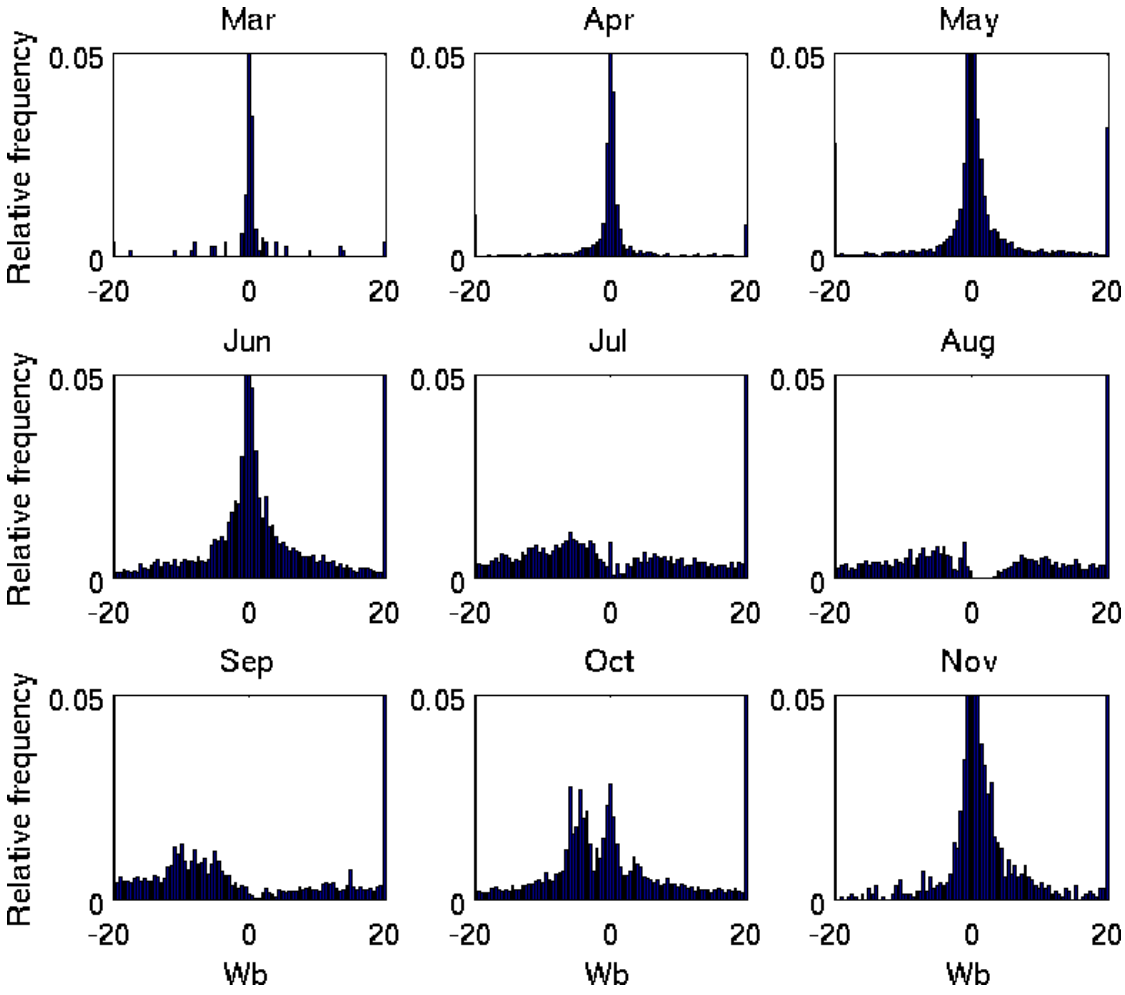

Figure 4.5: Monthly histograms of *Wb* for the period 1998 - 2008. Negative values of *Wb* indicate winds from the south which can lead to an upwards tilt of the thermocline near the southern shelf.

4.4 Overview of internal physical processes

Large scale motions of the water mass on the southern shelf are caused by two main forces - surface flow entering the lake from tributaries, and the wind. The wind generates surface waves and currents as well as internal waves. These processes, and their interactions, control the residence time of water on the southern shelf and the exchange between the shelf and the pelagic region of the lake.

When the wind is stable for a period of time the stress it applies over the surface of the lake causes downwind motions of water near the surface. This causes water to pile up near the downwind boundary of the lake, creating a tilt of the air-water interface such that the surface of the lake will become lower on the upwind end ("set down" of the surface) and higher on the downwind end of the lake ("set up" of the surface). Theoretically, the elevation gradient of the surface will continue to increase until it is large enough that the difference in potential gravitational energy it creates is large enough to balance the total force applied by the shear stress of the wind on the lake's surface (however, in reality a steady state is never reached). The (theoretical) time the wind must blow until reaching a steady state is a function of the geometry of the lake. The gradient of surface elevation is a function of the wind's magnitude. This gradient in surface elevation is not large - on the order of 1 cm difference in elevation over a length of 60 km in Cayuga Lake. However, the gradient in surface elevation has important effects on the internal dynamics of the lake. Since the wind causes advection of surface water in the downwind direction, conservation of mass requires that there be other motions of water in the upwind direction. The result is a current moving in the direction of the wind near the surface, and a return current in the opposite direction at the bottom of the epilimnion. This increases

internal mixing and transport within the lake.

In a stratified lake the downwind set up (increased elevation) of the surface will have another important effect. The increased elevation of the air-water interface at the downwind end of the lake, and the reduced elevation at the upwind end means that a different pressure exists at the same depth on either end of the lake (for a depth measured relative to the undisturbed surface). This pressure gradient acts on the thermocline and causes it to tilt as well, but in the opposite direction of the surface tilt. While the change in elevation of the air-water interface is of small magnitude, the corresponding change in elevation of the interface at the thermocline between higher and lower density layers will be much larger - on the order of tens of meters in Cayuga Lake. This is due to the fact that the density gradient across the air-water interface is orders of magnitude larger than the difference in density across the thermocline (e.g., density of water at $10°C$: $999.7\,kg/m^3$, density of water at $20°C$: $998.2\,kg/m^3$, density of air at $15°C$: $1.23\,kg/m^3$). The vertical movement of the free surface displaces air with water that has a much larger density: $\frac{\rho_{air}}{\rho_{surface\,water}} \approx 0.001$. Vertical movement of the thermocline causes a displacement of warmer water with colder, denser water. However, the ratio of densities here is much closer to unity: $\frac{\rho_{epilimnetic\,water}}{\rho_{hypolimnetic\,water}} \approx 0.998$. Therefore larger displacements are required to preserve the total potential energy of the water column - the density of water integrated over depth. (In other words, at the surface something heavy is moved a short distance, at the thermocline something light is moved a long distance - both require the same amount of work.)

Upwelling events on the shelf occur when the thermocline tilts to such an extent that its depth becomes less than that of the lake bottom on the shallow

shelf. This happens when the wind blows steadily from the south for a sufficiently long period of time, and results in the advection of water from the hypolimnion on to the shelf.

Conditions leading to upwelling events can be predicted by the Wedderburn (Wb) number (e.g., Imberger & Hamblin, 1982; Imberger, 1985; Monismith, 1985). Cayuga Lake's geometry lends itself to strong forcing of this type. The length of the lake's main axis, the fact that the main axis is well aligned with the prevailing winds in the area (figure 4.6), and the surrounding topography of steep hills that further channel the wind along the lake's axis create favorable conditions for the transfer of the wind's energy to the surface waters. A review of this and other physical processes in lakes and reservoirs is available in Imberger & Hamblin, 1982.

Different states of the longitudinal tilt of the thermocline in Cayuga Lake, the conditions that create them, and the interaction with the south shelf are illustrated in figure 4.7 and described in section 4.4.1, along with their potential impact on mixing and transport dynamics on the southern shelf.

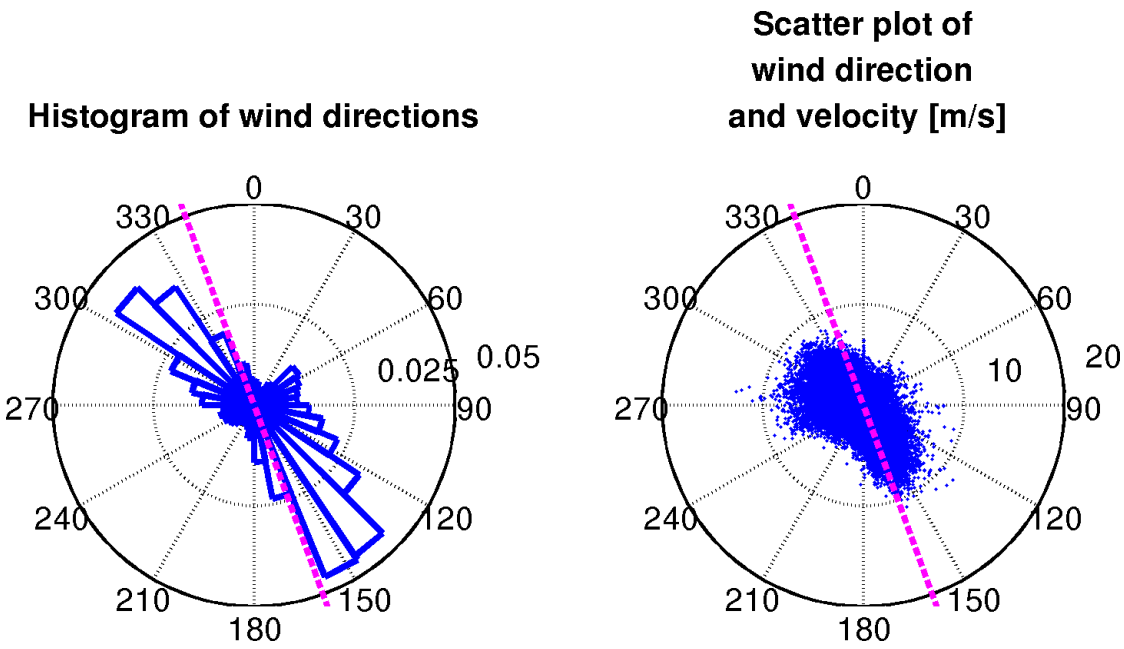

Figure 4.6: Histogram of wind direction and scatter plot of wind direction and velocity during April - October as measured at the Game Farm Road meteorological station. Dashed line marks approximate orientation of Cayuga Lake's main axis - 340° – 160°. Directions plotted are relative to true north.

4.4.1 Internal seiche and (longitudinal) tilting of the thermocline

The following is a general overview of the main effects of the tilt of the thermocline proposed in the thesis. It is intended to provide a simplified description of the main effect of the thermocline's longitudinal tilt near the shelf break. In reality the dynamics on the shelf will be more complex. The forcing conditions of the shelf constantly change and there is a balance of the different processes, operating on different timescales, that controls the movement of water on the shelf - the wind's forcing of internal motions as described here, the oscillations

of the internal seiche, inflows from tributaries, wind generated surface waves and currents etc.

***Wb* > 1; thermocline tilted down near shelf (figure 4.7a)** When the wind blows out of the north it causes advection of water near the surface towards the south end of the lake. This creates a deepening of the epilimnion in this area. The result is an increase in transport between the epilimnion on the two sides of the shelf break (loads entering the southern shelf get mixed out to the north more rapidly).

$|Wb| \gg 1$; general case, thermocline horizontal (figure 4.7b) If the magnitude of the wind is small, or if it does not blow stably from a constant direction, the shear stress of the wind on the lake's surface will not be strong enough to tilt the thermocline from its horizontal state. In reality the thermocline will never be horizontal for any meaningful length of time. After an event with winds strong enough to tilt the thermocline has ended, the thermocline will oscillate around the horizontal until this motion is dampened by friction. However for the lake to reach a quiescent state the winds need to remain very weak for a period on the order of weeks that is required to dissipate the energy in the oscillations. This does not normally happen in Cayuga Lake.

***Wb* < −1; thermocline tilted up near shelf (figure 4.7c)** When the wind blows out of the south it will advect surface water to the north, causing a thinning of the epilimnion near the southern shelf and a corresponding tilt of the thermocline upwards near the shelf break. Mixing across the shelf break, within the epilimnion, will be reduced due to the fact that the epilimnion becomes thinner

near the shelf break, essentially creating a "bottleneck". The result is a lower rate of transport across the shelf break (loads entering the shelf get mixed out to the north less rapidly).

Depending on the mean depth of the thermocline and the strength of the wind, the depth of the thermocline may become shallower than the lake depth on the shelf, causing hypolimnetic water to advect on to, and off of, the shelf with the periodic motions of the internal seiche. The shear of the water moving along the stationary bottom of the lake, as well as with respect to the epilimnion, creates turbulence that increases mixing between the epilimnetic water on the shelf and hypolimnetic water advected onto the shelf.

***Wb* ~ −1; upwelling onto southern shelf (figure 4.7d)** If the wind blows out of the south for a long enough duration at a strong enough magnitude (causing *Wb* to approach unity), the thermocline will tilt up to such a degree that it approaches the free surface of the lake. The result is advection of hypolimnetic water onto the shelf. However a second result is that the epilimnetic water in the southern part of the shelf will become isolated from the epilimnion in the main basin of the lake to the north of the shelf break. The density difference between the upwelling waters and the ambient water on the shelf will reduce mixing between these two phases, resulting in a "blocking" effect which will increase residence time on the shelf.

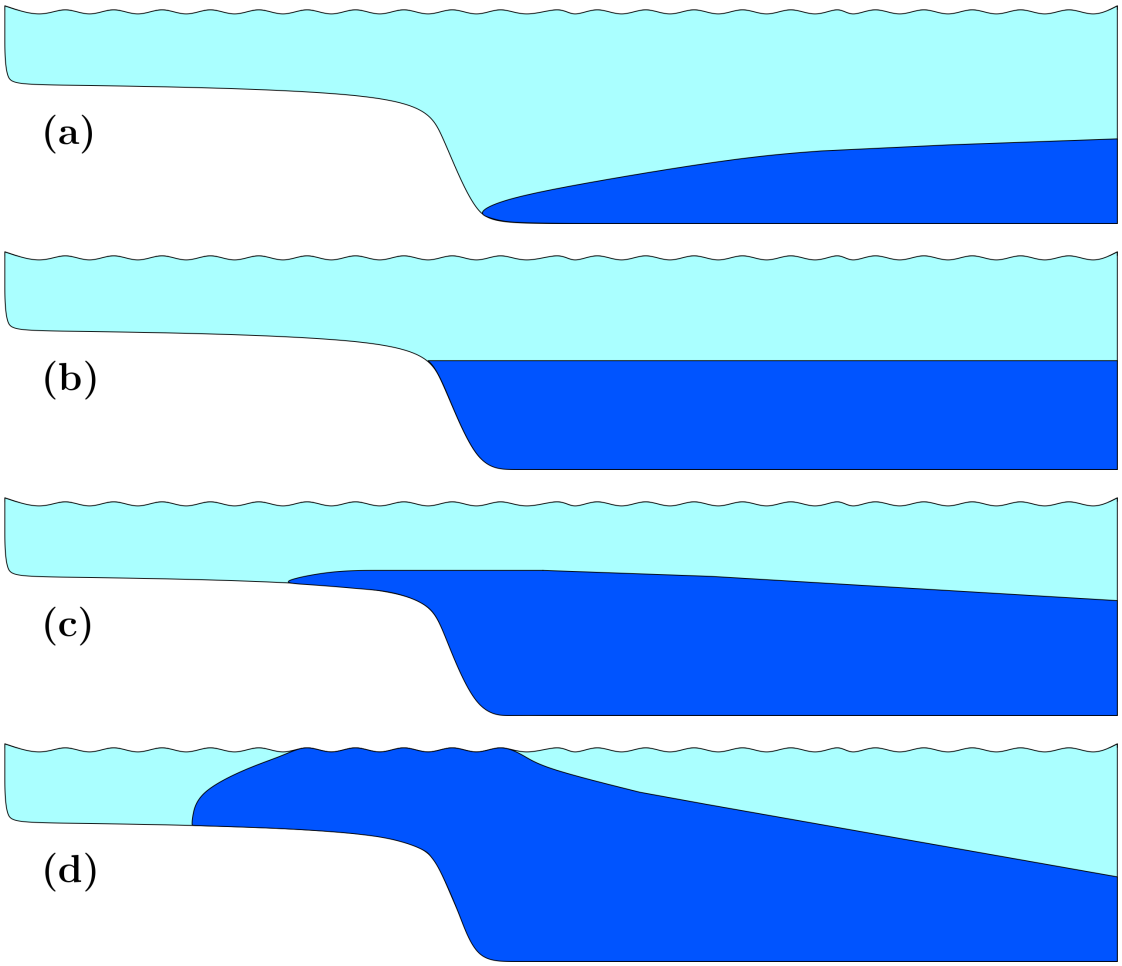

Figure 4.7: Illustration of thermocline tilt under various forcing conditions (not drawn to scale): (a) Winds out of the north, tilting thermocline down at southern shelf, (b) Quiescent state, thermocline not tilted, (c) Winds out of the south, tilting thermocline up at southern shelf, (d) Sustained winds out of the south, causing upwelling of hypolimnetic water onto the southern shelf.

4.4.2 Dynamics (seiching)

The dynamics described thus far assume the wind continues to apply the same constant shear stress to the free surface. Once the wind changes and that shear stress is removed there is nothing to balance the gradients in elevation of the

two surfaces, and they will both begin to move back towards their horizontal state of equilibrium. However due to momentum each interface will overshoot its equilibrium location, and begin to oscillate around it. The result is a long standing wave, or seiche, on the free surface (barotropic wave) and internally along the thermocline (baroclinic wave). In reality the wind will not always remain steady for extended periods of time, and motions of the interface at a given time will be determined by the input of wind energy to the system over preceding period (order several days or a week) and interaction with the existing internal wave field.

4.5 Effects of the earth's rotation

In addition to the longitudinal tilt of the thermocline described in the previous section, a lateral (east-west) tilting can also exist due to effects of the earth's rotation and due to differences in bathymetry across the width of the lake. The earth's rotation causes the direction of flow of fluid to be deflected to the right (in the northern hemisphere). The same effect applies to motions of water created by the internal seiche.

If the time scale of the earth's rotation is short relative to other time scales of fluid motion rotational effects can be important. The Rossby number (Ro) represents the importance of accelerations due to the rotation of the earth (i.e., the Coriolis force) relative to other motions.

$$Ro = \frac{inertial\ forces}{rotational\ forces}$$

$$if \quad Ro = \frac{rotation\ period}{advection\ time} = \frac{1/f}{L/u} = \frac{u}{Lf} < 1 \quad rotation\ is\ important\ to\ advection$$

$$if \quad \frac{\sqrt{gH}}{Lf} = \frac{Ro}{Fr} < 1 \quad rotation\ is\ important\ to\ long\ surface\ waves$$

$$if \quad \frac{internal\ wave\ frequency}{rotational\ frequency} = \frac{\omega}{f} < 1 \quad rotation\ is\ important\ to\ internal\ waves$$

The Burger number (S) represents the relative importance of gravity and rotation to internal waves. It is the ratio of the Rossby radius (c_i/f) to a length scale of the basin (Pedlosky, 1987; Antenucci & Imberger, 2001):

$$S = \frac{gravity}{rotation} = \frac{c_i}{\phi f}$$

where c_i is the phase speed of the wave, ϕ is the basin length scale (width of the lake) and f is the rotational frequency of the earth.

Rotation is certainly important for $S < 1$. It has also been shown to be important in cases where $S \sim 1$ and theoretically for values as high as $S \approx 1.5$ (Antenucci & Imberger, 2001; Antenucci, 2005).

Using values typical to Cayuga Lake we can predict the expected relative importance of the various processes (timescales):

$f = 2\Omega_0 \sin\Theta$ where: Θ = latitude of lake ($42°35' \rightarrow 42°45'$), $\Omega_0 \approx 7.3 \times 10^{-5}\ rad/s$ (one rotation every sidereal day - 23 hr, 56 min, 4.1 s), ϕ =width of the lake ($2 \rightarrow 5km$).

$$\Rightarrow \quad f = \quad 2 \times 7.3 \cdot 10^{-5} \times \sin(42°35') = 9.87 \cdot 10^{-5}$$

$$f = \quad 2 \times 7.3 \cdot 10^{-5} \times \sin(42°45') = 9.90 \cdot 10^{-5}$$

Substituting in these values we have:

for internal waves,

$$\frac{\omega}{f} = \frac{internal\,wave\,frequency}{rotational\,frequency} = \frac{2\pi/\left(2.4_{days} \times 24 \times 3600\right)}{f} \approx \frac{3 \cdot 10^{-5}_{rad/s}}{f} \approx 0.3 < 1$$

$$\begin{aligned} S_i &= \frac{c_i}{\phi f} = \frac{c_i}{2000_{meters} \times 9.87 \cdot 10^{-5}} \rightarrow \frac{c_i}{5000_{meters} \times 9.90 \cdot 10^{-5}} \\ &= \frac{c_i}{0.2} \rightarrow \frac{c_i}{0.5} \end{aligned}$$

where c_i is the internal wave phase speed.

For advective currents,

$$Ro = \frac{1/f}{\phi/u} = \frac{u}{\phi f} = \frac{u}{0.2} \rightarrow \frac{u}{0.5}$$

where u is the current velocity and, for long surface waves,

$$\frac{\sqrt{gH}}{\phi f} = \frac{Ro}{Fr} = \frac{\sqrt{9.81 \cdot 55}}{\phi f} = \frac{23.2}{0.2} \rightarrow \frac{23.2}{0.5} \gg 1$$

Thus we see that rotation can have an effect on currents at low speeds, on the order of $0.2 - 0.5\,m/s$ or slower, or on internal waves with phase speeds of the same order. Currents on the shelf during the summer have been observed to be on the order 2 cm/s (Ahrnsbrak, 1986), and the phase speed of an upwelling front onto the shelf in one case was estimated to be on the order 4 cm/s based on the time lag between the temperature signature at the RUSS and at the piling cluster (section 5.2.2), which is within the velocity range for which rotation is important. We would not, however, expect to see a noticeable effect of rotation on the surface wave field.

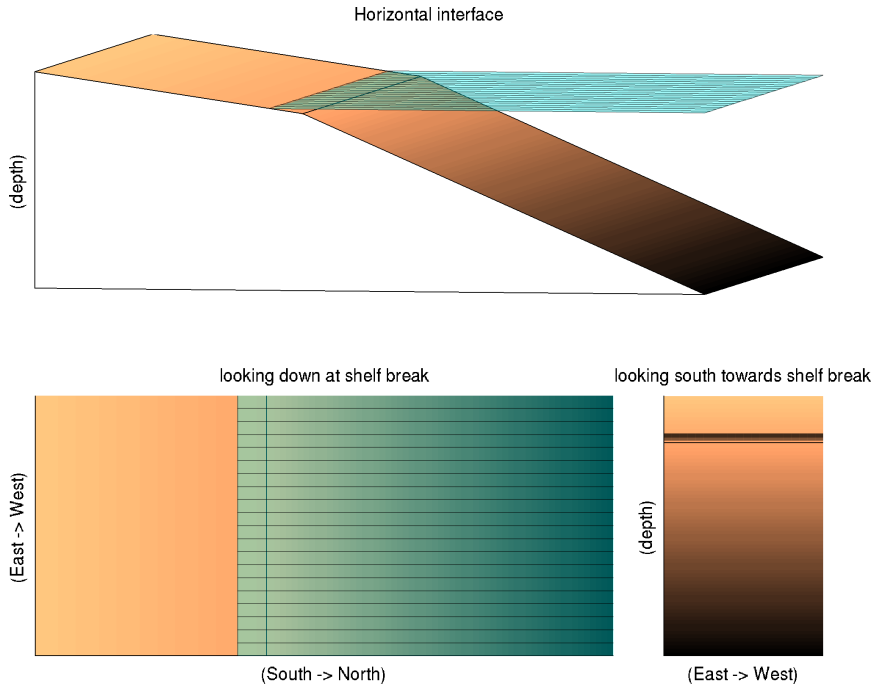

Figure 4.8: Illustration of internal seiche runup on southern shelf, ignoring the earth's rotation

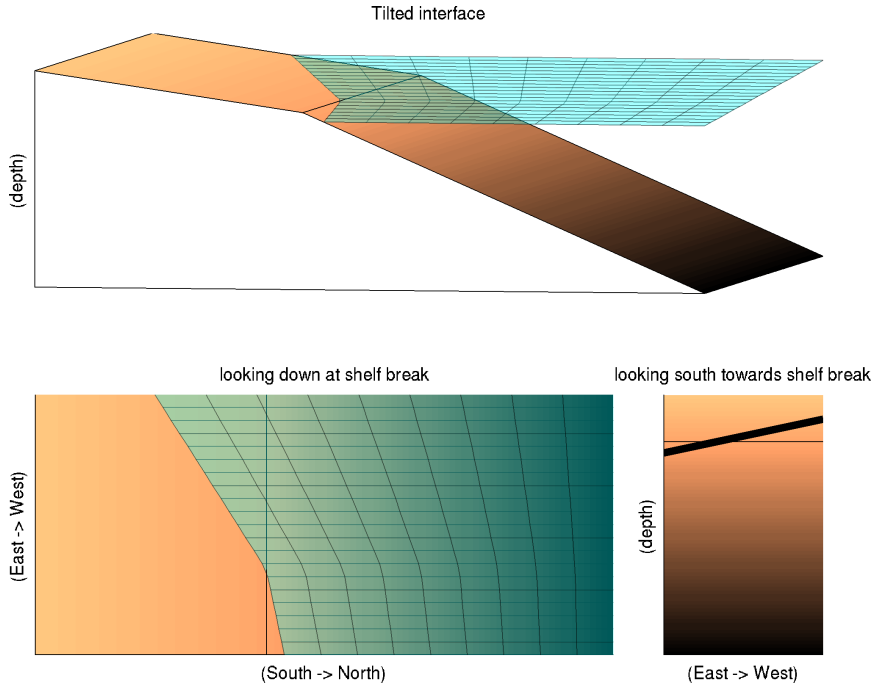

Figure 4.9: Illustration of internal seiche runup on southern shelf, with interface tilted due to rotation

The effect of rotation in Cayuga Lake is to laterally tilt the thermocline so that it becomes deeper in the east and shallower in the west. This can be important to transport and exchange dynamics on the southern shelf, since a shallower thermocline on the western side near the shelf break means that hypolimnetic water will be advected onto the shelf at less extreme longitudinal tilts of the thermocline than on the eastern side (illustrated in figure 4.8 and figure 4.9). The effect is amplified by the fact that the bathymetry of the lake is deeper in the west than the east in the vicinity of the shelf break, leading to reduced bottom friction on this side as the density front progresses up the shelf break. The end result is hypolimnetic water being advected farther onto the shelf on the western side of the lake than on the eastern side. This leads to increased mixing between the shelf water and hypolimnetic water on the western side of the shelf relative to the eastern side. Lower concentrations of chlorophyll-*a* have been observed at site 4 relative to other sites after the onset of stratification, possibly as a result of this gradient in mixing. This topic is discussed in greater detail in section 5.1.3.

CHAPTER 5

BASELINE CONDITIONS AND THE RESPONSE OF THE SHELF TO FORCING EVENTS

This chapter discusses the observed water quality properties of the shelf under baseline forcing and during forcing events. Shelf-averaged values are used in the discussion in an attempt to represent conditions on the shelf using a single number for simplicity. In any place that the term "shelf-average" is used it was calculated by averaging observed values at sites 1 and 7, and then taking the mean of this number and the values observed at sites 3, 4 and 5, i.e:

$$\text{shelf-average} = \frac{\frac{site\,1 + site\,7}{2} + site\,3 + site\,4 + site\,5}{4} \tag{5.1}$$

This method has been used in the annual reports on the LSC facility since 1998 (UFI, 2000*a*,*b*, 2001, 2002, 2003, 2004, 2005, 2006, 2007; Cornell University, 2008, 2009). Site 2 is excluded from this average since it is strongly affected by its proximity to the IAWWTF outfall (section 2.2.2). Sites 1 and 7 are averaged together to a single value to avoid over representing the eastern side of the shelf. References to deep water sites indicate the averaged values of observations at sites 6, 8 and the LSC Intake.

Several box plots are presented in this chapter to facilitate comparison of observed water quality properties at different locations or under different forcing conditions. These are standard box plots (e.g., Tukey, 1977) in which the central black line represents the median of the data plotted and the grayed area around it denotes the 95% confidence interval of the median. The extent of the box indicates the inter-quartile range (IQR, i.e., 25^{th} percentile to the 75^{th} percentile of the data), the whiskers denote the extent of $1.5 \times IQR$ beyond these limits. Any

values beyond the limits of the whiskers are considered outliers and are plotted individually. In some plots in which the range of data is especially large, extremely high (or extremely low) values are "compressed", i.e., the scale of the plot changes beyond the vertical dashed line in order to fit all the data into the plot. The color of the boxes has no meaning beyond grouping certain elements of the plot for easier visual comparison. The number of samples included in each element of the plot is indicated on the right margin and the conditions for inclusion are indicated on the left.

5.1 Baseline water quality record

A strong south to north gradient of water quality is observable from the median monthly and annual water quality values calculated over the entire 11 year period of data (presented in the following sections). Higher values of TP, SRP, Tn are observed in the shallower, southern sites. Differences between measurements at the three deep water sites (6, 8 and the Intake) are small, strengthening the assumption that the waters of the lake are well mixed in the deep portions and horizontal spatial gradients are not significant within the main basin of the lake.

Some evidence of an east to west gradient exists, however the case is less clear here for a number of reasons. First, of the nine sites sampled only sites 1, 4 and 7 are significantly removed from the centerline of the lake (the Intake site is also not located directly along the centerline, but it is closer to it, is located over deep water, and is much more distant from the nearest neighboring sampling sites). Sites 1 and 4 are located at similar distances from the southern end of the lake and at similar locations relative to the centerline and shore line east

and west of the center. Site 3 is on the centerline of the lake located midway along an East to West transect through sites 1 and 4. These sites provide the best comparison of east-west gradients in the lake. Site 7 is near the eastern shore but has no equivalent "mirror" site on the west. Additionally, site 7 is located near point and non-point sources that likely have a localized effect - the CHWWTP outfall, LSC discharge and the geese population at Stewart Park. Site 7 is also nearest to residential areas and some concerns have been raised regarding septic systems and minor tributaries entering the lake nearby.

A further analysis of the horizontal spatial gradient was conducted in the following manner: For each sampling date, the measured values of each parameter were ranked by site from the highest to the lowest. The frequency distribution of this set of synoptic rankings of relative values was then analyzed. The results answer the question "on what fraction of sampling dates was site x ranked i^{th} in relation to the other sites". This approach was used due to challenges working with the water quality data set from a statistical point of view. The water quality data are generally not normally distributed. Furthermore, strong inter- and intra-annual variations exist in the data caused by the seasonality of forcing and interannual variation of meteorological conditions. An observed value that might be considered high one year might therefore not be considered high when compared with observations from a different year with different nutrient loading (e.g., due to higher precipitation which leads to increased surface runoff). For these reasons the comparison of rankings has proved useful. For the same reasons medians and percentiles are given preference to means and standard deviations in many places throughout the thesis.

Flow rates in the tributaries and the accompanying nutrient loadings are

substantially higher in April than in following months due to runoff from melting snow and ice in the surrounding hills (figure 4.1). Also, The lake has not yet begun to stratify and chlorophyll-*a* levels are generally very low in April, possibly suggesting less biological uptake of nutrients than in warmer months (discussed in section 5.1.3). For these reasons data from April were dropped when calculating annual estimates of various parameters in the lake water.

5.1.1 Turbidity

Baseline turbidity values are presented in figures 5.1, 5.2 and 5.3. A strong south to north gradient is evident during the high runoff month of April, and to a lesser extent in the following months (table 5.1). Annual median turbidity values are of order 2.5 NTU at the southern, and southeastern most sites, and order 1 NTU at the deep water sites.

Sites 8 and LSC Intake have very similar turbidity values suggesting that water in the deeper part of the lake is well mixed (table 5.1). The effect of high surface runoff on turbidity is also apparent from these plots. Turbidity values are at their highest in April during the spring snow melt and then drop off substantially the next month before climbing somewhat in the warmer months when plankton levels increase, as is evident from the seasonal trend of chlorophyll-*a* levels plotted in figure 5.16. Interannual variation of runoff is also evident: 1999 was a year with extremely low surface runoff and correspondingly low turbidity values were measured in the lake. High flow rates in 2000 and 2004 led to high measured turbidity values.

A histogram of the relative ranking of turbidity at each site is presented in

figure 5.3. Plotting the resulting histogram of rankings for the 8 sites clearly indicates the gradient from the SE corner of the lake (site 7) to the northern deep water (site 8). The histograms of turbidity at each site and month presented in figure 5.2 and the monthly box plots of turbidity on and off of the shelf in figure 5.4 show that turbidity levels are generally higher on the shelf than in deeper parts of the lake, and that in general they are highest during the spring melt runoff period and drop off as the season progresses, with a slight increase during the growing season.

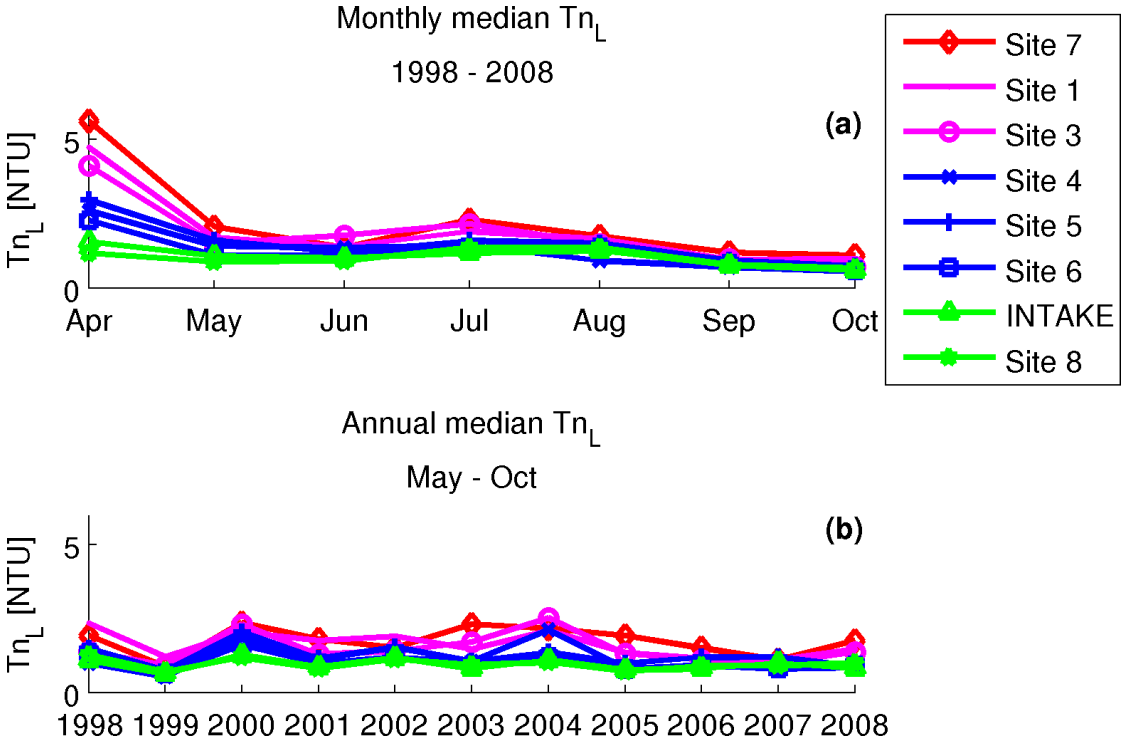

Figure 5.1: Median turbidity levels at each sampling site. a) monthly median turbidity at each site (median of all values in each month across all years) b) annual median turbidity at each site (median of all values in each year)

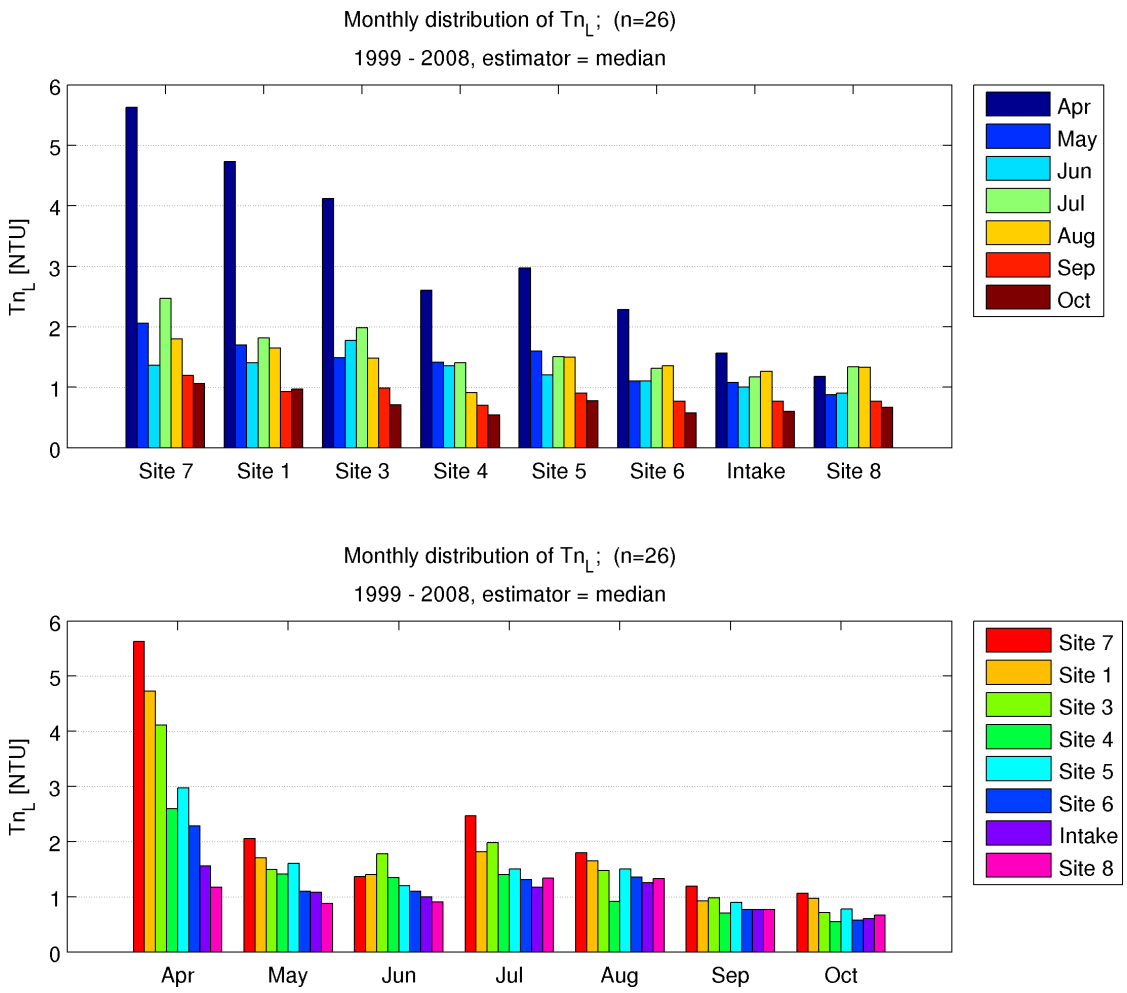

Figure 5.2: Monthly median turbidity grouped by site and by month. Order of sites is geographical by distance from the southeast corner of the lake.

Table 5.1: p-values of paired Tn comparisons, May - October, n=156. In each case the null hypothesis that the means/medians of respective sets are equal is tested against the listed alternative hypothesis.

hypothesis	**paired t-test**	**signed rank test**
deep water < shelf	<0.001	<0.001
Site 8 ≠ Intake	0.818	0.319

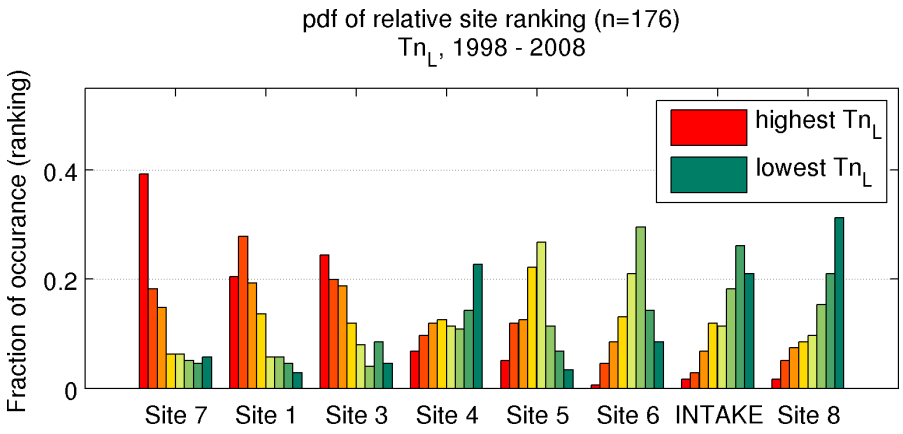

Figure 5.3: Probability distribution function of relative observed Tn at each site. For each sampling site the leftmost bar represents the fraction of all sampling dates on which the site had the highest observed Tn of all sites and so on to the rightmost bar which indicates the fraction of sampling dates on which it had the lowest value. Order of sites is geographical by distance from the southeast corner of the lake.

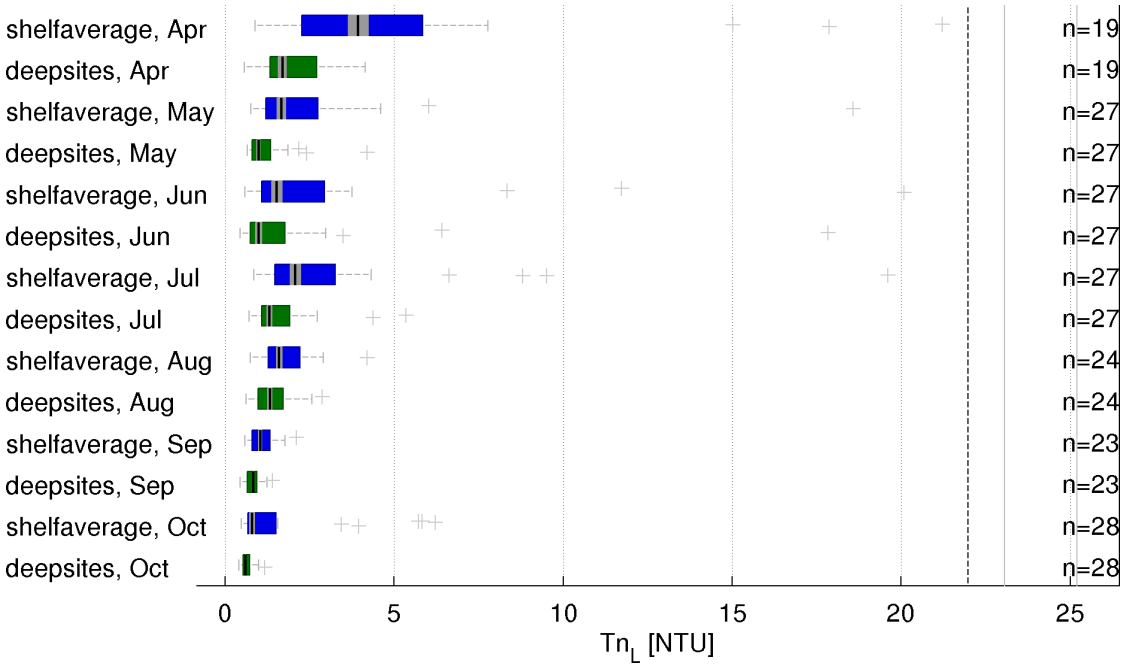

Figure 5.4: Box plots of shelf-averaged and mean deepwater (sites 6, 8, Intake) Tn for each month, over the entire record. The horizontal scale is compressed to the right of the dashed black line in order to fit outlying values into the plot.

5.1.2 Phosphorus

Baseline phosphorus values are presented in figures 5.5, 5.6 and 5.9 (TP), and figures 5.7, 5.8 and 5.11 (SRP). A strong south to north concentration gradient is evident with the highest concentrations (both TP and SRP) observed in the southernmost, or southeastern-most sampling locations (table 5.2 and table 5.3).

Phosphorus concentrations observed at site 2 are elevated compared to those of nearby sites throughout much of the sampling record. This is most likely due to the proximity of this site to the outfall of the IAWWTF. For this reason, measurements taken at site 2 are not included in most of the discussion in this thesis. Following upgrades to the IAWWTF (installation of tertiary treatment) phosphorus concentrations measured at this site have dropped considerably, but are still elevated relative to neighboring sites on the shelf. The site still reflects the water quality of the IAWWTF effluent to a greater extent than it does the general water quality on the shelf.

Mean TP (both monthly and annual) at sites 8 and LSC Intake are nearly identical (table 5.2), suggesting that the intake site is in the well mixed section of the lake.

Table 5.2: p-values of paired TP comparisons, May - October, n=156. In each case the null hypothesis that the means/medians of respective sets are equal is tested against the listed alternative hypothesis.

hypothesis	**paired t-test**	**signed rank test**
deep water < shelf	<0.001	<0.001
Site 8 ≠ Intake	0.330	0.160
Site 1 > shelf	0.006	0.015
Site 3 > shelf	0.003	0.095
Site 7 > shelf	<0.001	<0.001
Site 4 < shelf	<0.001	<0.001
Site 5 < shelf	<0.001	<0.001

Table 5.3: p-values of paired SRP comparisons, May - October, n=156. In each case the null hypothesis that the means/medians of respective sets are equal is tested against the listed alternative hypothesis.

hypothesis	**paired t-test**	**signed rank test**
deep water < shelf	<0.001	<0.001
Site 8 ≠ Intake	0.908	0.943

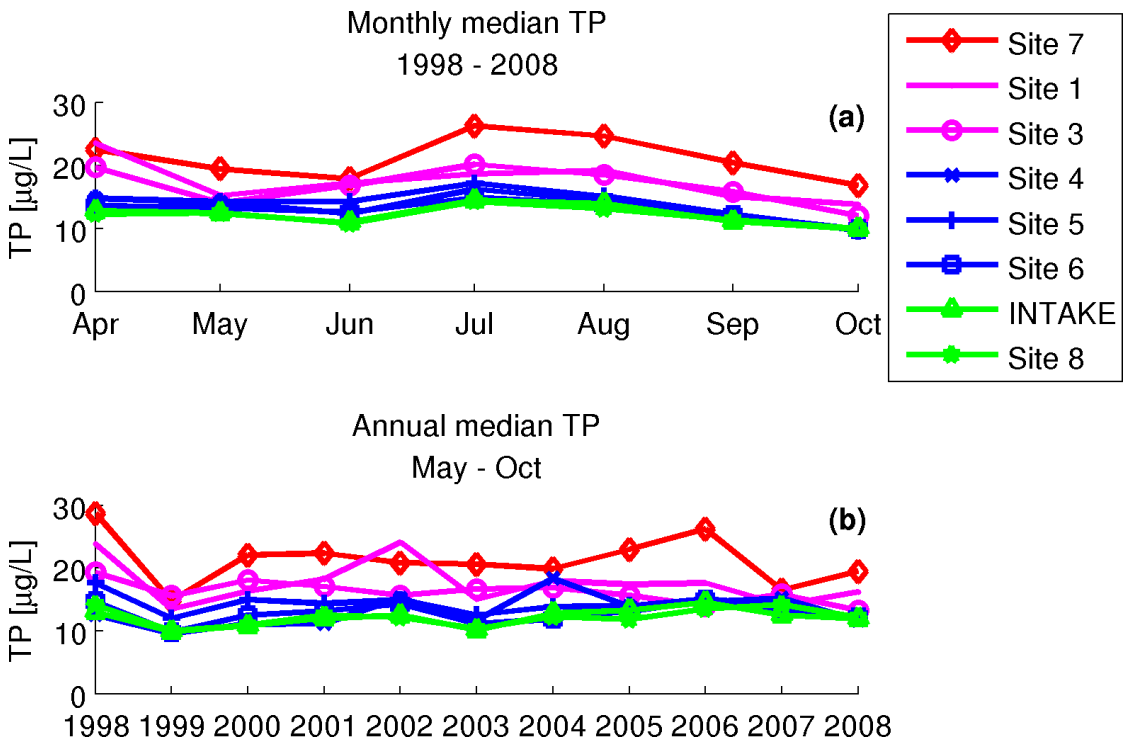

Figure 5.5: Median TP levels. a) annual median concentration at each site (all months of each year averaged) b) monthly median concentrations at each site (values of each month in all years averaged)

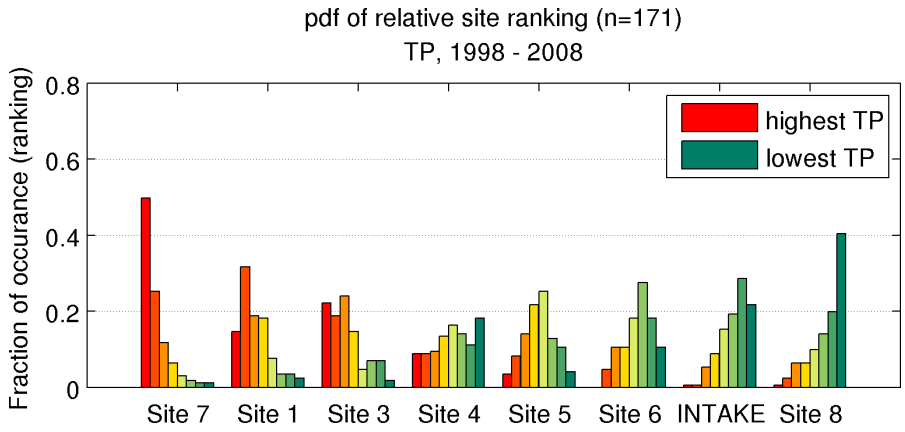

Figure 5.6: Probability distribution function (PDF) of relative observed TP at each site. The leftmost bar represents the fraction of sampling dates on which the site had the highest observed TP and so on to the rightmost bar which indicates the fraction of sampling dates on which it had the lowest value. Order of sites is geographical by distance from the southeast corner of the lake.

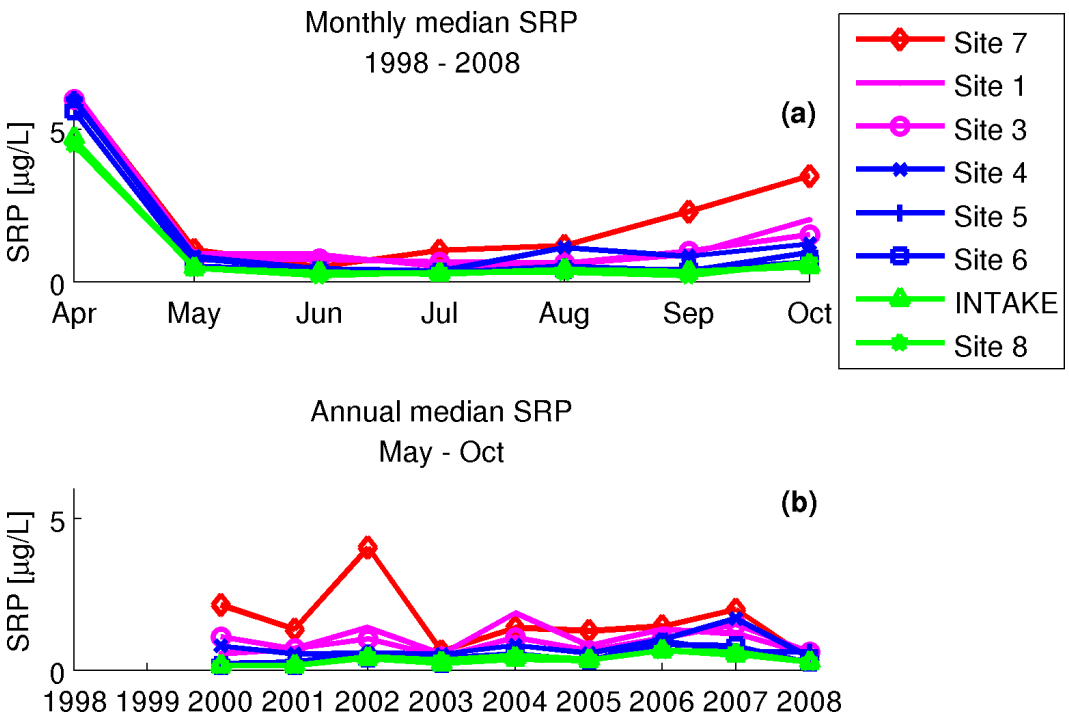

Figure 5.7: Median SRP levels. a) annual median concentration at each site (all months of each year averaged) b) monthly median concentrations at each site (values of each month in all years averaged)

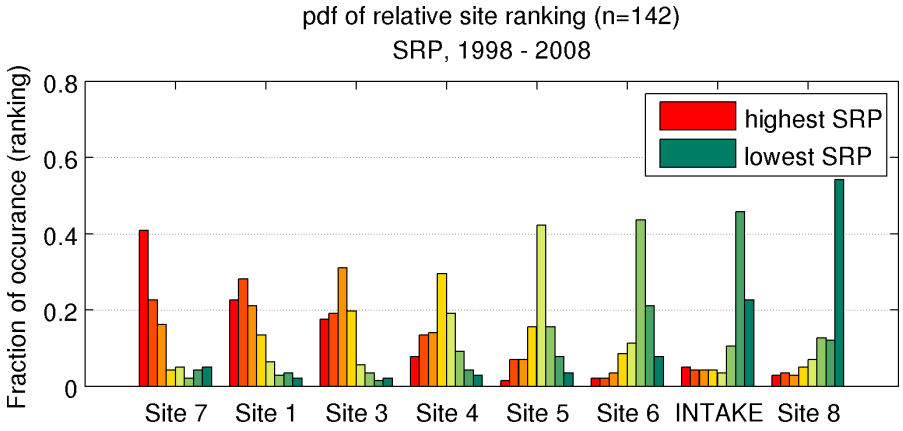

Figure 5.8: Probability distribution function (PDF) of relative observed SRP at each site. For each sampling site the leftmost bar represents the fraction of all sampling dates on which the site had the highest observed SRP of all sites and so on to the rightmost bar which indicates the fraction of sampling dates on which it had the lowest value. Order of sites is geographical by distance from the southeast corner of the lake.

The histograms in figure 5.9 and figure 5.11 and the box plots in figure 5.10 and figure 5.12 compare the seasonal trends of TP and SRP at the different sites and on the shelf and deep water sites. Median TP values are high on the shelf in April ($18\,\mu g/L$) and then drop somewhat before peaking in July ($21\,\mu g/L$) and continuing to decline until the end of the season. The deep water sites follow a similar trend but with lower values ($13\,\mu g/L$ in April and $14\,\mu g/L$ in July).

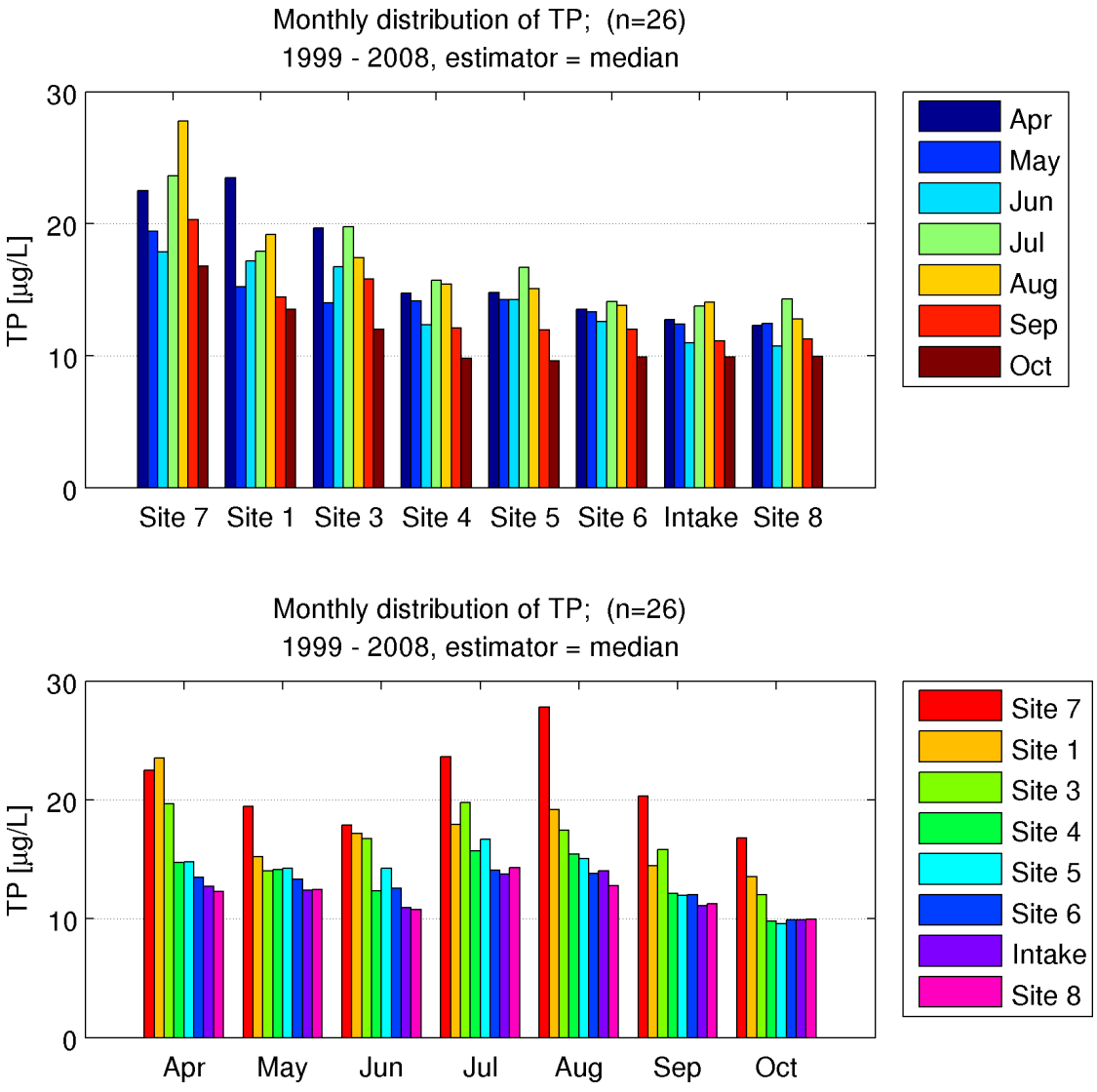

Figure 5.9: Monthly median TP turbidity grouped by site and by month. Order of sites is geographical by distance from the southeast corner of the lake.

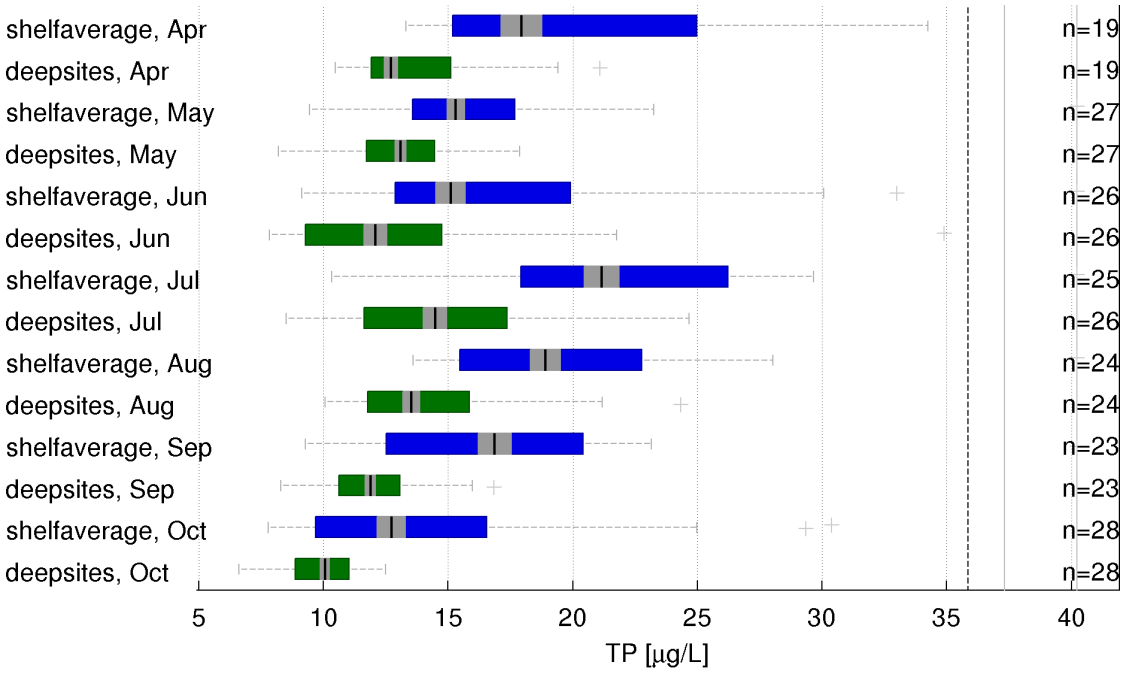

Figure 5.10: Box plots of shelf-averaged and mean deepwater (sites 6, 8, Intake) TP for each month, over the entire record. The horizontal scale is compressed to the right of the dashed black line in order to fit outlying values into the plot.

SRP is observed to be highest in April at all sites during the high runoff season before the lake has stratified. After dropping considerably over May and June (median 6.3 $\mu g/L$ on the shelf in April, 0.8 $\mu g/L$ in May) it rises slowly until October (1.8 $\mu g/L$ on the shelf). Observations in the deep water sites show a median peak of 4.8 $\mu g/L$ in April dropping to 0.5 $\mu g/L$ in May and staying fairly constant until October. The rising shelf-averaged SRP from May to October is observed at most shelf sites, however it is driven primarily by increasing SRP at site 7 (figure 5.11).

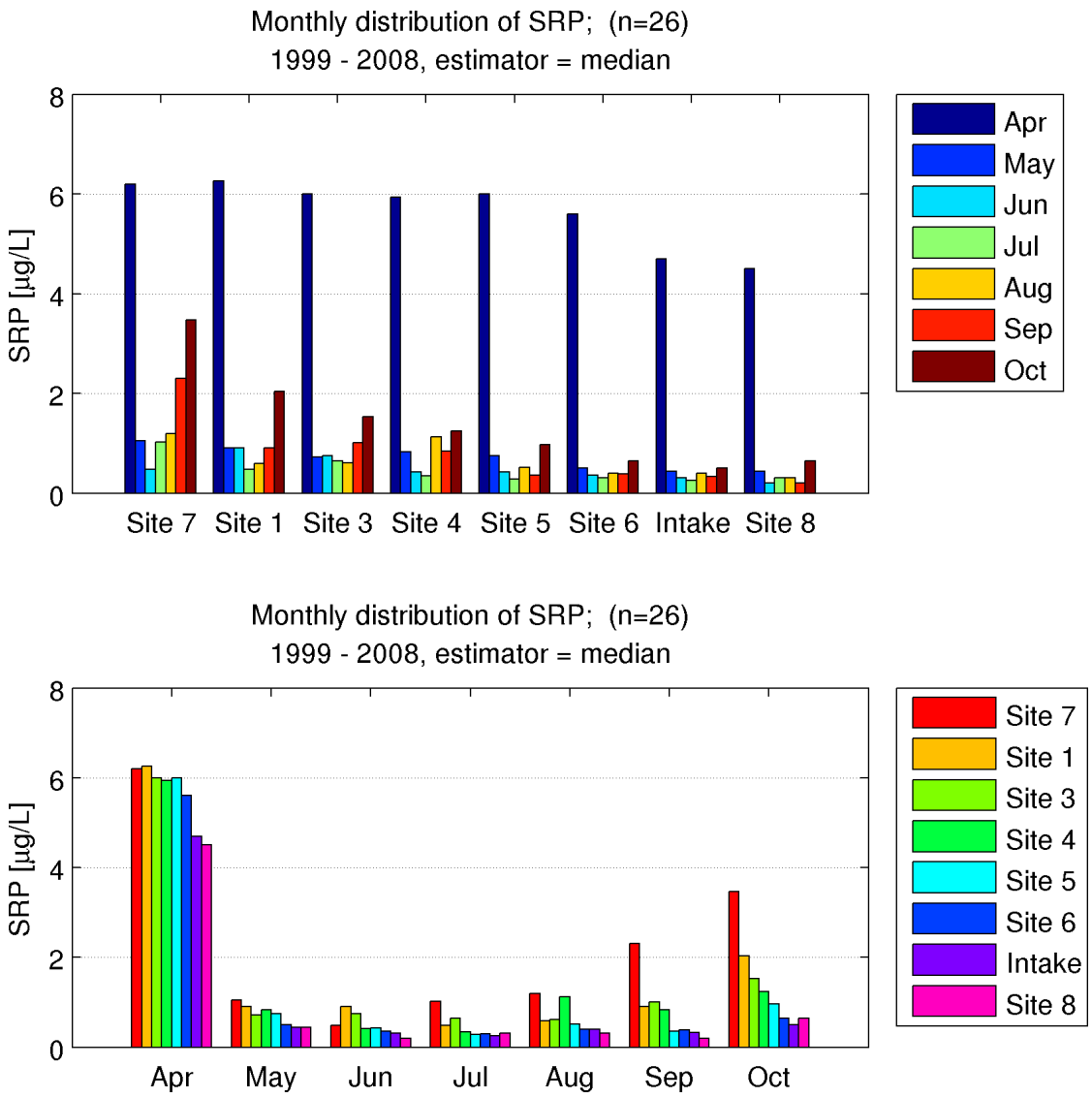

Figure 5.11: Monthly median SRP grouped by site and by month. Order of sites is geographical by distance from the southeast corner of the lake.

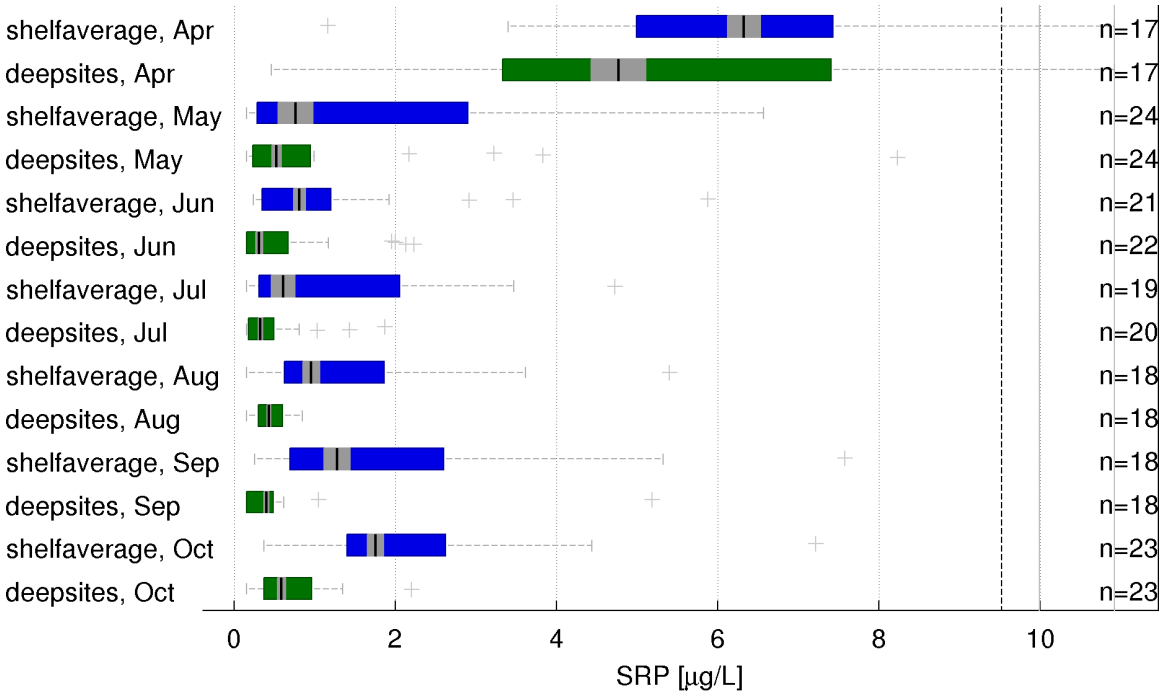

Figure 5.12: Box plots of shelf-averaged and mean deepwater (sites 6, 8, Intake) SRP for each month, over the entire record.The horizontal scale is compressed to the right of the dashed black line in order to fit outlying values into the plot.

Scatter plots of TP at the shelf sites and the weighted shelf-average are presented in figure 5.14 and of TP for the weighted shelf-average and mean of the deepwater sites in figure 5.13. TP concentrations at sites 1, 3 and 7 tend to be higher than the shelf-averaged concentration - the majority of mass of the scatter is located on that side of the equal concentration line in the respective plots. Sites 4 and 5 tend to have lower TP concentrations than the shelf-average (table 5.2; recall that Shelf-average $= \frac{(Site\,1+Site\,7)/2+Site\,3+Site\,4+Site\,5}{4}$ so as not to over represent the eastern side of the shelf). Site 7 tends to have higher TP concentrations when compared with each of the other shelf sites, site 5 tends to have the lowest. Shelf-averaged TP is higher than at the deep water sites on all but a few of the sampling dates in the 11 year record. This is not surprising since the

majority of phosphorus load entering the entire lake does so on the south shelf .

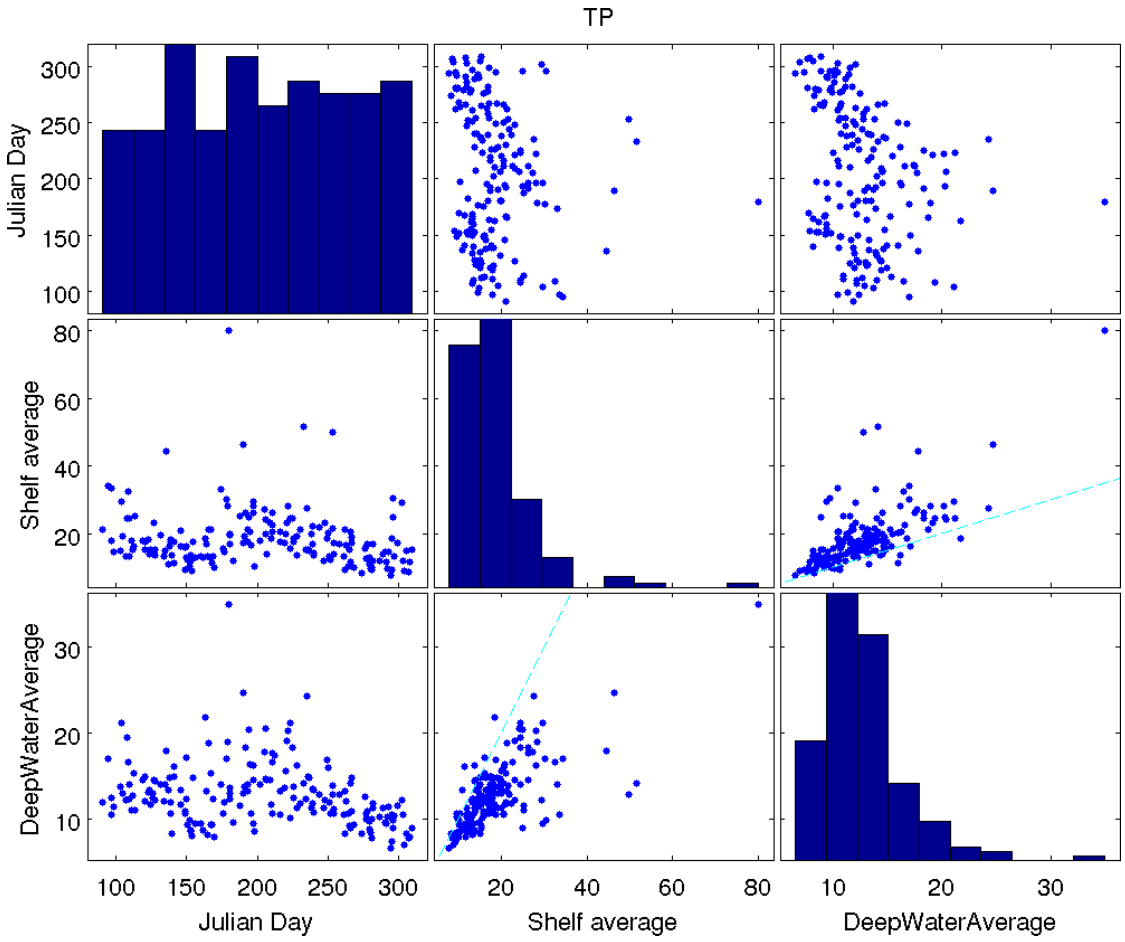

Figure 5.13: Scatter plots of observed shelf-averaged TP and averaged deep water (sites 6, 8, Intake). TP values are in $\mu g/L$. Dashed lines indicate location of perfect correlation (i.e., lines of $x = y$). Plots along the diagonal are histograms of the corresponding metric. Plots that are located symmetrically relative to the diagonal compare the same data, but are presented with different aspect ratios.

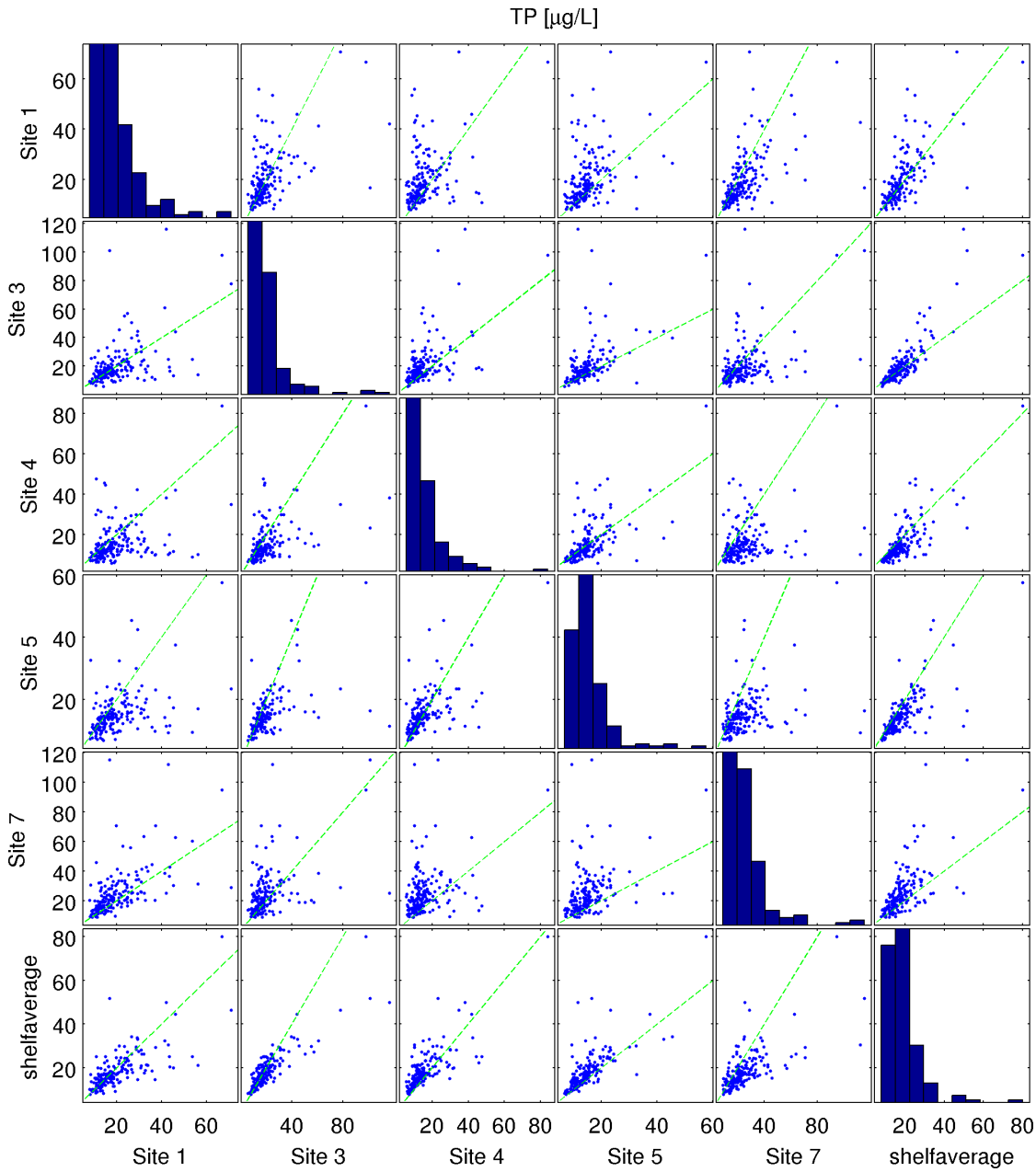

Figure 5.14: Scatter plots of observed TP at the shelf sites, during the stratified season (August - October). Each plot in this figure shows a scatter of two forcing parameters over the eleven year record, with each dot representing a single sampling date. TP values are in $\mu g/L$. Dashed lines indicate location of perfect correlation (i.e., lines of $x = y$). Plots along the diagonal are histograms of the corresponding metric. Plots that are located symmetrically relative to the diagonal compare the same data, but are presented with different aspect ratios.

5.1.3 Chlorophyll-*a*

Baseline chlorophyll-*a* values are presented in figures 5.15, 5.16, 5.17 and 5.18. Differences between the various sampling sites are small for this metric in comparison to those observed for turbidity and phosphorus (i.e., the spatial gradient is not as obvious). Levels observed at site 4 are generally lower than the shelf-average and those at site 7 and the deep water sites are generally higher than the shelf-average (table 5.4). The data from 2006 - 2008 show significantly (table 5.5) increased (~double) values at the deep water sites - 6, 8, and the Intake. An increase in phosphorus in the lake's hypolimnion has been observed leading up to those years (UFI, 2006, 2007; Cornell University, 2008, 2009). The increased chlorophyll-*a* concentrations are possibly a result of this apparently lake wide increase in phosphorus.

The seasonal trend of chlorophyll-*a* levels is typical of lakes in the region, with low levels (order 1 $\mu g/L$) at all sites in the start of the season in April which rise as the season progresses to warm and nutrients enter the lake, peaking in August. Chlorophyll-*a* concentrations then decline at all sites but at different rates - there is a clear spatial gradient in the rate of decline of chlorophyll-*a* with concentrations at the southern sites (1, 3, 4, 5 and 7) dropping more rapidly than the deep water sites (6, 8, Intake; figures 5.16 and 5.17). Site 4 exhibits seasonal trends that are somewhat different from the other sites. Early in the season changes in chlorophyll-*a* concentrations at site 4 are similar to those at the other sites. However, beginning in August the chlorophyll-*a* concentration at site 4 drops considerably, while it continues to rise at the other sites (figures 5.16 and 5.17). The drop in chlorophyll-*a* at site 4 coincides with the onset of stratification. A possible explanation for this is increased mixing with hypolimnetic water at

site 4 due to runup of internal waves during the stratified season. This would be consistent with the rotational effects discussed in section 4.5.

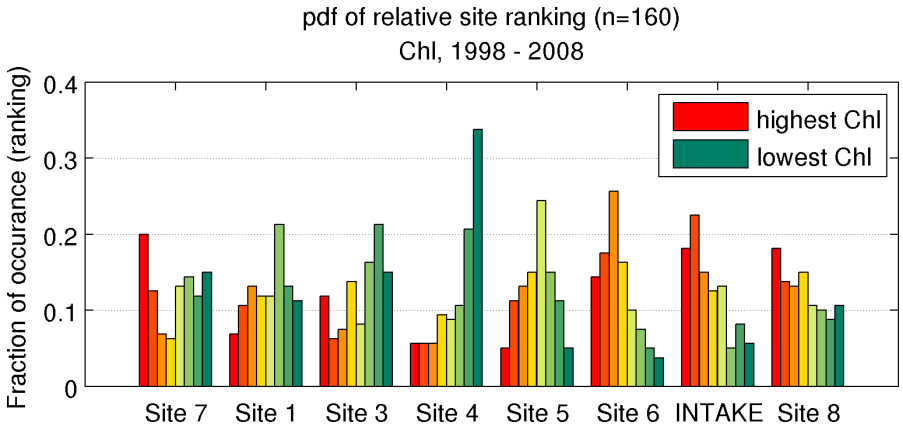

Figure 5.15: Probability distribution function (PDF) of relative observed chlorophyll-*a* at each site. For each sampling site the leftmost bar represents the fraction of all sampling dates on which the site had the highest observed chlorophyll-*a* of all sites and so on to the rightmost bar which indicates the fraction of sampling dates on which it had the lowest value. Order of sites is geographical by distance from the southeast corner of the lake.

Table 5.4: p-values of paired chlorophyll-*a* comparisons, May - October, n=156. In each case the null hypothesis that the means/medians of respective sets are equal is tested against the listed alternative hypothesis.

hypothesis	**paired t-test**	**signed rank test**
deep water > shelf	<0.001	<0.001
Site 8 ≠ Intake	0.053	0.020
Site 4 < shelf	<0.001	<0.001
Site 7 > shelf	0.001	0.008

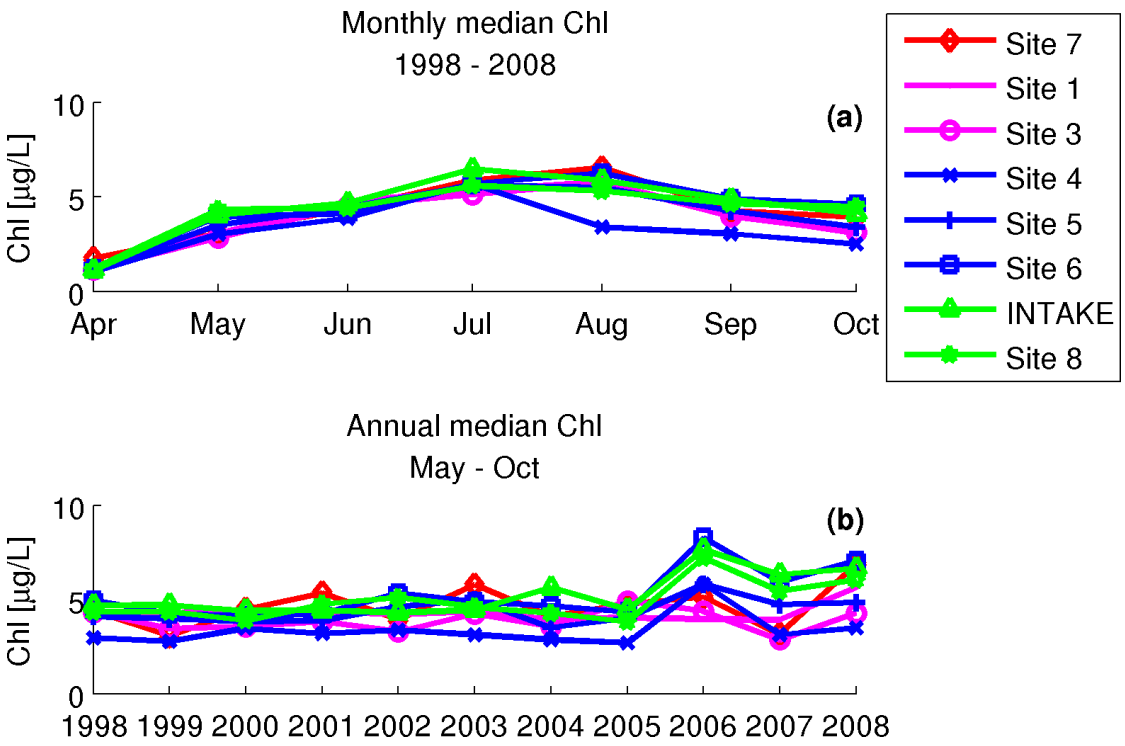

Figure 5.16: Median chlorophyll-*a* levels. a) annual median concentration at each site (all months of each year averaged) b) monthly median concentrations at each site (values of each month in all years averaged)

Table 5.5: p-values of two-sample chlorophyll-*a* comparisons, May - October, n=156. In each case the null hypothesis that the means/medians of respective sets are equal is tested against the listed alternative hypothesis.

hypothesis	**two-sample t-test**	**rank sum test**
deep water 1998-2005 < 2006-2008	0.005	0.001

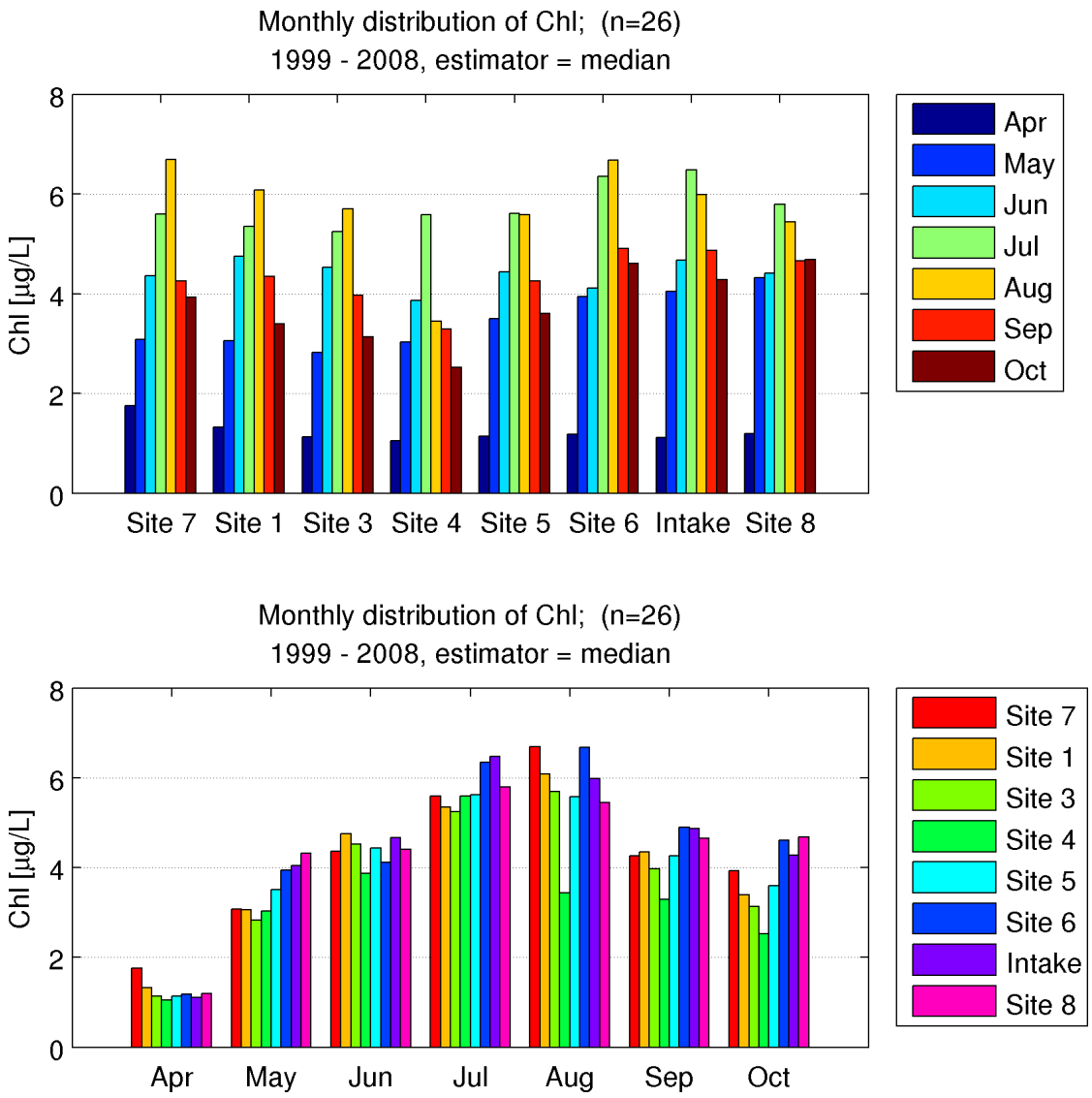

Figure 5.17: Monthly median chlorophyll-*a* grouped by site and by month. Order of sites is geographical by distance from the southeast corner of the lake.

Scatter plots of chlorophyll-*a* observed synoptically at the shelf sites are presented in figure 5.20. Correlation of individual sites with each other and with the weighted shelf-average is generally high, with the exception of site 4, which tends to be lower than the other sites and site 7 which tends to be higher. The seasonal trends of chlorophyll-*a* concentrations both on the shelf and in the deep

water sites are also evident from the scatter plots of synoptic shelf-averaged and deep water observations in figure 5.19.

In contrast to the case with phosphorus, the mean deep water site chlorophyll-*a* concentration tends to be higher than the weighted shelf-average chlorophyll-*a* (TP tends to be higher on the shelf). Differences between the shelf and the deep water sites are smaller for observed chlorophyll-*a* concentrations, however (figure 5.13).

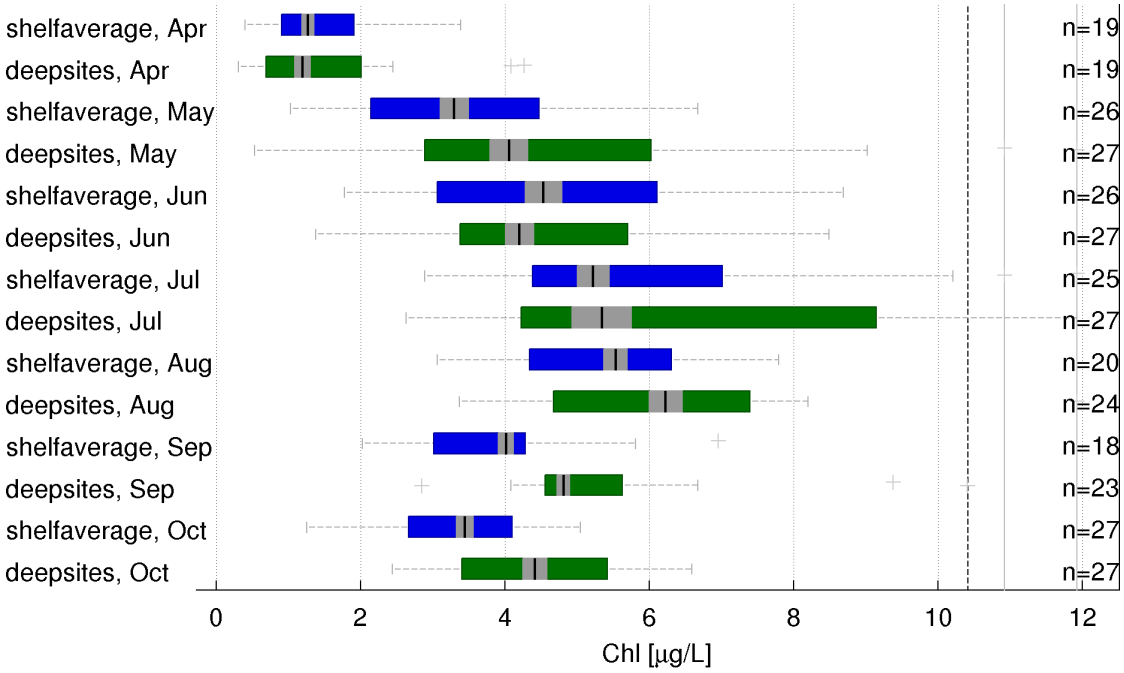

Figure 5.18: Box plots of shelf-averaged and mean deepwater (sites 6, 8, Intake) chlorophyll-*a* for each month, over the entire record. The horizontal scale is compressed to the right of the dashed black line in order to fit outlying values into the plot.

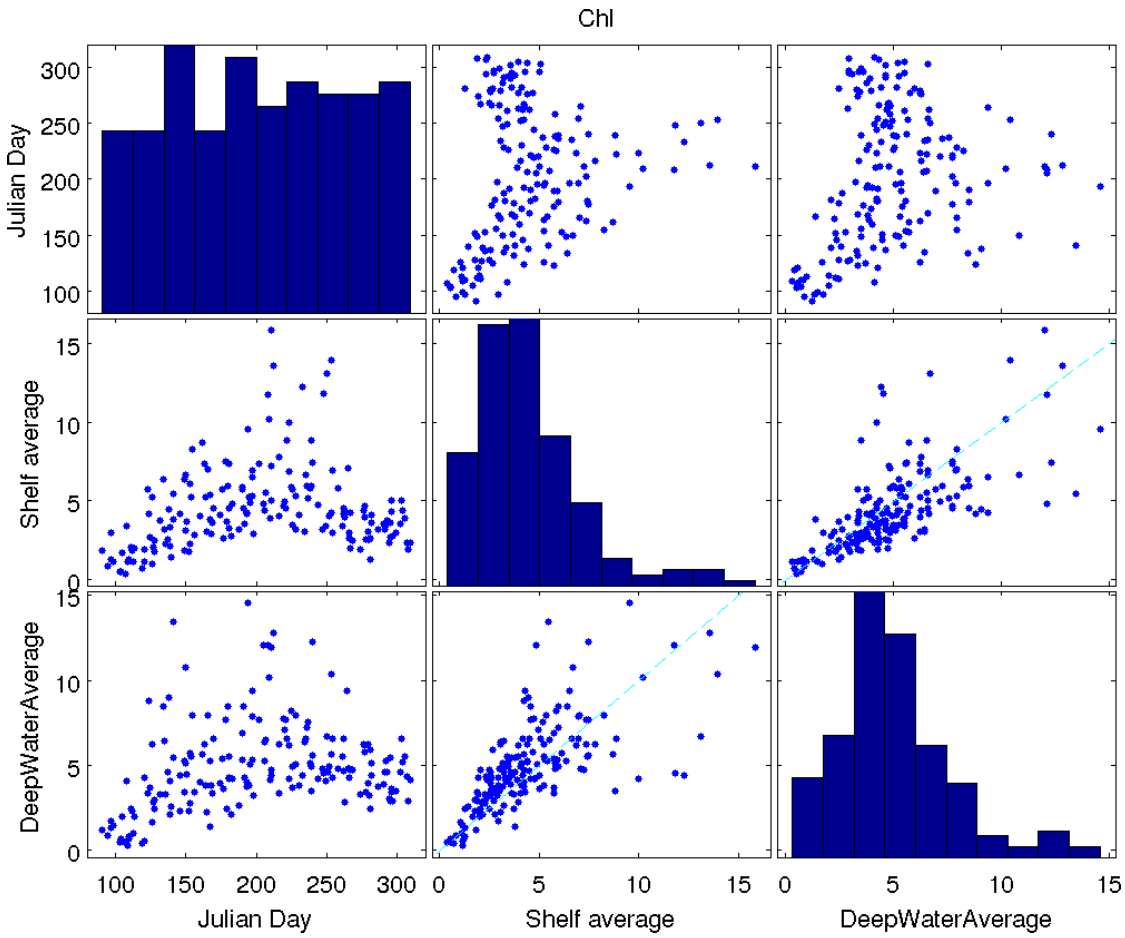

Figure 5.19: Scatter plots of observed shelf-averaged chlorophyll-*a* and averaged deep water (sites 6, 8, Intake). Each plot in this figure shows a scatter of two forcing parameters over the eleven year record, with each dot representing a single sampling date. Chlorophyll-*a* values are in $\mu g/L$. Dashed lines indicate location of perfect correlation (i.e., lines of $x = y$). Plots along the diagonal are histograms of the corresponding metric. Plots that are located symmetrically relative to the diagonal compare the same data, but are presented with different aspect ratios.

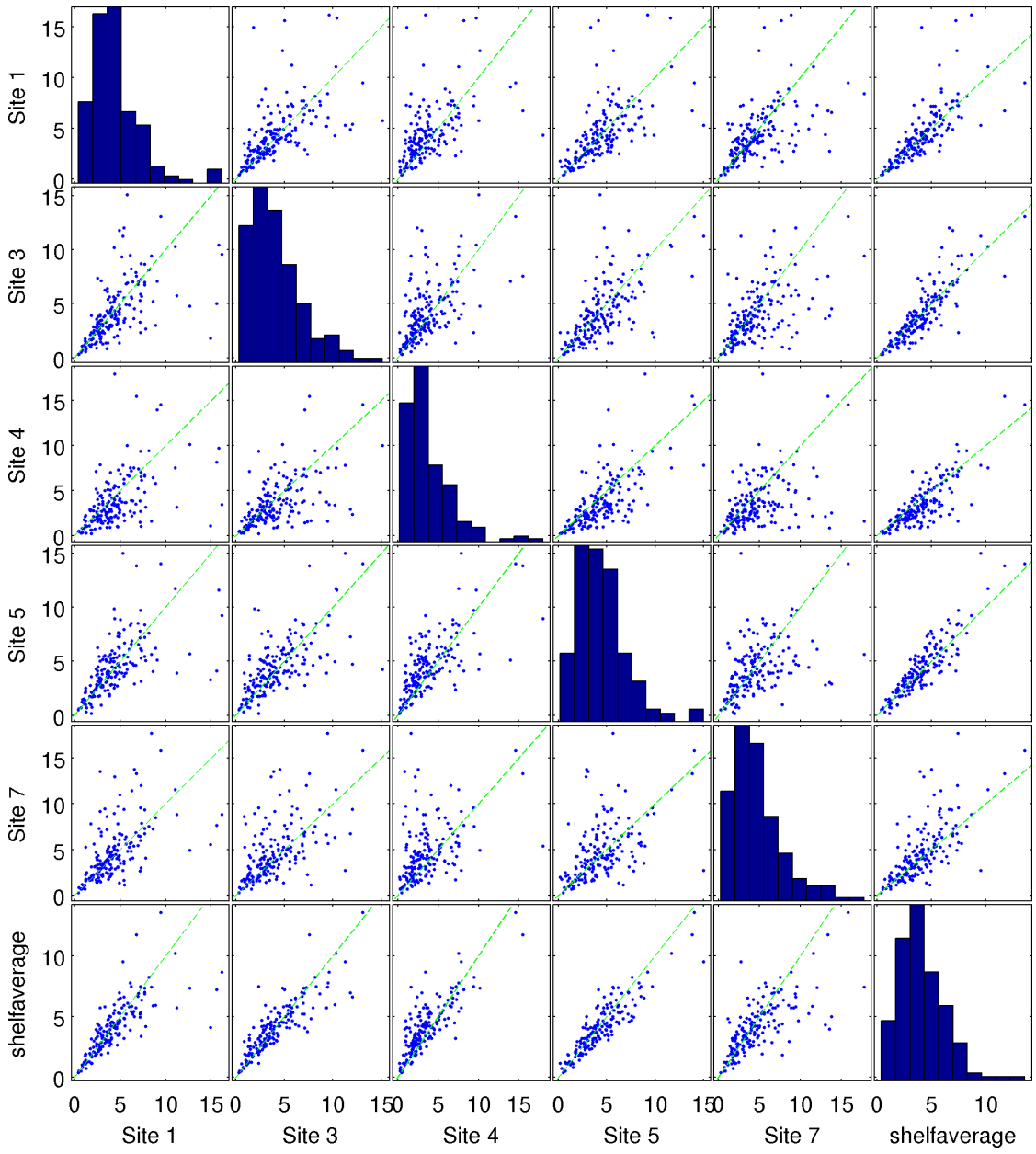

Figure 5.20: Scatter plots of observed chlorophyll-*a* at the shelf sites, during the stratified season (August - October). Each plot in this figure shows a scatter of two forcing parameters over the eleven year record, with each dot representing a single sampling date. Chlorophyll-*a* values are in $\mu g/L$. Dashed lines indicate location of perfect correlation (i.e., lines of $x = y$). Plots along the diagonal are histograms of the corresponding metric. Plots that are located symmetrically relative to the diagonal compare the same data, but are presented with different aspect ratios.

5.2 Event related water quality record

The distributions of observed shelf-averaged (equation 5.1) values of the four measured water quality parameters from the entire 11 year period are presented in figure 5.21. These distributions are strongly skewed, especially the TP and turbidity distributions which have several extreme values not continuous with the rest of the distribution. The SRP and chlorophyll-*a* are also strongly skewed but they are more continuous even in the higher range of values. The forcing conditions surrounding the dates of some of the extreme TP and turbidity observations are discussed in the following sections. While the specific cases discussed here are examples of exceptionally high water quality parameter observations, the forcing conditions that caused them are not as exceptional when considering the full forcing record (including in between sampling dates). It is therefore likely that similarly high levels of TP and turbidity existed on the shelf at several other times but were missed because they they did not occur on scheduled sampling dates. Capturing the response of the shelf's water quality to these forcing conditions depends on the coincidence of sampling dates and forcing conditions. This is one of the limitations of a fixed schedule of sampling of such low temporal resolution (biweekly sampling while the timescale of major flow events and upwelling events is on the order of days).

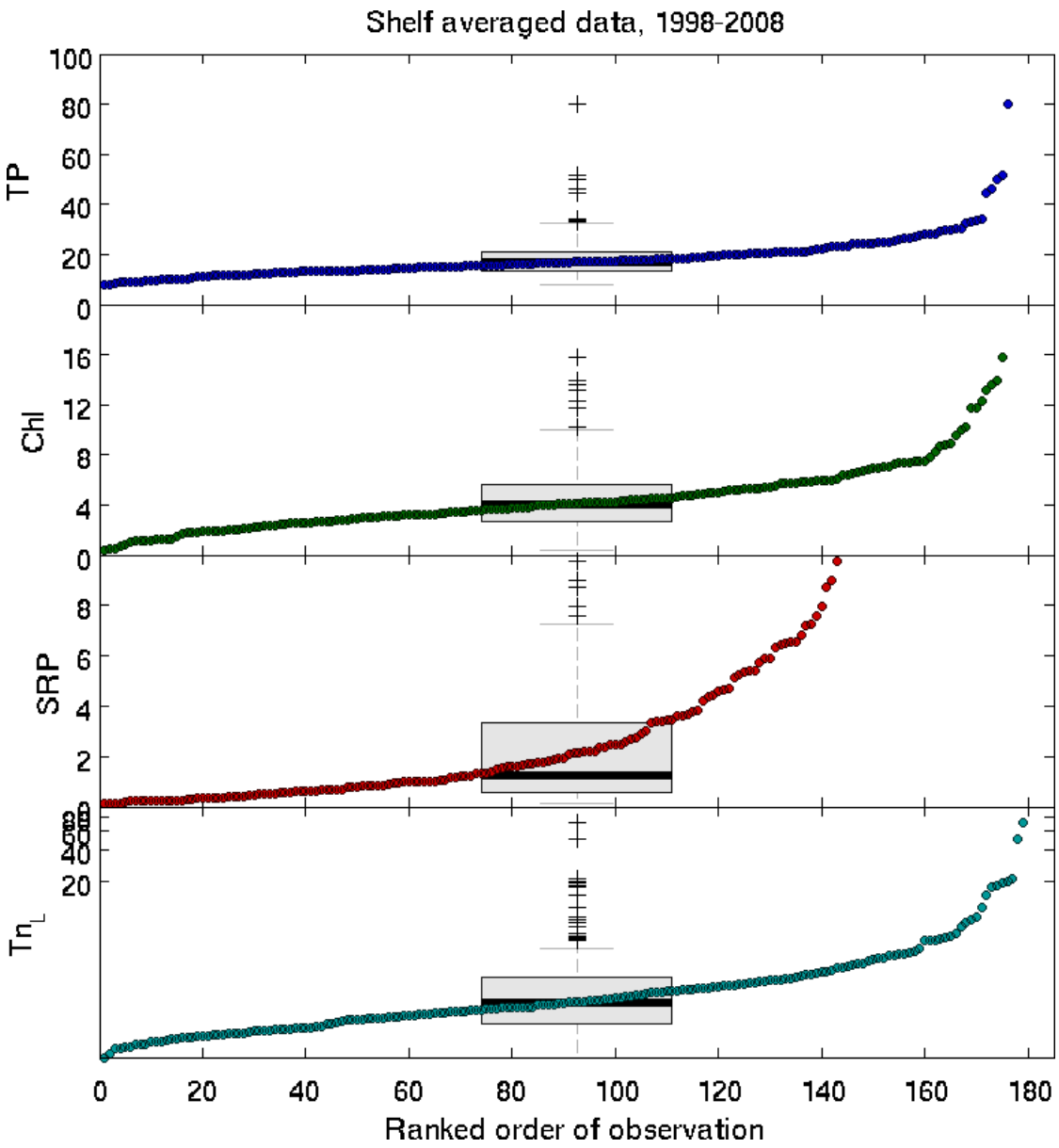

Figure 5.21: Ranked values of shelf-averaged water quality parameters from the entire 1998 - 2008 period (SRP data are from 2000-2008), and box plots of their distributions. Note the logarithmic scale on the turbidity plot.

The following is a discussion of the forcing conditions and water quality response of the shelf on the three dates on which highest shelf-averaged TP was observed. These three dates are used as examples of forcing conditions

and the response of the shelf in the form of elevated TP and Tn, in order to illustrate various processes that affect the water quality of the shelf. These are extreme examples and as such they are useful to isolate the effects of certain forcing conditions. In most cases the forcing of the shelf is more moderate, but the same processes described here will still play a part in determining the water quality on the shelf.

In the first example (section 5.2.1) high tributary flow leads to a shelf-wide response. In the second and third examples upwelling conditions coupled with high loading from point sources (section 5.2.2) or moderately elevated tributary flow (section 5.2.3) cause a more localized response on the shelf.

5.2.1 06/29/2006, shelf-averaged TP = 80.0 $\mu g/L$

The highest shelf-averaged value of TP observed during the entire sampling period was $80\,\mu g/L$ recorded on 06/29/2006. The highest shelf-averaged turbidity value in the record was also observed on this date (70 NTU). This sampling date coincided with a very high tributary flow event - daily mean discharge in Fall Creek peaked at 60 m^3/s the previous day. Forcing conditions and water quality response are presented in figure 5.22. This plot summarizes the forcing conditions and observed water quality on the shelf in 2007. Wb numbers are presented in the range $|Wb| < 10$. As discussed in section 4.3.2 the range of Wb is of more interest than its precise value for the purposes of the analysis presented here. When $Wb \approx 0$, such as in April and May, it signifies the lake not yet being stratified (the calculated Wb is valid under these conditions, but it does not have much utility). In the later months of the year the Wb lies outside of the plotted

range much of the time. Since the significance of $|Wb| \gg 1$ is the same regardless of its actual value - it means that the wind is not strong enough to play an important role - it is not plotted here.

High flow rates in the tributaries are generally accompanied by increased turbidity. The main source of TP to the shelf is from the tributaries, with large or dominant fractions in the form of particulates, which increases during high flow events (e.g., UFI, 2007). As shown in table 5.6 both turbidity and TP were extremely high on this date on all shelf sites and even as far north as site 6.

Table 5.6: Shelf water quality as observed on 06/29/2006

Site	**TP** $\mu g/L$	**Tn** NTU
shelf-average	80.03	70.39
Site 1	66.8	56.2
Site 2	105.6	124.0
Site 3	97.9	84.0
Site 4	83.9	78.4
Site 5	57.5	42.4
Site 6	58.1	43.3
Site 7	94.8	97.3
Site 8	22.5	3.6
LSC Intake	24.1	6.6

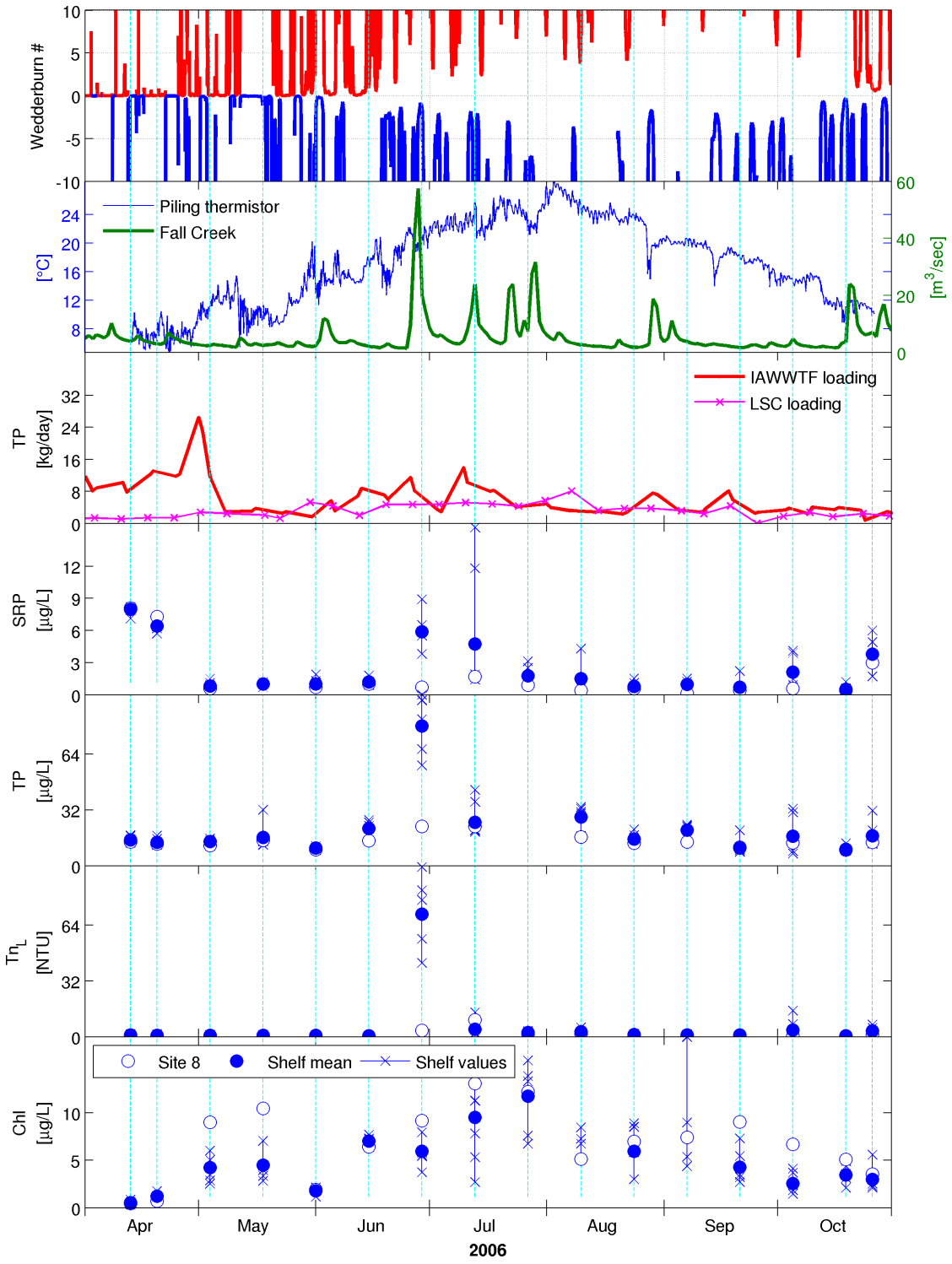

Figure 5.22: Forcing conditions and resulting water quality, 2006

5.2.2 08/21/2007, shelf-averaged TP = 51.7$\mu g/L$

The second highest shelf-averaged TP value of the 11 year record was observed on 08/21/2007. On this date the shelf-averaged TP was 51.7$\mu g/L$, mainly due to extremely high levels (> 100$\mu g/L$) at site 3 and site 7 (table 5.7). Tributary flow on this day and during the preceding days was base flow (Fall Creek flow rate was <1 m^3/s, typical for August). The apparent cause of the high concentrations of TP observed on this day is loading from the two wastewater treatment plants, coupled with the hydrodynamic effects of an upwelling event (figure 5.23). TP concentration in the IAWWTF effluent (as measured by the plant's operators) was 330 $\mu g/L$ on 08/20/2007 and 270 $\mu g/L$ on 08/21/2007. Detailed data on the CHWWTP discharge on this date were not available, however the average effluent concentration of TP from that source was approximately 500$\mu g/L$ during the month of August at a flow rate about one-fifth that of the IAWWTF (mean August 2007 discharge rate was $19.6 \cdot 10^3\ m^3/day$ from the IAWWTF and $4.1 \cdot 10^3\ m^3/day$ from the CHWWTP).

The proposed effect of the upwelling event on this day was reduction of mixing and transport of the loads from the two wastewater effluents. As described in section 4.4.1, when an upwelling event occurs the interface between the epilimnion and hypolimnion tilts to such an extent that it approaches the lake's surface in the vicinity of the shelf break. This causes the southern portion of the shelf to become isolated from the main lake's epilimnion (figure 4.7d). Mixing between the trapped shelf water and the upwelled hypolimnetic water occurs at a relatively low rate because of the difference in density between these two fluids. The effect is of "blocking" exchange off of the shelf, which leads to increased TP concentrations in the vicinity of the loading sources.

Interestingly, although TP concentrations were elevated at site 2, the site most proximate to the IAWWTF outfall, they were much lower than those measured at site 3 and site 7 which are located near the IAWWTF and CHWWTF outfalls, respectively. The fact that TP concentrations measured at site 2 were not as high as those measured at site 3 can perhaps be due to meandering of the effluent plume, or to site 2 being located more directly in the path of the inflow from the two major tributaries.

Other potential loading sources that might have caused the increased TP levels can be ruled out for the following reasons:

Tributary flow: Not only was the flow rate in the tributaries very low as recorded by the USGS stream gage on Fall Creek, but measured turbidity levels in the lake were very low on that day (less than $2\,NTU$ on all shelf sites except site 2, less than at site 1 and site 3 - similar to turbidity measured off the shelf at site 6 and site 8). Any significant flow from surface runoff would be accompanied by elevated turbidity. Turbidity in the effluents of the three point sources is generally very low (less than $1\,NTU$).

LSC: The LSC discharge's TP concentration was $16.3\,\mu g/L$ on 08/20/09 and was at similar or lower levels during the weeks surrounding this date. In general, as is evident from figure 5.23, the TP concentration in the LSC discharge is much lower than that of the two wastewater treatment plants' discharges. The LSC discharge can not therefore be the cause of highly elevated TP concentrations observed on the shelf on this and other occasions.

Exchange between the shelf and the hypolimnion: The LSC discharge is essentially a sample of hypolimnetic water, so the TP concentration measured there is the same as that of any water advected on to the shelf due to internal seiching or upwelling events. This TP concentration is too low (by about 85%) to be a cause of the elevated TP measured on the shelf on 08/21/2007. Runup of internal waves on the shelf's slope could theoretically cause resuspension of phosphorus rich sediments or pore water. However the extremely high TP levels were observed only at two of the sites that are among those most distant from the shelf break, and resuspension would cause an increase in turbidity which was not observed. More importantly the TP levels observed at site 1 and site 5, which is near the shelf break, were essentially identical to that measured in the LSC outfall (table 5.7) which is a sample of the hypolimnion. Measurements at site 5 are most likely the best indication of direct interaction of shelf waters with the hypolimnion or the effects of shoaling internal waves. It is therefore very unlikely that the extreme TP levels observed at sites 3 and 7 were caused by interaction with the hypolimnion.

Although the loading from IAWWTF on 08/21/2007 was above average, concentrations of 330 $\mu g/L$ in that effluent are not very unusual even after the plant's tertiary treatment was installed. Prior to 2005, when upgrades to the plant's treatment significantly reduced TP phosphorus output, TP concentrations in the effluent were typically around 500 $\mu g/L$ (daily discharge volumes have remained similar before and after the upgrades, a summary of loading rates is presented in table 3.3). It is therefore logical to assume that high TP concentrations in the plant's effluent are not by themselves enough to cause

such a strong response on the shelf (recall that this is the second highest shelf-averaged TP value of the entire 11 year period). Moreover during the following sampling date, 09/04/2007, the IAWWTF effluent TP concentration was still well above the seasonal average (though not as high as on 08/21/2007), tributary flows were similar but no upwelling occurred on that date (figure 5.23). On 09/04/2007 none of the shelf sites had significantly elevated TP (shelf-average of 11.9 $\mu g/L$ with a maximum of 15.8 $\mu g/L$ at site 7 excluding site 2).

A note on the timing of the upwelling event: At first glance at figure 5.23 it might look like the upwelling event occurred after the sampling date. This is not actually the case. Although the maximum dip in the temperature record at the piling cluster thermistor did indeed happen after the sampling date this marks the time at which the upwelling front reached the location of the thermistor (which is between site 2 and site 3). An upwelling front progresses up the shelf from the north for a period of hours or even days before reaching the piling cluster depending on the strength and stability of the wind and the density difference across the front. As the front progresses up the shelf from north to south little or no information of this happening is available at the piling cluster (although in this case a small drop in temperature at the piling cluster was seen a day or two before the main front arrived). In fact in cases in which the *Wb* number drops low enough to cause upwelling but not for a sufficient period for the front to reach all the way up the shelf to the piling cluster no indication of upwelling may be present in the thermistor record. This type of situation is easily found at several times in the record during 2007 and other years. The thermal record at the piling cluster alone tells only a partial story - it only captures the most extreme of upwelling events.

A closer look at the wind forcing and a comparison of the temperature record at the piling cluster and surface water temperature measured by the RUSS is presented in figure 5.24. The time lag between the two markers on the respective RUSS and piling cluster records is 9.25 hours from which an approximate rate of 4 cm/s is calculated for the progress of the front up the shelf. This is a loose estimate - comparing the time at which equal temperatures were recorded at the two sites is imperfect due to entrainment as the front progresses along the shallow shelf.

Table 5.7: Shelf water quality as observed on 08/21/2007

Site	**TP** $\mu g/L$	**Tn** NTU
shelf-average	51.65	1.36
Site 1	16.7	0.9
Site 2	39.5	2.1
Site 3	101.1	0.8
Site 4	23.1	1.7
Site 5	16.4	1.6
Site 6	14.2	0.8
Site 7	115.3	1.8
Site 8	14.2	0.9
LSC Intake	13.9	1.0

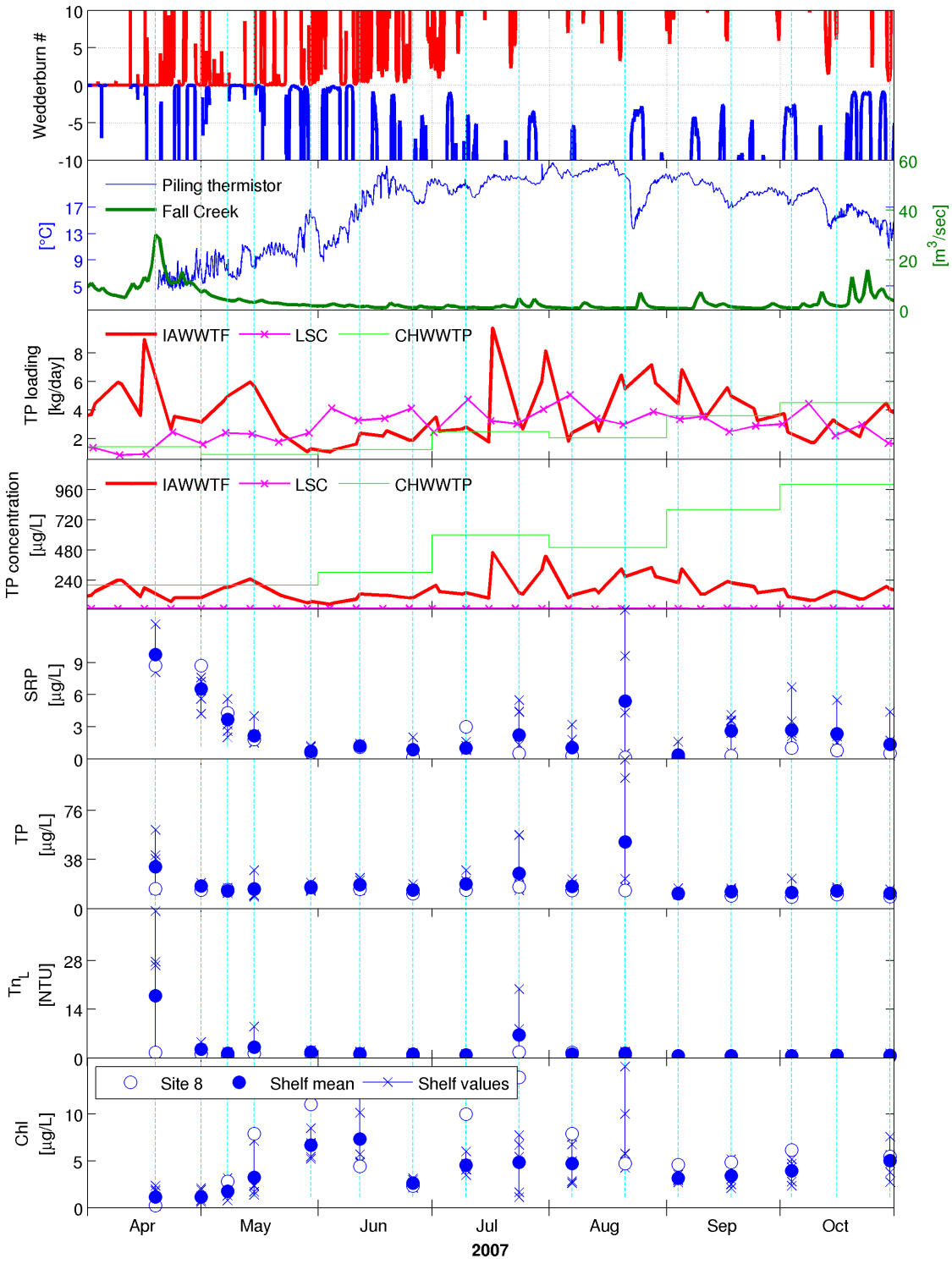

Figure 5.23: Forcing conditions and resulting water quality, 2007

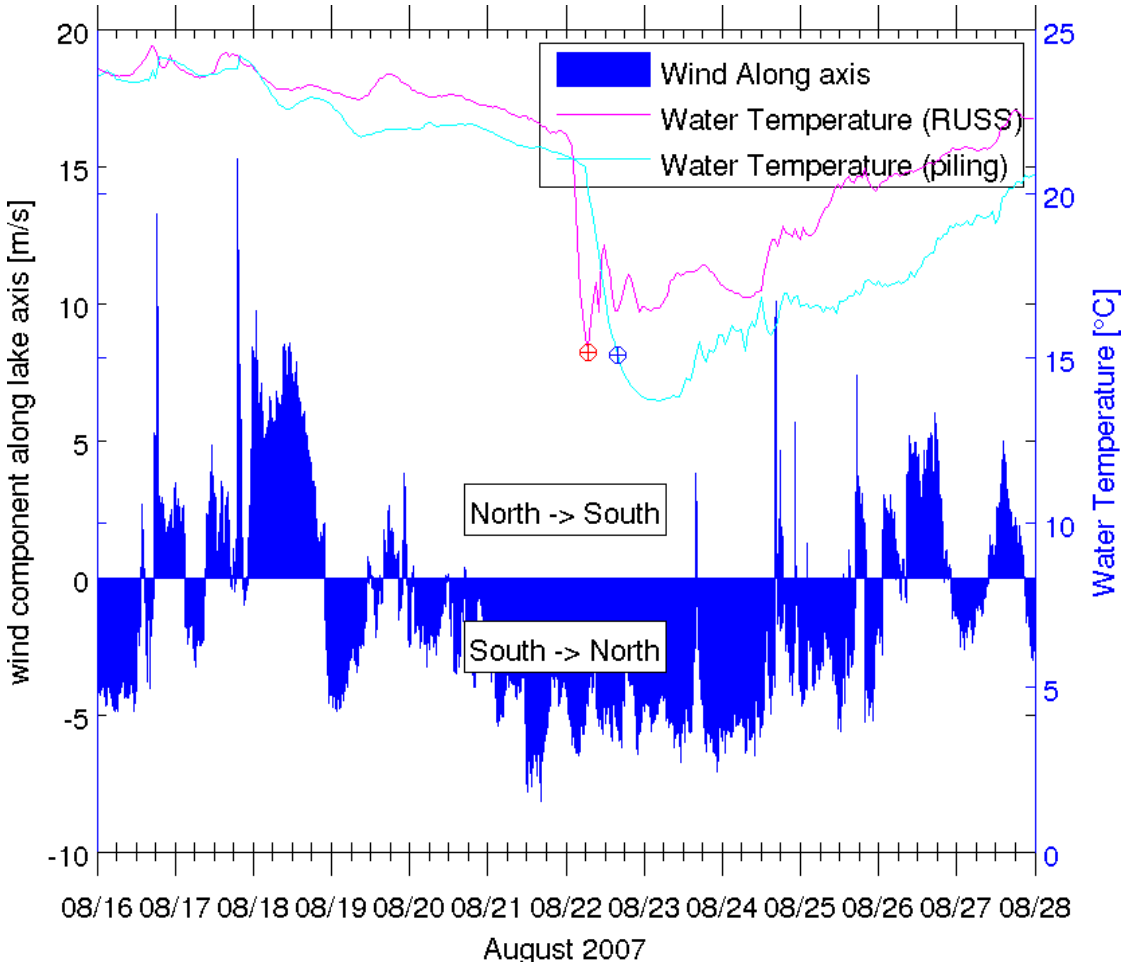

Figure 5.24: Comparison of temperature record at RUSS and piling cluster, 08/21/2007. Analysis of the time lag between two measurements of equal temperature at the RUSS and piling thermistors (indicated by the $\oplus$ symbols) yields an upwelling front progression rate of approximately 4 cm/s.

5.2.3 09/09/2004, shelf-averaged TP = 49.9 $\mu g/L$

The third highest shelf-averaged value of TP observed was 49.9 $\mu g/L$ recorded on 09/09/2004. This sampling date coincided with a moderately high tributary flow event - daily mean discharge in Fall Creek peaked at 25 m^3/s the same day

that water samples were collected. In addition, upwelling conditions existed on the shelf on and around this date. TP and turbidity values measured during this event are listed in table 5.8 and are presented along with the forcing conditions in figure 5.25. Extremely high TP and turbidity was observed at site 3 and site 2. TP was elevated at sites 1 and 4, and to a lesser extent at site 7 as well. Turbidity was observed to be elevated at sites 1, 2, 3 and 4 but not at site 7. A likely explanation for this is that the source of high TP and Tn at sites 1, 2, 3 and 4 was from surface runoff, but the elevated TP at site 7 was a result of phosphorus loading from the CHWWTP outfall since it was not accompanied by increased turbidity. The flow from the tributaries enters the lake south of sites 2 and 3, and the plume subsequently widened causing the elevated metrics at sites 1 and 4. The effect of the upwelling event was to slow the rate at which the plume from the tributaries mixed out into the main lake basin (i.e., it increased the residence time on the shelf). This would explain why elevated TP and Tn were observed on the shelf on this day, but not on other sampling days on which similar surface runoff conditions existed (e.g., a runoff event on the last sampling date in July of the same year on which surface flow was similar but TP levels observed on the shelf were much more moderate; figure 5.25). The main differences in forcing conditions between this event and the one observed on 06/29/2006 (section 5.2.1) were much lower tributary flow rates in this case (25 vs. 60 m^3/s daily average flow rate in Fall Creek), and the fact that upwelling conditions existed on the shelf for several days leading up to the storm event. In the 06/29/06 event the highest TP and turbidity levels measured were actually not as high as those observed on the 09/09/2004 event, despite the fact that tributary flow rates were more than twice as high. However highly elevated levels of TP and turbidity were observed at all the shelf sites and even as far north as

site 6. In the current event the response of the shelf was more localized. This event therefore could be characterized as having extreme localized effects, with very strong spatial gradients between sites on the shelf. The main source of TP and turbidity in this event was tributary flow, and the highest values of both of these metrics were observed at sites 2 and 3 which lie directly in the path of the inflow from Fall Creek and the Cayuga Inlet. The surface flow coincided with upwelling conditions on the shelf, which reduced the rate at which the high TP and Tn water was mixed out into the main basin of the lake. This is evident from the increased levels of TP and Tn at sites 1 and 4 - on the shelf - and the sharp gradient between site 3 and site 5. Site 5 is located north of site 3, closer to the shelf break. TP and Tn values measured at site 5 during this event were essentially at baseline levels, which was possibly caused by the upwelling event blocking the high TP and Tn water from reaching this site.

Table 5.8: Shelf water quality as observed on 09/09/2004

Site	**TP** $\mu g/L$	**Tn** NTU
shelf-average	49.9	49.74
Site 1	42.1	15.0
Site 2	144.5	118.0
Site 3	116.3	182.0
Site 4	38.3	7.3
Site 5	11.4	1.2
Site 6	12.1	1.0
Site 7	25.2	2.0
Site 8	13.4	0.8
LSC Intake	12.8	1.0

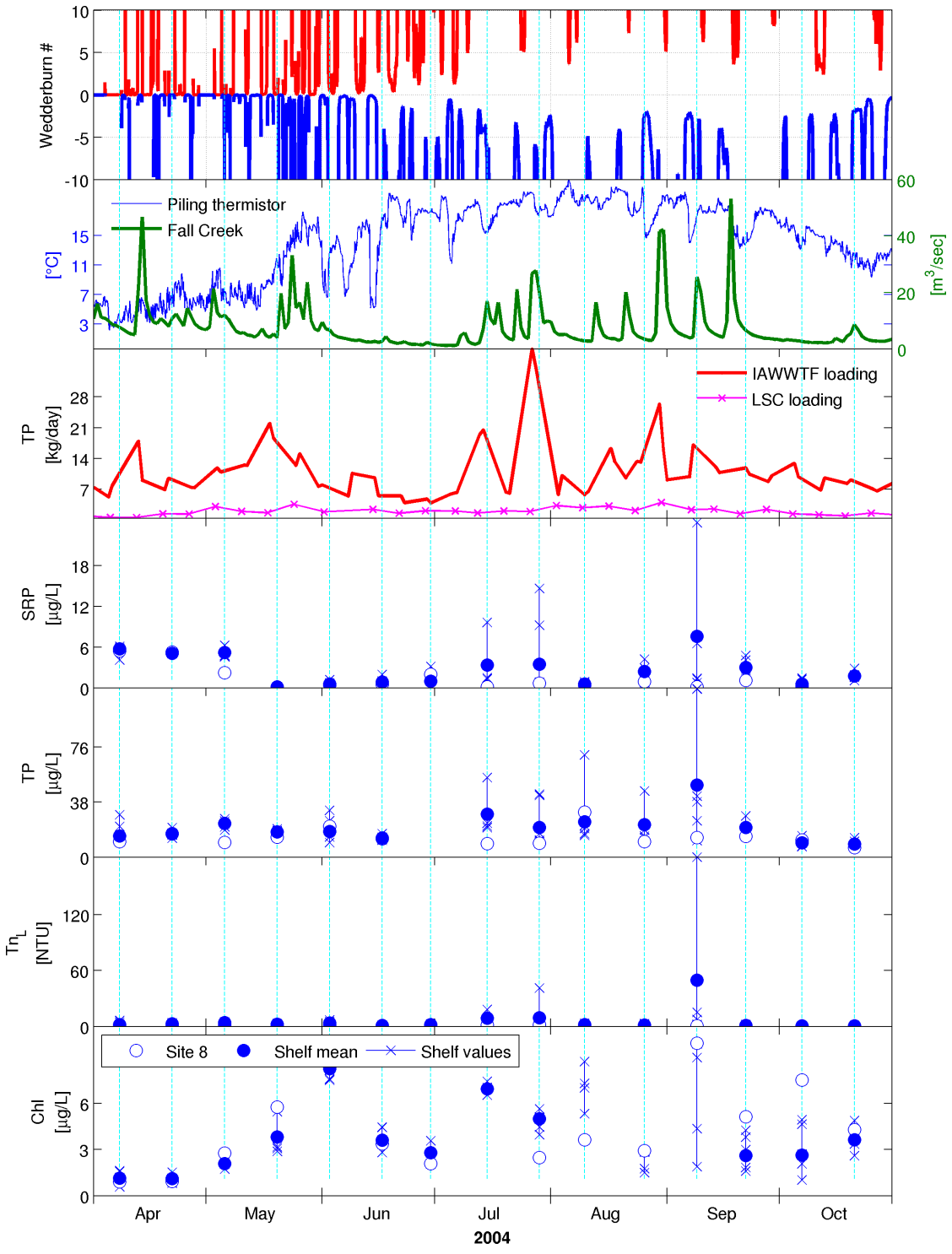

Figure 5.25: Forcing conditions and resulting water quality, 2004

5.3 Temporal correlation of various forcing conditions

The temporal correlation of different forcing factors is presented in figure 5.26. Each plot in this figure shows a scatter of two forcing parameters over the eleven year record, with each dot representing a single sampling date. Histograms of the various forcing conditions are plotted along the diagonal. Units plotted are mass loading in kg/day for the LSC and IAWWTF and Fall Creek flow rates in cfs representing flow in tributaries.

From this figure it is apparent that the IAWWTF loading is not well correlated with any of the other parameters, Wb values are essentially zero during the early and late season when the lake is not stratified and are negative (indicating thermocline tilted up near the southern shelf) more often than positive during the stratified period. The LSC loading follows a seasonal pattern with peak loadings during the hottest months due to increased flow rates - whereas tributary flows rates are much higher in the early season (April-June) than later in the season. For this reason higher LSC loading rates generally occur at times of lower tributary flow rates. The majority of the time during which Wb is non-zero is during lower tributary flow periods of the season.

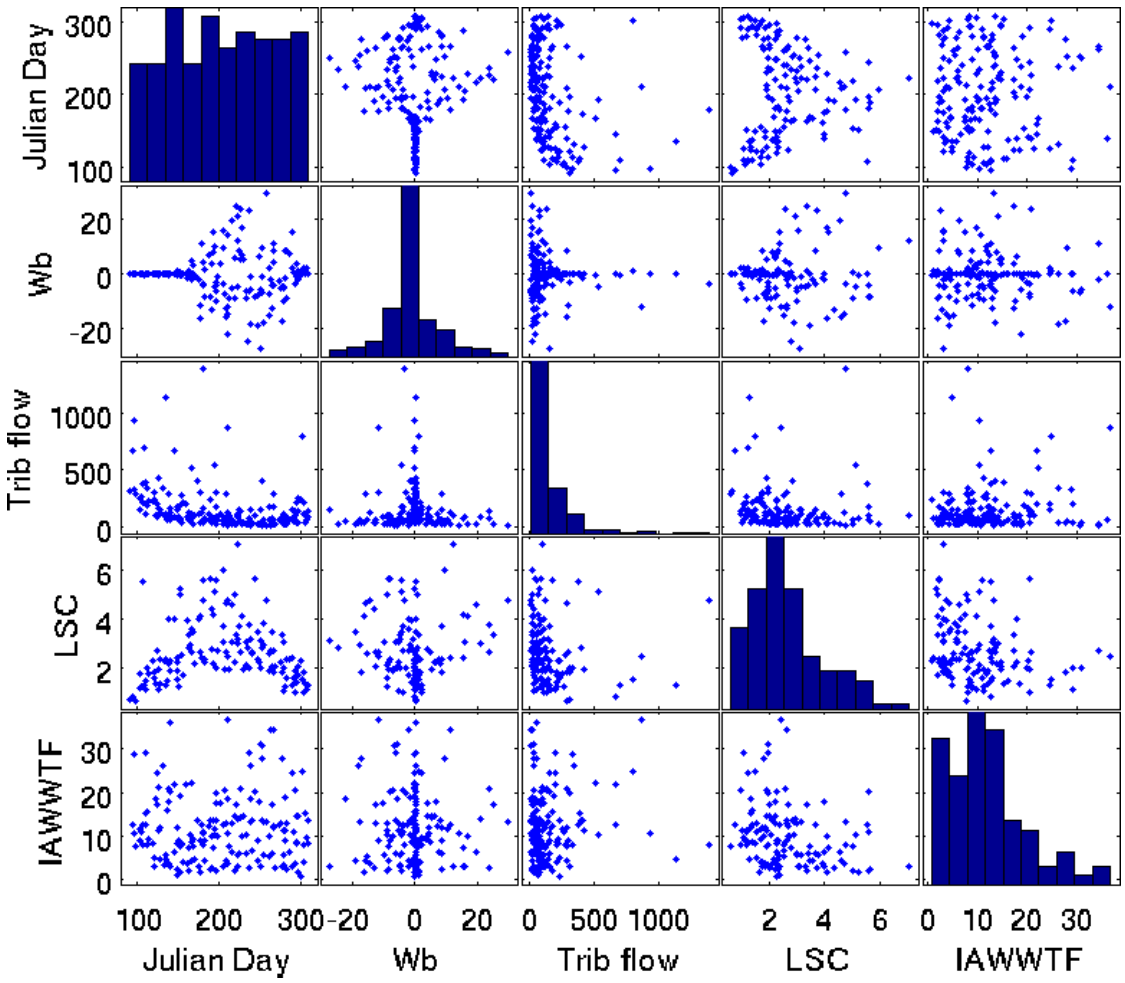

Figure 5.26: Temporal correlation of forcing conditions. Each plot in this figure shows a scatter of two forcing parameters over the eleven year record, with each dot representing a single sampling date. Histograms of the various forcing conditions are plotted along the diagonal. Tributary flow is in cfs, LSC and IAWWTF loading are in kg/day TP. Plots that are located symmetrically relative to the diagonal compare the same data, but are presented with different aspect ratios.

5.4 Correlation of forcing conditions and water quality observations

As discussed in section 5.2 the data strongly suggest that extreme forcing events can have a dramatic effect on the water quality of the shelf. The following sections examine the effects of more moderate forcing conditions. In order to do so, a time history of forcing conditions was constructed including the forcing caused by IAWWTF and LSC (TP loading), flow rates in Fall Creek and the *Wb* number on and around each sampling date.

For this purpose, mean values of mass loading from IAWWTF, LSC and the mean flow rate in Fall Creek were calculated over a period beginning two days before each sampling date (the point source data are reported on a weekly or semi-weekly basis and daily values were linearly interpolated from those data for the purpose of this calculation). The selection of a three day window for this averaging is somewhat arbitrary, but is based on an estimated flushing rate of the shelf of order 1 day (timescale of renewal of all water on the shelf) as estimated by Effler *et al.*, Submitted December 2009). For the *Wb* history the median value of *Wb* was calculated from a period beginning two days before the sampling date and ending one day after it. The averaging window was extended until after the actual sampling date to include upwelling events that had begun but were not yet fully developed at the time of sampling (see discussion in section 5.2.2). The median (rather than the mean) was selected as an estimator for this metric since *Wb* can have a very large range of values in a short period of time as the wind fluctuates (recall from equation 4.1 that the square of the velocity of the wind appears in the denominator of *Wb*).

The figures in this section include box plots similar to those described in the introduction to this chapter. The plots include comparisons of the distribution of water quality properties observed under specific forcing conditions i.e., a set of forcing conditions was defined, then the 11 year sampling record was examined to find dates matching these conditions and the water quality properties were calculated from observations on those dates. The forcing conditions used to select each subset of sampling data are listed on the plots. They include some or all of the following for each element of the plots - sampling sites, month of sampling, condition on Wb; either $Wb < 0$ for upwelling or $Wb > 0$ for downwelling, and percentile for point source loading and flow in Fall Creek. Percentiles were calculated out of the set of values on the sampling dates (as described in this section). The percentages listed on the plots are the percentiles and if the condition was over or under this value (e.g., IAWWTF<35% indicates all instances in which loading from the IAWWTF was below the 35^{th} percentile). If a forcing condition is not listed, all values of that parameter would be acceptable in creating the subset of sampling dates.

5.4.1 South to north gradients

The south to north gradient in TP described in section 5.1.2 is examined more closely here. From figure 5.27 we see that when observed TP levels at sites 3, 5, and 6 are compared during the stratified (August - October) and non-stratified months (April - July), similar distributions of observed values exist but they are shifted down during the stratified period. Site 3 has the highest median and widest distribution of observed values in both cases. The record during the stratified period is also plotted in the same figure separating sampling dates

around which IAWWTF loading was above and below its median loading value (median of loading on each sampling date in the 1998 - 2008 record). This subdivision makes little difference to values at sites 5 and 6 - in both cases the distributions for these sites are similar to that of the combined set. However the record at site 3 shows higher values of TP at times when loading from IAWWTF is above its median value. Median TP values under various conditions are presented in table 5.9.

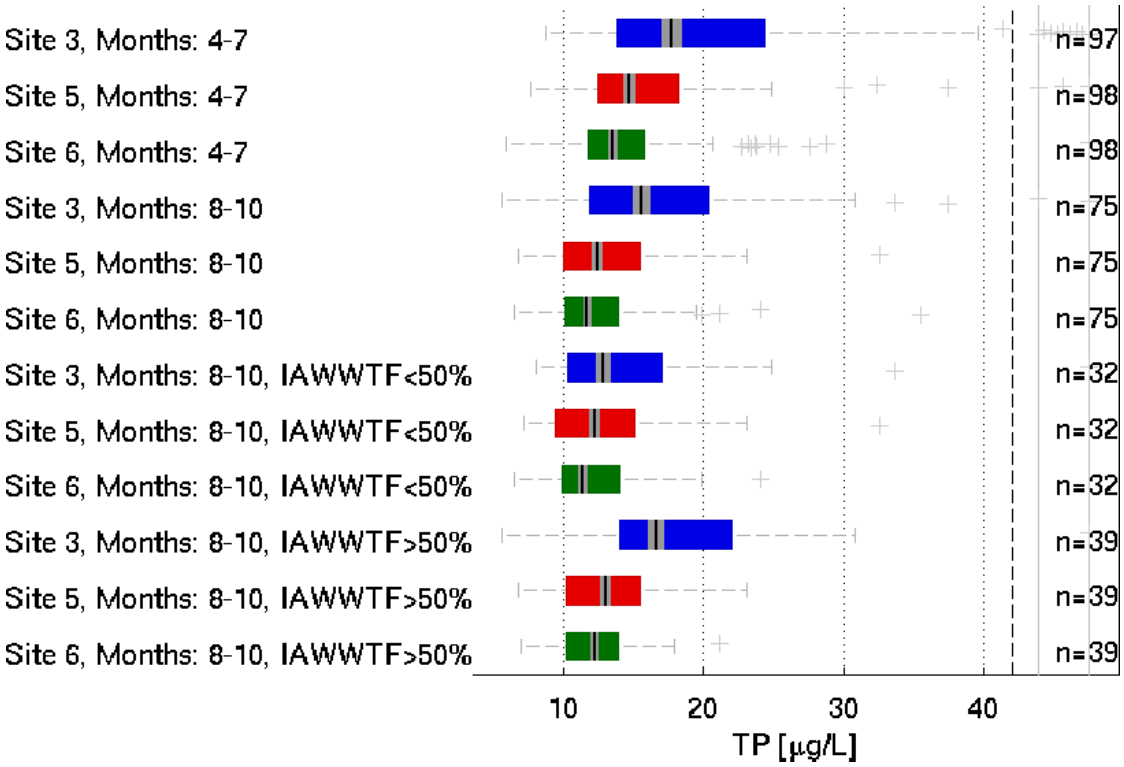

Figure 5.27: Box plots of TP measured at sites 3, 5, 6 during unstratified period (months 4-7), stratified period (months 8-10), stratified period with below median IAWWTF loading and stratified period with above median IAWWTF loading. Bold lines mark median values, grayed area around the median is the 95% confidence interval. The horizontal scale is compressed to the right of the dashed black line in order to fit outlying values into the plot.

This subset of the data is subdivided further in figure 5.28 which presents the TP distributions during the stratified months on dates when IAWWTF loading was above median, for all values of the Wb number, as well as separately for dates on which $Wb < 0$ (thermocline tilted up) and days on which $Wb > 0$ (thermocline tilted down). Median TP at site 3 was the same for the general case and when $Wb < 0$, and slightly lower when $Wb > 0$ (table 5.9), although the difference is not statistically significant (table 5.10). TP at sites 5 and 6 was lower when $Wb < 0$ than for the general case and higher when $Wb > 0$.

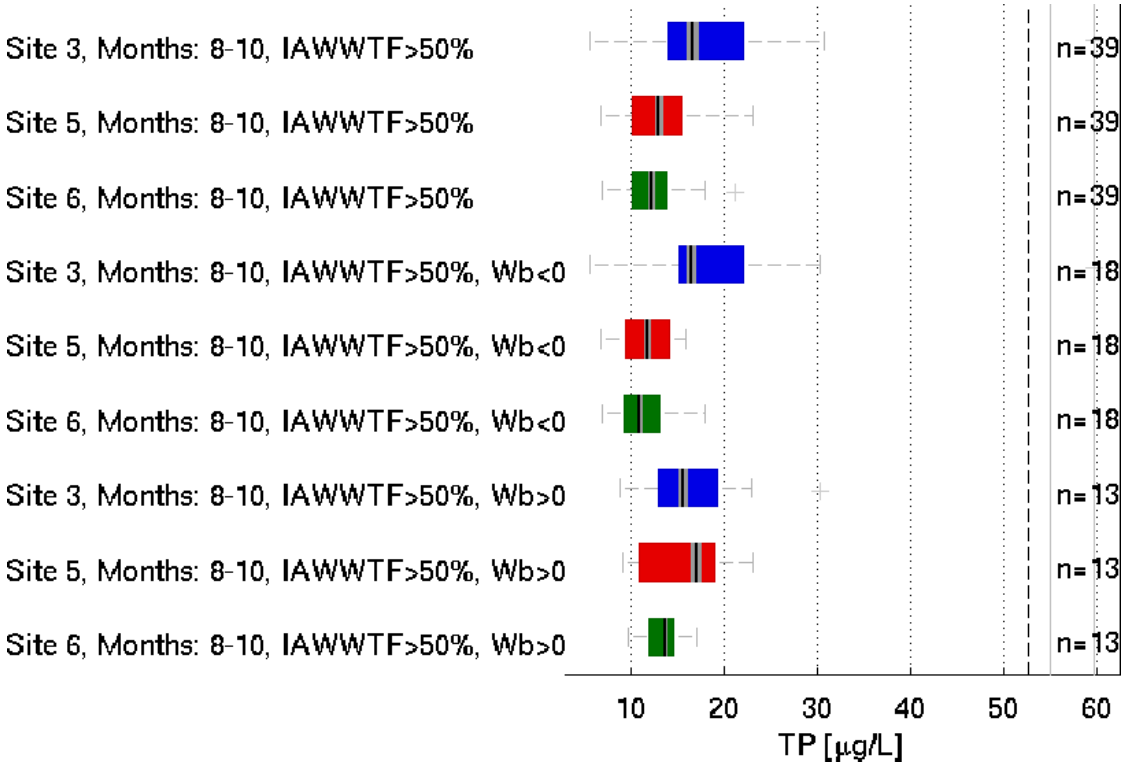

Figure 5.28: Box plots of TP measured at sites 3, 5, 6 during stratified period (months 8-10) with IAWWTF above median for any Wb value, and for conditions where the thermocline is tilted up ($Wb < 0$) or down ($Wb > 0$) near the shelf. Bold lines mark median values, grayed area around the median is the 95% confidence interval. The horizontal scale is compressed to the right of the dashed black line in order to fit outlying values into the plot.

Table 5.9: Median TP at sites 3, 5, 6 under various forcing conditions

Forcing conditions	**Site 3**	**Site 5**	**Site 6**
April - July	17.7	14.7	13.5
August - October	15.6	12.4	11.7
August - October, IAWWTF < 50% loading	12.9	12.2	11.4
August - October, IAWWTF > 50% loading	16.6	13.0	12.2
August - October, IAWWTF > 50%, Wb<0	16.5	11.8	11.0
August - October, IAWWTF > 50%, Wb>0	15.6	17.0	13.7

Table 5.10: p-values of two-sided TP comparisons. Tests were performed on sampling days in the range August - October when loading from IAWWTF was above median. In each case the null hypothesis that the means/medians of respective sets are equal is tested against the listed alternative hypothesis.

hypothesis	**two-sample t-test**	**rank sum test**
(Site 3, $Wb < 0$) > (Site 3, $Wb > 0$)	0.187	0.487
(Site 5, $Wb < 0$) < (Site 5, $Wb > 0$)	0.003	0.006
(Site 6, $Wb < 0$) < (Site 6, $Wb > 0$)	0.003	0.002

The following explanation of these observations is offered, under the assumption that phosphorus loading from IAWWTF and the state of the internal seiche are indeed the main factors driving the differences in TP levels at sites 3, 5 and 6 as shown here. It should be noted that the condition of above median IAWWTF loading was chosen somewhat arbitrarily, and applied to the entire 11 year record. As discussed in section 3.2 loading from IAWWTF was significantly reduced after 2005, and indeed all sampling dates on which IAWWTF loading

was above median are pre-2007, and all but two are pre-2006 (there is a total of 170 sampling dates in the record). Prior to 2006 it is fair to assume that on days when IAWWTF loading was high during August - October it was the dominant source of TP loading onto the shelf since loadings from the IAWWTF were relatively high in those years, and flow in the tributaries, which is the other main source of TP, is low during those months. However this is not the case in the years following the plant upgrades (table 3.1, table 3.2). The discussion in this section is therefore best viewed as a discussion of hydrodynamics on the shelf in which TP is used as a tracer, rather than any kind of discussion of the effects of TP loading from IAWWTF, especially after the plant upgrades.

During the early months of the sampling season (i.e., April until June/July depending on the weather each year) the lake is not stratified and runoff volume and nutrient loading from the tributaries is high. Under these conditions the surface flow sources are the dominant factor that controls the water quality on the shelf. During the stratified period (August through October/November) the situation is different. Flow volume and the accompanying loading from the tributaries is minimal most of the time outside of storm events. When a storm occurs, such as the one that coincided with a sampling date on 06/29/2006 and is described in section 5.2.1, it can radically change the conditions on the shelf (TP levels during that event were 5-6 times higher than those discussed here). However, although there might be several such storms during the stratified period of any given year their duration is short and aside from bringing a load of sediment and nutrients into the lake their effects are short lived. During the majority of the stratified season the factors that control the water quality on the shelf are less dramatic, but more persistent. The main phosphorus loading source to the shelf (in terms of mass of phosphorus) is the IAWWTF outfall.

Therefore it is not surprising to see higher TP concentrations observed at times when the IAWWTF loading is higher. The main physical process controlling exchange between the shelf and the pelagic is the internal seiche and wind driven tilt of the thermocline. When the wind blows from the north ($Wb > 0$) the thermocline deepens causing the epilimnion to become much thicker, and hence larger in volume, near the shelf break. The result is increased exchange between epilimnetic water on the shelf - closer to the loading sources - and the epilimnion to the north in which TP levels are generally lower. It therefore follows that the phosphorus load entering the shelf near its southern end will be transported towards the north at an increased rate. This is indicated by the higher TP levels at sites 5 and 6, and the similar or lower TP at site 3, nearest the loading source, under these conditions. Conversely when the wind blows out of the south ($Wb < 0$) the thermocline tilts up in the vicinity of the shelf break, or even reaches close to the surface when Wb approaches -1. Therefore at sites 5 and 6 which are near the shelf break there should be more exchange across the thermocline (or rather the same rate of exchange would have a larger impact on the observed TP concentration since the volume of the epilimnion in that area will be smaller). Sites located farther south such as site 3 in the previous discussion and sites 7 and 3 during the extreme upwelling event on 08/21/07 discussed in section 5.2.2 are more isolated from these effects in all but the most extreme upwelling conditions. Furthermore in the case where the thermocline tilts up and essentially isolates the southern shelf from the rest of the epilimnion (e.g. figure 4.7d) the situation would be one in which the same mass loading (e.g., TP from IAWWTF, CHWWTP) to the southern shelf would be mixed throughout a smaller volume of water, thereby causing increased concentrations such as those observed on 8/21/2007 (section 5.2.2).

5.4.2 East to west gradients

Comparison of TP values observed at site 1 and site 4 during the stratified season sheds light on the effects of internal movements on transport onto the shelf. As shown in figure 5.14 TP levels measured at site 1 are generally higher than those measured at site 4 during the stratified season. However from figures 5.29 and 5.30, TP at the two sites, and especially the difference in TP between the two sites on the same sampling day, responds differently to Wb values less than or greater than zero (i.e., to conditions where the wind tilts the thermocline up or down near the shelf). While TP at site 1 is generally higher than at site 4 under any forcing conditions, TP at site 1 tends to be higher under conditions where the thermocline is tilted down ($Wb > 0$) while TP at site 4 does not. The difference $TP_{Site\,1} - TP_{Site\,4}$ is smaller when the thermocline is tilted up ($Wb < 0$; median 1.98 vs. 5.70 $\mu g/L$; figure 5.29; tables 5.11 and 5.12).

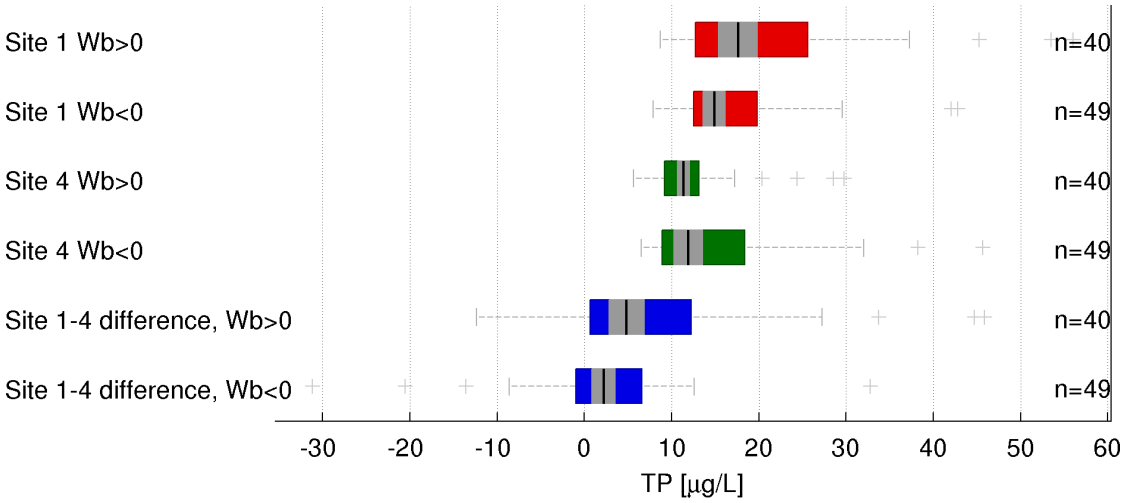

Figure 5.29: Comparison of TP at site1 and site 4 under different Wb number cases, during the stratified season (August - October). Darkened region around the median marks 95% confidence interval of the median.

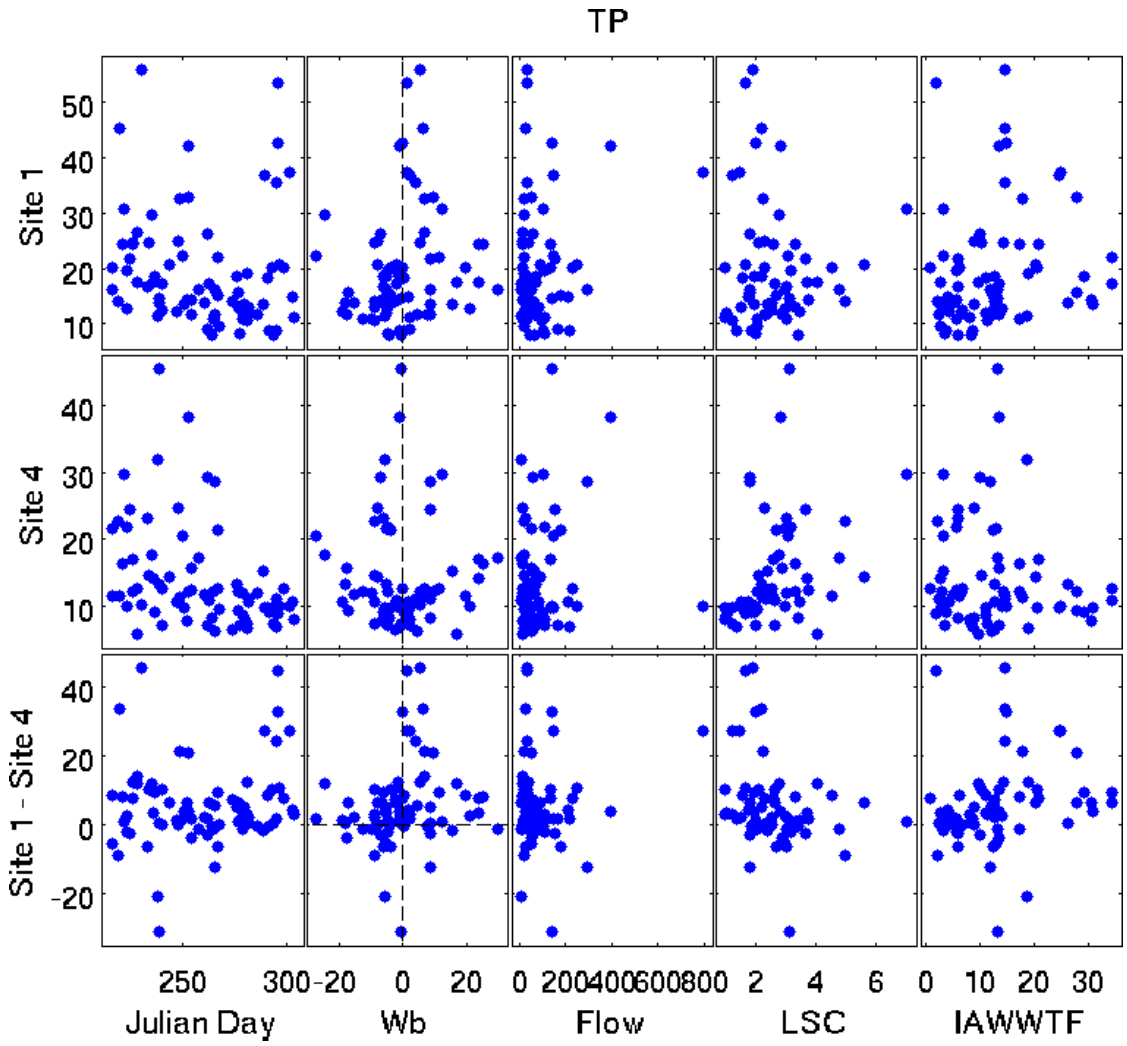

Figure 5.30: Comparison of TP at site 1 and site 4 under different forcing conditions, during the stratified season (August - October). TP values are in $\mu g/L$, flow in cfs, LSC and IAWWTF loading in kg/day of TP.

Table 5.11: p-values of paired TP comparisons at sites 1 and 4, August - October, n=40 ($Wb > 0$), n=49 ($Wb < 0$). In each case the null hypothesis that the means/medians of respective sets are equal is tested against the listed alternative hypothesis.

hypothesis	**paired t-test**	**signed rank test**
Site 1 > Site 4, when $Wb < 0$	0.097	0.013
Site 1 > Site 4, when $Wb > 0$	<0.001	<0.001

Table 5.12: p-values of two-sample TP comparisons at sites 1 and 4, August - October, n=40 ($Wb > 0$), n=49 ($Wb < 0$). Δ_{14} refers to the difference in TP between sites 1 and 4. In each case the null hypothesis that the means/medians of respective sets are equal is tested against the listed alternative hypothesis.

hypothesis	**two-sample t-test**	**rank sum test**
(Site 1, Wb>0) > (Site 1, Wb<0)	0.010	0.022
(Site 4, Wb>0) < (Site 4, Wb<0)	0.085	0.304
(Δ_{14}, $Wb > 0$) > (Δ_{14}, $Wb < 0$)	0.002	0.006

One possible explanation for this is advection of hypolimnetic water onto the shelf when the thermocline is tilted up or during upwelling conditions. Hypolimnetic TP concentrations are generally in the range 10-15 $\mu g/L$ (Cornell University, 2009). When $Wb < 0$ (thermocline tilted up near shelf) concentrations at both site 1 and site 4 are closer to this range, although they approach it from different directions - TP increases at site 4 and decreases at site 1. The higher levels of TP at site 1 relative to site 4 during general ($|Wb| \gg 1$) conditions is most likely due to loading from the point sources and tributaries. Site 1 is closer to the CHWWTP and LSC discharges than site 4, however the main sources of

phosphorus loading to the shelf are the tributaries and the IAWWTF outfall (at least prior to the IAWWTF plant's upgrades in 2005), both of which are located at similar distances from the two sites in question. A general Coriolis-induced counter clockwise circulation pattern on the shelf would therefore cause more of the phosphorus load onto the shelf to be advected towards site 1 rather than site 4. Additional evidence that this is the case may perhaps be found in figure 5.14, which shows that TP concentrations are better correlated between site 3 and site 1 than site 3 and site 4, indicating that the southeastern region of the shelf is better mixed than the southwestern region. If the main phosphorus loading sources on the shelf are the tributary flows and the IAWWTF, a counter clockwise rotation pattern would be consistent with similar TP concentrations at sites 3 and 1. If the main phosphorus loading sources are CHWWTP and LSC, the correlation in TP between sites 1 and 3 would indicate a clockwise advection pattern, which in turn would imply that the loading from the tributaries and IAWWTF be advected towards site 4. This is not consistent with the low TP concentrations observed there.

CHAPTER 6

DISCUSSION

6.1 Conceptual models of the impact of internal dynamics on the shelf water mass

6.1.1 The shelf as a well-mixed reactor with varying volume

If the shelf is considered to be a well mixed reactor (i.e., without significant spatial gradients in concentration) the average concentration of any passive tracer will be equal to its total mass divided by the volume of the shelf $\left(C = \frac{M}{V}\right)$ therefore the concentration will increase with net inputs of mass, and will also increase as the total volume of the reactor becomes smaller (with a fixed amount of mass). If we assume that the flux of mass into and out of the reactor is approximately equal, then for a constant loading rate the average concentration on the shelf will be governed by the rate of change of the volume of the reactor.

The lateral boundaries of this idealized reactor are fixed - the shoreline. The upper boundary is fixed at the water's free surface. However the bottom of the reactor is essentially in constant motion - on the shallow shelf it is defined by the lake's bottom but in the region near the shelf break it is determined by the location of the thermocline, which oscillates with the internal seiching of the lake. During upwelling conditions this bottom moves to a shallower depth or even moves up on to the shelf itself. This reduces the volume available for mass inputs to mix in, resulting in higher concentrations at some locations on the shelf but also more spatial variation since the boundary created by the upwelling

front can essentially separate some parts of the shelf from the loading sources.

During downwelling conditions the conceptual mixed reactor extends farther to the north, towards site 5 and even site 6 just beyond the beginning of the shelf break. The result is that measured concentrations of TP or other parameters will be elevated at more locations, however the concentrations will not be as high as in the upwelling case since the mass is now mixed with a larger volume of water.

If the weighted shelf-average of sites 1, 3, 4, 5 and 7 is used as an estimator of water quality on the shelf upwelling and downwelling conditions could each affect it in a different manner. Upwelling conditions, with very high values at only a few locations would lead to an elevated shelf-average since the one or two sites with high values would raise the mean. Under downwelling conditions the variation from baseline conditions at each site would not be as extreme, however since increased values would be observed at more locations the result would be a similarly increased shelf-average.

All of the preceding discussion assumes a high localized mass loading without significant inflow of water. This is typical of low tributary flow conditions when the main loading is from the wastewater treatment plants. During higher surface flow events the momentum of the inflowing water will alter the mixing dynamics on the shelf, and the prevailing upwelling or downwelling conditions on the shelf become of secondary importance.

6.1.2 Lateral tilting of the thermocline near the shelf break

As shown in section 4.5 the rotation of the earth can be expected to be important to long internal waves (i.e., basin scale seiche). The effect is a lateral (east to west) tilting of the thermocline as it shoals on the south shelf, so that the interface approaches the surface faster on the western side of the lake than on the east. This means that forcing conditions of borderline magnitude (e.g., say $|Wb| \sim 10$ as opposed to $|Wb| \sim 1$) would affect the western side of the shelf, but not the eastern side. Furthermore, although the main component of the wind over the lake is usually along the north - south direction, it generally lies to the west of the lake's main axis (figure 4.6), which leads to the thermocline becoming deeper on the eastern side of the lake and shallower on the west. Finally, the bathymetry of the lake in this region likely enhances this effect further - the lake is deeper close to the western shore so the progressing internal wave will encounter less bottom friction on that side. This lateral tilting of the thermocline has been described as far back as Henson *et al.* (1961), although there it was attributed to the Coriolis force acting on surface inflows from the tributaries (as opposed to affecting water motions stemming from the internal seiche, however the two processes are connected). The result is twofold: First if the mixed reactor with varying volume model is considered it will have the effect of confining that mixed reactor to the southeast corner of the shelf. Since that is where most of the loading sources are located the effect could be significant. Anecdotal evidence of this "blocking" effect exists in the form of aerial photos of plumes from Fall Creek and the Cayuga Inlet during moderate flows such as in figure 6.1. The plume can be observed to stay very near the south eastern shoreline. During higher surface flow events the momentum of the water flowing in from the tributaries is sufficient to overcome any density differences with upwelled water on

the shelf and cause increased mixing.

The second effect is to cause exchange between the shelf and the pelagic to be unequal between the eastern and western sides of the shelf, with hypolimnetic water being advected on and off of the shelf primarily on the western side. This result is increased exchange in the vicinity of site 4 which could explain why water samples collected from that site tend to have lower turbidity and TP than the other shelf sites. The increased exchange with the hypolimnion could also partially explain the lower chlorophyll-*a* levels observed at site 4 - existing chlorophyll-*a* is diluted more rapidly due to increased mixing with low chlorophyll-*a* hypolimnetic water, and local production is reduced due to lower residence times in that region.

This increased exchange on the western side of the shelf is due to the continuous runup of the internal seiche in this area, which over time leads to higher mixing rates between the shelf water and hypolimnetic water, e.g., due to turbulence generated from friction between water flowing up along the shelf break and the bottom. Its effect can be observed over long time scales, such as average values of water quality metrics in this part of the shelf. This is different from the reduced exchange rates discussed during upwelling events in which the southern shelf becomes isolated from pelagic waters. In that situation the effect is isolation from the main basin's epilimnion, and the effects are observable over shorter time scales.

Figure 6.1: Aerial photo of the southern shelf of Cayuga Lake

6.2 Summary

A summary of water quality properties observed on the southern shelf of Cayuga Lake over the 1998 - 2008 period has been presented along with measurements and discussion of the relevant physical forcings of the system. Spatial gradients have been shown to exist with higher levels of phosphorus and turbidity on the southern shelf than in the main basin of the lake to the north. The water quality on shelf has been shown to respond strongly to extreme physical forcing events, but in the absence of such conditions the water quality on the shelf is determined by a subtle balance of nutrient and sediment loading from natural and anthropogenic sources, and the interaction of the dynamics of

the lake with the shelf region in a manner similar to that described in Rueda & Cowen (2005*a*,*b*). Two conceptual models of the mechanisms controlling such factors as the residence time at different locations on the shelf were presented.

While it is likely that these two suggested mechanisms have significant importance for mixing and transport across and onto the shelf, these are subtle processes. Furthermore since the point sources are concentrated at the south-eastern corner of the shelf, and there is evidence of localized non-point sources of nutrient loading in that area as well it is very difficult to tease apart the effect of these various processes from the currently available data. This is mainly due to its low temporal and spatial resolution. However since these processes exist continuously throughout the stratified season, whereas strong forcing such as runoff events is intermittent especially during the peak of the stratified period it it likely that their importance is significant.

BIBLIOGRAPHY

AHRNSBRAK, WILLIAM 1986 Water movements in the south end of Cayuga Lake. report to engineering department, City of Ithaca NY. *Tech. Rep.*. Included as an appendix in the LSC DEIS.

AMOROCHO, J & DEVRIES, JJ 1980 A new evaluation of the wind stress coefficient over water surfaces. *JOURNAL OF GEOPHYSICAL RESEARCH-OCEANS AND ATMOSPHERES* **85** (NC1), 433–442.

ANTENUCCI, JP 2005 Comment on "Are there internal kelvin waves in Lake Tanganyika?" by jaya naithani and eric deleersnijder. *GEOPHYSICAL RESEARCH LETTERS* **32** (22).

ANTENUCCI, JP & IMBERGER, J 2001 Energetics of long internal gravity waves in large lakes. *LIMNOLOGY AND OCEANOGRAPHY* **46** (7), 1760–1773.

BIRGE, E. A. & JUDAY, CHANCEY 1914 *A limnological study of the Finger Lakes of New York.*. Washington: Govt. Print. Off.

BIRGE, EDWARD A. & JUDAY, CHANCEY 1921 *Further limnological observations on the Finger Lakes of New York*. Washington, D.C.: Govt. print. off.

BOEGMAN, L, IVEY, GN & IMBERGER, J 2005 The energetics of large-scale internal wave degeneration in lakes. *JOURNAL OF FLUID MECHANICS* **531**, 159–180.

CALLINAN, CLIFFORD W. 2001 Water quality study of the Finger Lakes. *Tech. Rep.*. NYSDEC.

CORNELL UNIVERSITY 2008 Cayuga Lake water quality monitoring, related to the LSC facility: 2007. *Tech. Rep.*. DeFrees Hydraulics Laboratory, School of Civil and Environmental Engineering, Cornell University.

CORNELL UNIVERSITY 2009 Cayuga Lake water quality monitoring, related to the LSC facility: 2008. *Tech. Rep.*. DeFrees Hydraulics Laboratory, School of Civil and Environmental Engineering, Cornell University.

EFFLER, SW, MATTHEWS, DA, PERKINS, M & JOHNSON, DL 2002 Patterns and impacts of inorganic tripton in Cayuga Lake. *HYDROBIOLOGIA* **482** (1-3), 137–150.

EFFLER, S. W., PRESTIGIACOMO, A. R., MATTHEWS, D. A., RAKESH, K. G., PENG, F, COWEN, E. A. & SCHWEITZER, S. A. Submitted December 2009 An analysis of phosphorus loading, trophic state, and clarity for southern Cayuga Lake, ny: A prelude to TMDL modeling. *Fundamental and Applied Limnology* .

GFLRPC 2000 Cayuga Lake watershed preliminary watershed characterization. *Tech. Rep.*. Genesee/Finger Lakes Regional Planning Council, 1427 Monroe Avenue Rochester, New York 14618 www.gflrpc.org 716-442-3770.

HAITH, DOUGLAS A., HOLLINGSHEAD, NICHOLAS, BELL, MATTHEW L., KRESZEWSKI, STEPHEN W. & MOREY, SARA J. 2009 Estimation of nutrient and sediment loads to Cayuga Lake using the GWLF watershed model. *Tech. Rep.*. Cornell University and The Cayuga Lake Watershed Network.

HENSON, EB 1959 Evidence of internal wave activity in Cayuga Lake, New-York. *Limnol. Oceanogr.* **4** (4), 441–447.

HENSON, E. BENNETTE, BRADSHAW, A. S. & CHANDLER, D. C. 1961 The physical limnology of Cayuga Lake, New York. Cornell University, Agricultural Experiment Station, New York State College of Agriculture, Ithaca, N.Y.

IMBERGER, J. 1985 The diurnal mixed layer. *Limnology and Oceanography* **30** (4), 737–770.

IMBERGER, J & HAMBLIN, PF 1982 Dynamics of lakes, reservoirs, and cooling ponds. *ANNUAL REVIEW OF FLUID MECHANICS* **14**, 153–187.

KITCHELL, J. F., SCHINDLER, D. E., HERWIG, B. R., POST, D. M., OLSON, M. H. & OLDHAM, M. 1999 Nutrient cycling at the landscape scale: The role of diel foraging migrations by geese at the Bosque del Apache National Wildlife Refuge, New Mexico. *Limnology And Oceanography* **44** (3), 828–836.

MAIDMENT, DAVID R. 1993 *Handbook of hydrology*. New York: McGraw-Hill.

MONISMITH, SG 1985 Wind-forced motions in stratified lakes and their effect on mixed-layer shear. *Limnol. Oceanogr.* **30** (4), 771–783.

MONSEN, NANCY E., CLOERN, JAMES E., LUCAS, LISA V. & MONISMITH, STEPHEN G. 2002 A comment on the use of flushing time, residence time, and age as transport time scales. *Limnology and Oceanography* **47** (5), 1545–1553.

OGLESBY, R. T. 1978 *Lakes of New York State, Volume I Ecology of the Finger Lakes*, chap. The Limnology of Cayuga Lake, pp. 2–120. Academic Press.

OGLESBY, R. T. & SCHAFFNER, W. R. 1978 Phosphorus loadings to lakes and some of their responses .2. regression-models of summer phytoplankton standing crops, winter total p, ad transparency of New-York lakes with known phosphorus loadings. *Limnology and Oceanography* **23** (1), 135–145.

PEDLOSKY, JOSEPH. 1987 *Geophysical fluid dynamics*. New York ;Berlin [u.a.]: Springer.

R DEVELOPMENT CORE TEAM 2009 *R: A Language and Environment for Statistical Computing*. R Foundation for Statistical Computing, Vienna, Austria, ISBN 3-900051-07-0.

RUEDA, F. J. & COWEN, E. A. 2005*a* Exchange between a freshwater embayment and a large lake through a long, shallow channel. *Limnol. Oceanogr.* **50** (1), 169–183.

RUEDA, F. J. & COWEN, E. A. 2005*b* Residence time of a freshwater embayment connected to a large lake. *Limnol. Oceanogr.* **50** (5), 1638–1653.

SPIGEL, R. H. & IMBERGER, J. 1980 The classification of mixed-layer dynamics in lakes of small to medium size. *JOURNAL OF PHYSICAL OCEANOGRAPHY* **10** (7), 1104–1121.

STEARNS & WHELER 1997 Draft environmental impact statement - Lake Source Cooling prepared for Cornell University, NY. *Tech. Rep.*. NYSDEC Application No. 7-00009/00001.

SUNDARAM, T. R., EASTERBROOK, C. C.., PIECH, K. R. & RUDINGER, G. 1969 *An investigation of the physical effects of thermal discharges into Cayuga Lake (analytical study)*. Buffalo, NY 14221: Cornell Aeronautical Laboratory.

TUKEY, JOHN W. 1977 *Exploratory data analysis*. Reading, Mass.: Addison-Wesley Pub. Co.

UFI 2000*a* Cayuga Lake water quality monitoring, related to the LSC facility: 1998. *Tech. Rep.*. Upstate Freshwater Institute (UFI).

UFI 2000*b* Cayuga Lake water quality monitoring, related to the LSC facility: 1999. *Tech. Rep.*. Upstate Freshwater Institute (UFI).

UFI 2001 Cayuga Lake water quality monitoring, related to the LSC facility: 2000. *Tech. Rep.*. Upstate Freshwater Institute (UFI).

UFI 2002 Cayuga Lake water quality monitoring, related to the LSC facility: 2001. *Tech. Rep.*. Upstate Freshwater Institute (UFI).

UFI 2003 Cayuga Lake water quality monitoring, related to the LSC facility: 2002. *Tech. Rep.*. Upstate Freshwater Institute (UFI).

UFI 2004 Cayuga Lake water quality monitoring, related to the LSC facility: 2003. *Tech. Rep.*. Upstate Freshwater Institute (UFI).

UFI 2005 Cayuga Lake water quality monitoring, related to the LSC facility: 2004. *Tech. Rep.*. Upstate Freshwater Institute (UFI).

UFI 2006 Cayuga Lake water quality monitoring, related to the LSC facility: 2005. *Tech. Rep.*. Upstate Freshwater Institute.

UFI 2007 Cayuga Lake water quality monitoring, related to the LSC facility: 2006. *Tech. Rep.*. Upstate Freshwater Institute.

UFI 2008 A Before-After-Control-Impact Analysis for Cornell University's Lake Source Cooling facility. *Tech. Rep.*. Upstate Freshwater Institute.